THE INTERPLAY BETWEEN MICROBIAL METABOLISM AND SURVIVAL AT SURFACE-AIR INTERFACES

Implications for the Long-Term Storage of Used Nuclear Fuel

by

Wendy Stone

B.Sc. (Molecular Biology and Biotechnology), Stellenbosch University, 2007
M.Sc. (Microbiology), Stellenbosch University, 2011

A dissertation
presented to Ryerson University
in partial fulfilment of the
requirements for the degree of
Doctor of Philosophy
in the program of
Environmental Applied Science and Management

Toronto, Ontario, Canada, 2016

AUTHOR'S DECLARATION FOR ELECTRONIC SUBMISSION OF A DISSERTATION

I hereby declare that I am the sole author of this dissertation. This is a true copy of the dissertation, including any required final revisions, as accepted by my examiners.

I authorize Ryerson University to lend this dissertation to other institutions or individuals for the purpose of scholarly research.

I further authorize Ryerson University to reproduce this dissertation by photocopying or by other means, in total or in part, at the request of other institutions or individuals for the purpose of scholarly research.

I understand that my dissertation may be made electronically available to the public.

The Interplay Between Microbial Metabolism and Survival at Surface-Air Interfaces

Implications for the Long-Term Storage of Used Nuclear Fuel

©Wendy Stone

Doctor of Philosophy
Environmental Applied Science and Management
Ryerson University, Toronto
2016

ABSTRACT

The Nuclear Waste Management Organization of Canada was mandated with the safe, long-term containment of the mounting nuclear industry waste (NWMO, 2005). The engineering of a multi-level barrier system in deep geological repositories to prevent radionuclide escape into groundwater involves the multidisciplinary collaboration of physicists, modelers, engineers, policy makers and legislators. This extreme environment is largely inhospitable to life, nevertheless microbial ubiquity demands biological attention if we are to approach risk assessment with legislative integrity. Two decades of work driven by an engineer-turned-microbiologist (Stroes-Gascoyne et al., 2010) provided extensive data to support highly compacted bentonite clay for microbial suppression during repository saturation. However, interfaces still demand microbiological attention (Wolfaardt and Korber, 2012), and desiccated bentonite interfaces are thus the focus of this research. The foundational work (Chapter 2) developed tools for evaluating microbial activity in saturated and desiccated bentonite. Novel aspects included the evaluation of precipitated sulphides with fluorometry, and the use of closed-

loop CO_2 measurements to assess microbial metabolism at bentonite-air interfaces. These tools were employed (Chapter 3) to measure the influence of relative humidity (RH) on persistent microbial metabolic activity at bentonite-air interfaces, and the influence of metabolic activity on the clay matrix. It was shown that the combination of bentonite interfaces and high RH stimulated the metabolic persistence of microbial communities during desiccation, despite high RH inhibiting the long-term survival of viable communities. A number of hypotheses were built on these observations (Chapter 4). These extended the observation of the interactive influence of high RH and bentonite to another hygroscopic matrix, polyethylene glycol, confirming that hygroscopic interfaces and high RH improve microbial access to water vapor at surface-air interfaces. It was also shown that oligotrophy increases biofilm desiccation-resilience in a desiccation-tolerant species (*Arthrobacter*), but not a desiccation-sensitive species (*Pseudomonas*). An appreciation of the microbial ability to harness their matrix for access to water vapor, and the interaction of this metabolic persistence with long-term survival, is applicable in the modeling and engineering of these industrial environments, and is an intriguing picture of the response of these versatile organisms to the vast challenges within which they so remarkably persist.

FOR

My Parents and Sister
My All

Otini Kroukamp
Teacher

ACKNOWLEDGEMENTS

To Annalise, Samantha and John Stone, Bronwyn Ford, Janice Rachel Saunders, Louis and Pauline Rowles, Carel-J Rischmuller, Cathy Patel, Jessica Nevin, Daphne Page, Juanita Lenford, Qing Huang, Maryam Goudarzi, Karen Milley, Wakeela Kassim, Hilda Bursey and Annie Chu: a tenacious community spanning continents, cultures and generations. This is how novel ideas are borne, stories are told and challenges surmounted. I hope that each of your realms grew from our discussions as much as this work benefitted from your wisdom.

Elanna Bester, Lindsay Jackson, Romeo and Alex Dumitrache, Evan and Pat Ronan. It was a privilege to work with a group of people courageous and unusual enough to take on the off-beat territory typical of the Wolfaardt group. Robin Luong, you saved me too many times with your engineering skills and cheer. Karen Puddephatt, this degree somehow morphed into a love of teaching that was unexpected. In the moments I'm not throwing all my markers in frustration, thank you for sparking that newfound adventure with your passion.

Darren R. Korber and Jennifer McKelvie. The NWMO project was a privilege because of the exposure to this unusual field, but mostly because I was on your team. Your insight, experience and encouragement were indispensable and went far beyond the call of duty. You two also taught me Canadian levels of politeness, promptness and gentle respect; skills you may take for granted, but I thoroughly enjoy as both foreign and powerful.

Gideon M. Wolfaardt, you facilitated this adventure, managed remarkable insight and guidance from another continent, and paved the way back to Africa. You have a unique ability to see straight to the centre of things. Words are inadequate to express my gratitude and severe whiplash at the consequences of crossing your path. Otini Kroukamp, your patience, grace and wisdom are a little crazy. I strive for similar insanity daily and can't wait for the next collaborations.

CONTENTS

LIST OF FIGURES

LIST OF TABLES

LIST OF ABBREVIATIONS

NWMO	Nuclear Waste Management Organization of Canada
EBS	Engineered Barrier System
HCB	Highly Compacted Bentonite
DGR	Deep Geological Repository
CEMS	Carbon Dioxide Evolution Measurement System
MIC	Microbially Induced Corrosion
RH	Relative Humidity

CHAPTER 1

Introduction to Microbial Metabolism at Surface-Air Interfaces

Implications for the Long-Term Storage of Used Nuclear Fuel

1. Introduction

1.1 Used Nuclear Fuel Storage: Legislature, Policy and Emplacement

The Nuclear Waste Management Organization of Canada (NWMO) is an independent research body, commissioned under the *Nuclear Fuel Waste Act* to design and implement a process for the storage of Canada's accumulated used nuclear fuel (NWMO, 2005). In its Adaptive Phased Management plan, proposed in 2005 and federally initiated in 2007, the NWMO describes the disposal of nuclear waste in deep geological repositories (DGR's) under a multi-disciplinary management plan that spans 3 phases over 90 years. Under the APM plan, a program has been rolled out to select a geologically appropriate site in a willing and informed host community (NWMO, 2005; NWMO, 2010). In Canada, there are currently 22 operating Canada Deuterium Uranium (CANDU) nuclear generation facilities. According to the Nuclear Energy Agency of the Organization for Economic Co-operation and Development (OECD, 2012), nuclear power generates 50% of Ontario's total power supply. Canadian reactor site storage, as of 2014, had accumulated over 2.5 million CANDU bundles (ca. 50,000 tonnes of heavy metal, t-hm), with projections of 3.4 million fuel bundles (ca. 69,000 t-hm) at the time of DGR emplacement (Garamszeghy, 2010). The APM strategy was selected as a long-term solution, relying on both natural and engineered barriers in the DGR for radionuclide containment. The natural barrier system will involve emplacement under 500 m of low-permeability sedimentary or crystalline host rock, in geological formations assessed for stability. The Canadian engineered barrier system (Fig 1.1) consists of copper-coated steel used fuel containers, containing 48 CANDU bundles each, surrounded by highly-compacted bentonite (HCB) clay. The used fuel container is designed to provide containment for at least 100,000 years; whereas, the HCB clay and host rock

will be relied upon for isolation of radionuclides to one million years. A nearly-sterile zone is expected in the highly compacted bentonite directly surrounding the used fuel containers. However, the interfaces between the bentonite barrier and the host rock have been identified as potential zones of microbial activity warranting investigation (Stroes-Gascoyne et al., 2011A; Pedersen, 2010; Wolfaardt and Korber, 2012).

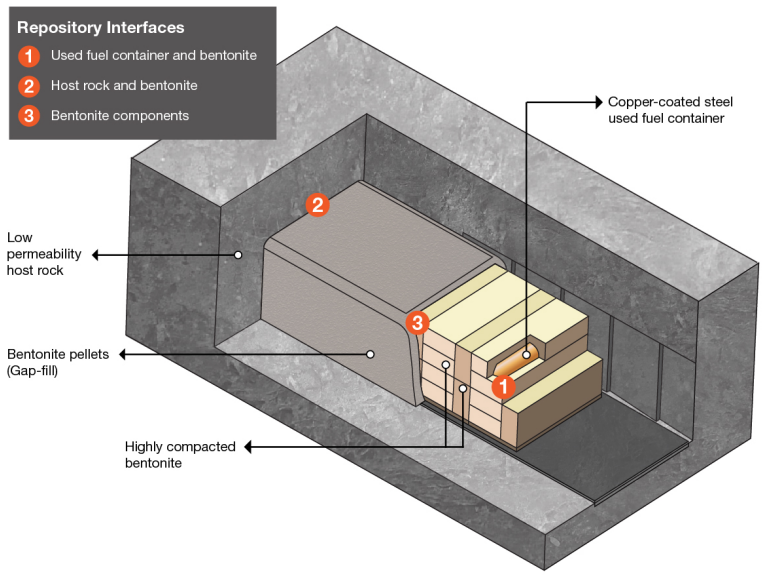

FIG 1.1 The Canadian Engineered Barrier System (EBS) in a deep geological repository for used nuclear fuel storage. The current Canadian design employs copper used fuel containers as a first barrier for the prevention of radionuclide escape from CANDU fuel bundles, and highly-compacted bentonite (HCB) blocks as a buffer between the used fuel containers and the host rock. The interface between the host rock and HCB is of greatest microbiological interest.

1.2 Used Nuclear Fuel Storage: Interface Microbiology

Microbes are adept at surviving diverse extreme conditions (Fredrickson et al., 2004; Dadachova and Casadevall, 2011; Hallbeck and Pedersen, 2012), and metabolism could have a variety of consequences in a DGR (Hallbeck and Pedersen, 2012; Stroes-Gascoyne and West, 1997). Microbial metabolism could create anaerobic zones due to oxygen consumption, metabolic by-products could cause Microbially Induced Corrosion (MIC), metabolic gas generation could cause cracks and channels of preferential diffusion through the compacted bentonite (Fig 1.2) and microbes could influence radionuclide migration by sorption or solubility. Indigenous microbial populations in the host rock may influence the storage of used nuclear fuel, as well as organisms introduced during the construction phase (Sherwood Lollar, 2011; Pedersen, 1997). Construction and waste placement will lead to aerobic, hot, dry, oxidizing conditions in the DGR; but upon emplacement and sealing, the environment should revert back to the initial anaerobic, cool, saturated, reduced conditions over time. This gradual change in conditions is predicted to take hundreds of thousands of years (NWMO, 2005).

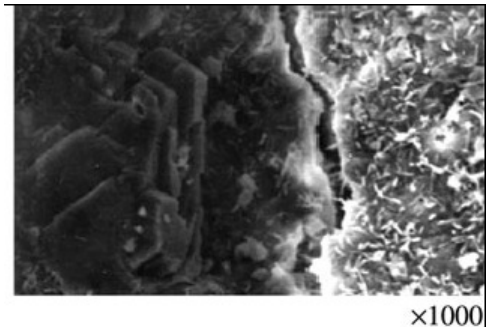

FIG 1.2 Potential microbial DGR consequences. Biogenic cracking of cement compounds in a surface repository after 4-5 years (Safonov et al., 2012).

The microbiology of this field has been extensively studied (Wolfaardt and Korber, 2012; Safonov et al., 2012; Fru and Athar, 2008; Stroes-Gascoyne et al., 2010; Stroes-Gascoyne et al., 2011A, B) and it was concluded that the surface area and compacted bentonite surrounding the used fuel containers are likely to be completely sterile for many hundreds of years due to extreme heat, radiation and desiccation. These may lessen over time, but compaction of bentonite to a dry density of 1.6 g/cm^3, with a corresponding saturation swelling pressure of >2 MPa and a_w of <0.96, limits culturable microbial numbers to background levels in as-received, powdered dry bentonite (Stroes-Gascoyne et al., 2010). Thus, the area directly surrounding the canisters is considered unlikely to pose any microbial threat to the storage structure integrity. However, the interfaces between the buffer and host rock could potentially present both the space and the nutrients for microbial survival and activity.

The potential for microbial metabolic activity in the nutrient-limited deep geological subsurface has been demonstrated (Kotelnikova, 2002). The organisms that have received the most attention in this environment are tellingly classified by their metabolic by-products, which have potential impacts in any deep subsurface endeavours, such as mining and repositories. They include the sulphate-reducing bacteria (SRB), acetogens and the methanogens (Wolfaardt and Korber, 2012), with corrosive sulphide production by SRB receiving the most focus in nuclear waste research. The compaction of the MX-80 bentonite buffer and resultant swelling pressure, combined with the natural salinity of groundwater, should prevent the growth of these organisms by lowering a_w (Stroes-Gascoyne et al., 2010; Masurat et al., 2010). However, these limiting parameters may not be maintained at HCB-host rock interfaces. Stroes-Gascoyne *et al*. (2011A) postulated that DGR moisture cycles could lead to non-homogenous bentonite swelling and the

transient release of microbial limiting parameters at buffer-host rock interfaces. Moisture levels may fluctuate due to heat gradients as a result of used fuel emplacement. When dry, the absence of water would be expected to limit microbial activity whereas upon saturation, clay swell pressure would physically limit microbial access to water. However, if these swell parameters are not met in non-uniform microenvironments during the periods between dry and wet phases, microbial activity could influence the bentonite matrix with the production of extracellular polymeric substances (EPS) and metabolites (Fig 1.3). In particular, biofilm formation at HCB-host rock interfaces has the potential to alter the transport of radionuclides and metabolites through the bentonite matrix, or provide microenvironments that promote microbial survival and activity. Such activity may influence key physical properties of bentonite, such as the clay swell index. Thus, the 2nd and 3rd Chapters of this dissertation investigates,

(i) the ability to measure microbial metabolism in bentonite in saturated and desiccated conditions,

(ii) the potential for microbial metabolism at surface-air interfaces,

(iii) the influence of relative humidity and clay on microbial metabolic persistence at surface-air interfaces and,

(iv) the impact of microbial metabolism on key bentonite properties, such as the clay swell index and water retention capacity.

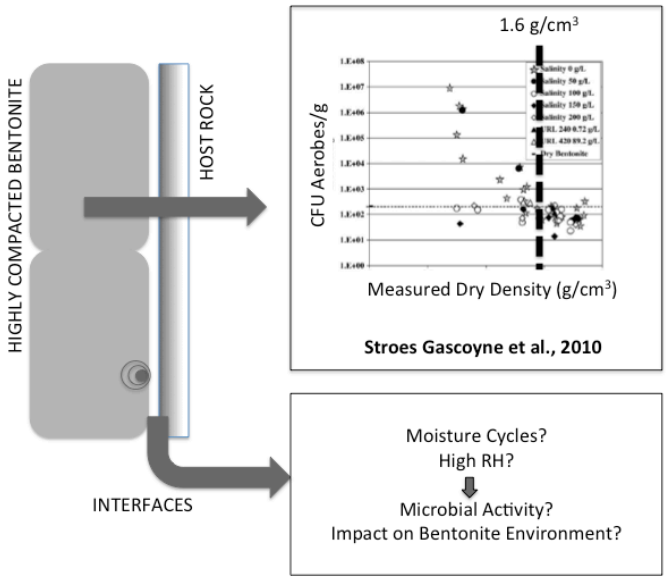

FIG 1.3 Research motivation schematic. Previous studies have demonstrated that bentonite compacted to 1.6 g/cm^3 limits a_w by swelling sufficiently to suppress microbial growth in saturated conditions. During liquid or gaseous moisture cycles, however, interface microenvironments may form with high enough a_w and low enough pressure for microbial activity. This work investigates the measurement of such potential microbial interface activity.

The distinction between microbial survival and persistent metabolism is fundamental, both in definition and consequent impact. Due to nutrient limitation and extreme conditions in subsurface environments, and the associated challenges in measuring microbial activity, subsurface microbiology has focused on microbial survival and species diversity. However, in the time-scales considered in DGR models, even slow metabolism could eventually influence the matrix. Thus, this research attempts to address microbial impact, rather than species diversity. Chapters 2 to 4 address the classification of an active community (with a measurable metabolic impact on their surroundings) and a potential community (with a potential for activity under ideal conditions), and discuss the relevance of both in the DGR. Particularly, the influence of relative humidity (RH) on microbial activity and survival is investigated.

1.3 What do Microbes Face upon Desiccation?

1.3.1 "Essentially Aquatic Organisms"

A microbial community relies on water as the source of the proton motive force for the ADP-ATP cycle, the basis of innumerable intra-cellular processes, and external water is similarly crucial for maintaining cell turgor, motility and molecular momentum across the membrane, including the export of toxins and import of substrates (Stotzky and Pramer, 1972).

As such, microbes have been referred to as "[regardless of their habitat…] aquatic creatures" (Stotzky and Pramer, 1972). The theory behind the availability of water to microbes at soil-air interfaces was extensively reviewed decades ago, and two excellent reviews will be summarized here for context (Stotzky and Pramer, 1972; Brown, 1976). Notably, both of these thorough reviews point out that the theory was rarely conclusively demonstrated *in situ*, due to the challenge of measurement techniques and the variability and diversity of natural soil and surface populations. The development of genetic techniques since then has facilitated an understanding of metabolism at surface-air interfaces (Billi et al., 2000; Deng et al., 2012), but low cell concentrations and reactions rates remain a hurdle to measuring true impacts in this field of study.

As proposed by Brown (1976), all prokaryotes and many microbial eukaryotes acquire nutrients from solution, and for a growing prokaryote, even a desiccated environment is thus essentially a "concentrated solution with which the microbial cell must come directly to thermodynamic terms".

Osmotic potential and **water activity** are the most well-researched indicators of microbial environmental access to water, since both are relatively easily measured. Water activity (a_w, described in Eq 1) describes the availability of environmental water to microorganisms, as opposed to quantification of the total water in the environment.

$$a_w = P_s/P_w = RH/100 \qquad \text{Eq 1}$$

where Ps = vapour pressure of the solution/environment, Pw = vapour pressure of pure water at the same temperature, and RH is the relative humidity (Brown, 1976).

However, as pointed out by Brown (1976), **water potential** is a much more thorough concept, since it includes osmotic potential (concentration of solutes, Ψ_o), pressure potential (Ψ_p), gravimetric potential (Ψ_g), potential due to humidity (Ψ_h) and the matric potential (Ψ_m) (Eq 2). All of these will have an influence on the availability of water to the microbial population at a surface-air interface.

$$\Psi = \Psi_o + \Psi_p + \Psi_g + \Psi_h + \Psi_m \qquad \text{Eq 2}$$

This equation demonstrates that the influence of desiccation on a microbial cell comprises more than pure limitation of liquid phase water molecules. Matric potential and osmotic potential, two distinct variables in the above-mentioned equation, have distinct morphological effects on both bacterial biofilms and eukaryotes (Chang and Halverson, 2003; Ramirez et al., 2004; Ritchie, 2006). In *Pseudomonas putida*, matric stress stimulates thicker biofilm EPS layers and solute stress stimulates filamentous morphology, both well-studied bacterial responses to desiccation

(de Goffau et al., 2011). The effects of water limitation on microbes are also determined by a number of extrinsic factors such as the availability of nutrients, the substrate upon which the cells are dried, the inoculum size, the cell growth phase, and the speed at which the cells are dried (Billi and Potts, 2002; Potts, 1994).

1.3.2 Desiccation at the Molecular Level: Cell Responses

There are two phases to the microbial desiccation response: an initial, rapid thermodynamic response and a slower metabolic, enzymatic and molecular adaptation during persistent growth (Brown, 1976). In the adaptation phase, growth at low a_w is due to (a) enzymes that have different conformations from non-adapted organisms or (b) the same enzymes as non-adapted organisms, within an intra-cellular environment that is controlled at higher a_w than the external environment, or a combination of the two. In halotolerant and halophylic bacteria, low a_w changes peptidoglycan and lipid structures to the extent that antibiotics like penicillin don't affect them. It also influences metabolism and stimulates pigment, gas vacuole and satellite DNA production. Thus, in exploring the influence of RH on microbial metabolism, the adaptation phase must be considered, and its influence on anabolic-catabolic rates.

1.3.3 Nutrient Cycling, Growth Rates and Desiccation

Water limitation is an effective and well-researched method for retarding microbial growth in the food industry, achieved by drying, freezing (limiting microbial access to liquid water) or adding solutes (Brown, 1976). Eukaryotes are much more tolerant of a wider range of water activity and

osmotic potential than prokaryotes (Table 1; Brown, 1976), and yeasts are notorious for contaminating honey, despite its high solute concentration and consequent low a_w (Snowdon and Cliver, 1996). However, desiccation is typically linked to starvation, since microbes faced with desiccation are often airborne, or on nutrient-poor surfaces (Billi and Potts, 2002; Potts, 1994). Brown (1976) describes an interesting discrepancy in the impact of the concentration of solutes that inherently accompanies desiccation in often nutrient-limited natural environments. At least during the initial phases of desiccation, the negative effects of water limitation increase concurrently with microbial access to nutrients. Similarly, the cell death and decomposition of susceptible species during desiccation provides resistant heterotrophs with extra nutrients. A desiccated biofilm community in a nutrient-poor environment may thus have access to more nutrients per cell than the same community under saturated conditions. Microbial mats have been shown to scavenge and tightly recycle limiting nutrients in water columns, thus, particularly within biofilms, similar nutrient cycling would likely occur during desiccation (Varin et al., 2010).

TABLE 1. *Approximate limiting water activities for microbial growth*[a]

Water activity (a_w)	Reference points	Foods	Bacteria	Yeasts	Fungi
1.00	Blood Plant wilt Seawater	Vegetables Meat, fruit	*Caulobacter* *Spirillum* spp.		
0.95		Bread	Most gram rods	Basidiomycetous yeasts	Basidiomycetes
0.90		Ham	Most cocci *Lactobacillus* *Bacillus*	Ascomycetous yeasts	*Fusarium* *Mucorales*
0.85		Salami	*Staphylococcus*	*Saccharomyces rouxii*, (in salt) *Debaryomyces* (in salt)	
0.80		Fruit cake Conserves		*S. bailii* (in sugars)	*Penicillium*
0.75	Salt lake	Salt fish	Halophils		*Wallemia* *Aspergillus*
0.70		Cereals Confectionary Dried fruit			*Chrysosporum*
0.65					*Eurotium*
0.60				*S. rouxii* (in sugars)	*Xeromyces bisporus*
0.55	DNA disordered				

[a] This table was obtained in its essentials from J. I. Pitt. With the exception of the halophilic bacteria, the organisms listed had a tolerance range from a_w 1.00 (approximately) down to their tabulated level. The halophilic bacteria, together with halophilic species of the alga *Dunaliella* and the halophilic actinomycete *Actinospora halophila*, have an upper limit as well (see text). The growth characteristics of halophilic bacteria suggest that they are limited at 0.75 a_w by the solubility of salt rather than by their physiology.

Fluxes in cell/community catabolic-anabolic balances are also an adaptive desiccation response, since microbes will expend energy to produce water when the external a_w is lower than the internal cellular a_w limit (de Goffau et al., 2011). Since the development of continuous flow cells, open systems have dominated biofilm studies of nutrient cycling, since most saturated natural biofilms (streams, drains, skin or oral infections, etc.) are better reflected by open systems (Benoit et al., 2010). However, nutrient cycles in desiccated biofilms will likely follow closed system, static dynamics more closely, with important consequent parameters like nutrient depletion and waste accumulation. Hydrodynamically, the no-slip boundary condition posits that there is zero flow at attachment surfaces in flow systems (Floryan and Rasmussen, 1989) and biofilms form "stagnant" internal phases with slow growth rates in the deeper regions (Xu et al., 1998), suggesting that even fast-growing saturated biofilms have phases adapted to "closed system" dynamics that would likely benefit a microbial community during desiccation.

It was shown in saturated biofilms that although the planktonic cell output is high, the carbon cost to the biofilm in the same time span was as low as 1.0±0.2% of the total carbon input (Bester et al., 2011). Thus, within a saturated biofilm, very low levels of carbon are required to prolifically produce cells. Such carbon balances suggest that cycles of cell production and degradation could provide sufficient nutrients to sustain persistent metabolism in a biofilm community at surface-air interfaces, particularly if adaptation includes slower metabolic processes.

An elegant technique was recently developed to measure slow environmental microbial growth rates at single cell level *in situ*, using the incorporation of heavy water into fatty acid synthesis (Kopf, 2015). The average *in situ* growth rate of *Staphylococcus aureus* in expectorated sputum from cystic fibrosis patients was between 12 hours and 4 days – radically longer than the typical laboratory culture generation time. This work proposes a revolution in our approach to laboratory studies, suggesting experimental growth rates be informed by much slower *in situ* growth rates. In most environmental systems, microbes have adapted to nutrient limitation, desiccation and low metabolic rates, suggesting that high growth rates or metabolic footprints are not necessarily measures of strong microbial communities. As Chesterton eloquently phrased this philosophy a century ago, "There is unfortunately one fallacy here into which it is very easy for men to fall… of supposing that because an idea is greater in the sense of larger, therefore it is greater in the sense of more fundamental and fixed and certain" (Chesterton, 1925). Such ubiquitous natural "slowness" could suggest that there is physiological, morphological and adaptive strength in metabolic pacing, which needs to inform laboratory experiments. Simply put, faster is not necessarily stronger. Thus, although exploring metabolism at surface-air interfaces is

challenging, the metabolic and survival dynamics may lead to deeper understanding of the true strength of microbes. Biofilm population or community morphology may permit metabolic persistence and pacing through interactions and cooperation, since macrobiological populations, for example birds in flight, often rely on population structure for pacing and energy conservation (Weimerskirch et al., 2001). Thus, the role of microbial morphological diversity in desiccation is introduced.

1.3.4 Morphology: Dormancy and Biofilms

Dormancy has long been marvelled at as a survival tactic allowing microbes to tolerate almost any environmental stress, including desiccation (Feofilova et al., 2012). The state of dormancy generally involves protective morphological changes, like spore formation and melanization, followed by the cessation of metabolic processes. These dormant spores germinate and regain their metabolic activity upon re-exposure to an ideal niche, generally one rich in nutrients and water. Such spore-formers can survive extreme environmental stresses ranging from desiccation to nutrient deprivation and high levels of radiation. Melanized spore-bearing fungi, for instance, were the first organisms to recolonize the Chernobyl site following radiation contamination (Zhdanova et al., 2000). Bacterial endospores, however, have an internal water content of approximately 21-58% and are therefore not considered strictly anhydrobiotic (Billi and Potts, 2002). The viable but nonculturable state (VBNC) of bacteria is another response to desiccation, albeit a poorly understood physiological state. This phenomenon describes a viable yet metabolically inactive state that bacteria enter in response to environmental stressors like desiccation (Kell et al., 1998; Oliver, 2005; Oliver, 2010).

Another vastly different microbial adaptation to such environmental stress, including desiccation, is their tendency to persist as multi-species biofilms. The fundamental difference between dormancy and biofilm response to desiccation is the biofilm maintenance of higher water activity and consequent potential persistent metabolic activity (Varin et al., 2010; Chang et al., 2007; Jordan et al., 1999). Extracellular polymeric substances (EPS) are fundamental constituents of biofilms and can improve the biofilm community's ability to scavenge both water and nutrients from the environment when either are limiting. EPS is also thought to protect cells from desiccation by providing a matrix for various water-stress proteins and polysaccharides such as trehalose (Billi and Potts, 2002). Biofilm production of EPS is enhanced in response to a plethora of harsh conditions, including desiccation (Auerbach et al., 2000; Chang and Halverson, 2003). In addition, synergism is enhanced in multi-species biofilms, creating metabolic networks that are more effective at harnessing the energetic potential in the environment, across both energetic redox and physical gradients, than pure or planktonic cultures (Pfeffer et al., 2012).

Biofilm forces also play a role in adaptation to extreme conditions. In saturated biofilms, liquid-air surface tension forces were proven sufficient to break the attractive Lifshitz-van der Waals forces, attractive and repulsive electrostatic interactions, and acid-base forces that attach biofilms to surfaces (Bos et al., 1999; Rutter and Vincent, 1988). The use of liquid-air interface tension forces for the detachment of particles has practical expression in the use of bubbles for the detachment of biofilms (Leenaars and O'Brien, 1989; Gómez-Suárez et al., 2001). However, during evaporation of water from a biofilm, these same physical surface-air interface forces will likely work in favour of the biofilm, forming a protective, concentrating physical force around the biofilm, rather than a disruptive force.

The physiological and metabolic responses of biofilms to harsh conditions have been extensively studied in saturated environments, since such biofilms are central to wastewater treatment, the food industry, hospitals and medicine. However, biofilm studies under desiccated conditions are rare due to the challenge of measuring morphology, physiology and metabolism at the lower limits of technological capabilities. Another challenge to the study of desiccation-induced mechanisms is the unravelling of the myriad stressors that often accompany desiccation, including nutrient limitations, temperature fluctuations, UV radiation and osmotic shock (Bauermeister et al., 2011). Halverson and Holden's groups have addressed some of these challenges and extensively described the formation of biofilms at surface-air interfaces using fluorescently labelled *Pseudomonas putida*, (Chang et al., 2007; Auerbach et al., 2000; Chang and Halverson, 2003; Li et al., 2010; Nielson et al., 2011). From these studies, cell association emerged as a common morphological response to desiccation, including the formation of cell tetrads or hyphae-like cell chains. Cell size can increase in some species, and decrease in others. However, their focus is almost exclusively on morphology and the biofilms were grown on relatively nutrient-rich, moist surfaces mimicking biofilms that form on leaves and soil particle surfaces. Despite the stark differences between these studies and the nuclear waste environment, they do emphasize two critical parameters when studying microbes at surface-air interfaces, and particularly their response to atmospheric water content: 1) the importance of attachment surface and 2) the importance of microbial community. Although technology has limited the study of desiccated biofilms, microbiology at surface-air interfaces has a few industrial and economic consequences that have driven progress despite the challenges.

1.3.5 Popular Interface Microbiology: Surface Weathering and Soil

The understanding of biofilms at solid-air interfaces has application in the fouling of statues, monuments, paintings and other structures. Weathering is thus one aspect of desiccated microbiology that has received some attention, along with some studies on diversity in air and arid soils (Alakomi et al., 2006; Gorbushina and Broughton, 2009; Gorbushina, 2007). Microorganisms at this boundary exist primarily in sub-aerial biofilms and are adapted to the stresses typical of these terrestrial environments, such as desiccation, temperature fluctuations, nutrient scarcity, and solar radiation (Gorbushina, 2007). These biofilms are often predominated by a specific group of eukaryotes known as microcolonial fungi, which have been shown to form subaerial biofilms on rocks in deserts (Gorbushina, 2007; Grishkan, 2011; Gostinčar et al., 2012). These tight, melanized hyphal clumps can penetrate rocks to depths in the range of mm. Eukaryotes are active at a much broader range of water activity extremes (Brown, 1976), form often-melanized spores in response to environmental stresses and their hyphal morphology allows them to access energy sources across physical distances (Pfeffer et al., 2012). In addition, eukaryotes adapted to deep subsurface aquifers were isolated from groundwater in the Aspo Underground Laboratory (Ekendahl et al., 2003) and from frozen arctic lakes at extremely limited a_w (Sterflinger et al., 2012), and need to be considered in extreme environments, particularly in weathering. The presence of eukaryotes in the DGR is addressed in Appendix A.

Another microbial surface-air habitat that has earned a scientific spotlight is soil, due to the agricultural impact of the soil microbiome. However, soil desiccation is often evidenced as a discontinuity of the liquid water phase, in contrast to the more consistent, homogenous water

limitation on rocks or walls (Stotzky and Pramer, 1972). Plants have adapted to obtain occluded water via root hairs, and microbes will also be concentrated in occluded water. Thus, microbial growth patterns measured in desiccated soil are not necessarily a reflection of microbial growth at low a_w, but possibly rather microbial growth in discontinuous liquid phases and microenvironments of higher a_w. The concept of water gradients and cycles also receives much attention in soil microbiology. This underscores the contention in this dissertation that at DGR bentonite-rock interfaces, microenvironments of concentrated occluded water or dampness could form microhabitats of high enough water potential and low enough swelling to sustain microbial metabolism. Bentonite is highly hygroscopic, and therefore both high relative humidity and water seepage are potential contributors to occluded microhabitats of higher water activity. Two critical physical parameters when studying microbial activity at a surface-air interface are thus (1) the RH of the environment and (2) the tendency of the surface to retain water, along with the ability of microorganisms to access both of these.

1.4 Microbial Access to Water: Vapour and Surface-Bound Water

1.4.1 Relative Humidity

The influence of the gaseous and liquid phases of water on microbial growth at surface-air interfaces need to be distinguished, since the atmosphere provides water in the gaseous phase, as well as precipitation. Gaseous water is discussed in terms of relative humidity (RH), defined as the amount of water vapour in the air and quantified as the ratio of the actual partial vapour pressure of water to the saturation vapour pressure of water at a particular temperature (Bauermeister et al., 2011). The influence of RH on desiccated bacterial survival at surface-air interfaces was shown to be species-dependent (Bauermeister et al., 2011; Turner and Salmonsen,

1973; Walters et al., 2005; Ronan et al., 2013). However, an emergent trend in these studies is that survival seems to be lower at high RH than at mid and low RH for most species, including desiccation-tolerant microorganisms. Desiccation-tolerant species are classified based on an internal water content survival threshold (Potts, 1994). An internal water content of approximately 0.7 g water/g dry weight is characteristic of an average bacterial cell in saturated conditions, and cellular water content below 0.3 g water/g dry weight is the threshold typically associated with cell death. When dried to equilibrium with air, the vast majority of organisms are irreversibly damaged, leading to cell death due to water limitations (Alpert, 2005). Tolerance to desiccation is an obvious evolutionary advantage due to the ubiquity of surface-air interfaces on earth. Organisms with the ability to survive at internal cellular water contents below 0.1 g water/g dry weight are classified as desiccation tolerant (Billi and Potts, 2002). It has been experimentally demonstrated that internal water contents of 0.1 g water/g dry weight can be achieved at ambient RH of 40%, whereas drying cells in air to equilibrium at 30% RH results in an internal cellular water content of 0.03 g water/g dry weight (Potts, 1994). Again, the majority of such studies have focused on the potential of microbes to survive these cellular thresholds, rather than metabolize.

Thus, the ambient water vapour equilibrium in the environment influences the internal cellular water content, which typically limits cell activity below these thresholds. Similarly, RH gradients have marked influences on cellular morphology in both bacteria and eukaryotes (de Goffau et al., 2009). However, a third critical aspect is the interaction between RH and the attachment environment on which the organism/biofilm is dried. Hygroscopic surfaces attract water, whilst hydrophobic surfaces repel water. Little research has been done on the effect of this on microbial

activity at surface-air interfaces. In bentonite clays, the hygroscopic nature of the matrix, in conjunction with the ambient water vapour, might influence long-term microbial activity at bentonite-air interfaces during DGR desiccation cycles.

1.4.2 Hygroscopic Clay Matrices

Having explored relative humidity, the next factor to engage, within the context of DGR microbiology and bentonite buffers, is the interaction between the hygroscopic clay surface and atmospheric water, and the accessibility of this water to microbes for metabolic persistence. The clay-microbe interaction, particularly the influence of clay on the activity of microbes, has largely been studied from the perspective of agricultural soil sciences and was, again, thoroughly reviewed decades ago (Filip, 1973). This review highlights the overwhelmingly positive effect of the addition of montmorillonite clays, such as bentonite, to agricultural soils. It results in higher crop yields, greater return of plant biomass to the soils, the reduction of carbon and nitrogen losses, increased humus content of the soil and an increase in microbial biomass and activity. It does not have a high nutrient content, and thus the positive influence is likely due to its structure. Clay minerals have a direct influence on microbial cells, as well as an influence on their environment. Sorption of microbial cells to clay is influenced by clay type, concentration, particle sizes, the cations in solution, as well as the microbial populations age, size and motility. Partial reduction is a crucial component of the hydrogen bonding and van der Waals forces involved in clay-cell sorption. Since clay and cells are predominantly negatively charged, sorption follows an ion exchange-like process. Montmorillonite added to soils decreases the sensitivity of bacteria to desiccation, temperature extremes and X-rays, promoting their survival.

Despite the positive influence of bentonite on microbial activity, the primary parameter of bentonite as a suppressive material in a DGR is the compaction and resultant swell pressure. However, this agricultural work suggests that at interfaces, where transient release of this pressure may occur in microenvironments, the bentonite-air interface is an environment of potential microbial protection and activity. The primary aspect of potential protection in this work is the interaction of the clay with water, and its influence on microbial metabolism.

1.4.3. Moisture Cycles

As pointed out above, soil is the most widely studied surface-air microbial habitat, yet much microbial activity in desiccated soil may be attributed to occluded water channels and precipitation cycles. Similarly, microbial growth on rocks in deserts, as well as in frozen lakes, may be attributed to precipitation cycles. Thus, most of these microbes could be adapted to switch to dormancy upon desiccation rather persisting metabolically. As studies typically focus on presence and diversity, rather than activity, the distinction in literature is elusive.

In this work, we contend that microbes may metabolize at surface-air interfaces, and that relative humidity and bentonite surface hygroscopicity could interact to create microenvironments of higher a_w, promoting microbial metabolism under desiccation. However, a laboratory predisposition is the classification of “low” versus “high” relative humidity. Whilst typical measurements relate microbial responses to these distinct conditions (Turner and Salmonsen, 1973; Walters et al., 2005; Ronan et al., 2013), microbes rarely face consistently low or consistently high relative humidity, unless in very unique (probably man-made) environments.

Biology constitutes cycles and is almost never static in any condition. The circadian rhythm is renowned as a fundamental biological determinant in response to external rhythms (Edgar et al., 2012; Trinder et al., 2015). Thus, the study of microbial metabolism during desiccation is more realistically pursued within the context of desiccation cycles. For example, natural water rhythms that will influence a soil microbial community include rainy and dry seasons, diurnal/nocturnal dew cycles, shadows cast over soil that move with the sun, and terrestrial disturbances (animal locomotion) (Stotzky and Pramer, 1972). In soils, desiccation cycles have been shown to significantly shift microbial community composition and influence activity (Kakumanu et al., 2013). Within man-made environments, such as bathrooms and kitchens, surfaces are exposed to precipitation cycles, humidity cycles, temperature cycles and splashing/drying cycles. Pipes and drains experience even greater cyclic extremes between desiccation and flow. Within the DGR, a moisture cycle is predicted due to the emplacement of heated waste, which, as pointed out, may facilitate transient microenvironments for microbial activity at buffer-rock interfaces, but may also drive adaptation and influence microbial community metabolic persistence. This study was limited to investigations of two consistent relative humidity points during desiccation. However, potential extension would be the investigation of the influence of relative humidity cycles and gradients on microbial metabolism and survival at surface-air interfaces.

1.5. Research Questions and Hypotheses

Perspective is important in this exploration. In certain applications, such as wastewater and bioremediation, science attempts to enhance and harness the metabolic activity of the biofilm

(Post et al., 2013). In contrast, in the food and medical realms the focus is predominantly on eliminating the biofilms, which often harbour pathogens and are more resistant to antimicrobial treatment than planktonic cells (Van Houdt and Michiels, 2010; Ghadakpour et al., 2014). In this study, the ecological and industrial perspectives are similarly distinct. Although persistent metabolism under desiccation may have greater metabolic impacts on the immediate bentonite environment, dormancy may result in a greater community potential upon re-saturation. These distinct biofilm energetic responses seem to be mutually exclusive, and need to be studied from the ecological perspective of biofilm robustness: essentially, from the perspective of the microbial community. A similarly interesting, but much more simple, question involved evaluating what can be measured in the bentonite environment, under saturated and desiccated conditions.

Thus, in Chapter 2, the measurement of microbial metabolism in bentonite is explored, under both saturated and desiccated conditions. The novel techniques of (1) fluorometry and (2) carbon dioxide evolution at bentonite-air interfaces are introduced, and the limitations of both are expounded upon.

Chapter 3 employs some of these tools to explore a number of fundamental questions regarding the potential for microbial metabolism in bentonite, and at bentonite-air interfaces:

(i) the potential for microbial metabolism at clay-air interfaces,

(ii) the influence of relative humidity and clay on microbial metabolic persistence at surface-air interfaces and,

(iii) the impact of microbial metabolism on key bentonite properties, such as the clay swell index and water retention capacity.

Chapter 4 extends these observations into theories, proposing a number of hypotheses to test these theories. In this chapter, the (1) strength of CO_2 as a metabolic indicator at surface-air interfaces was further evaluated, (2) the notion that hygroscopic surfaces and high relative humidity promote microbial communities' access to water was strengthened by extending the observation to synthetic hygroscopic surfaces and (3) the proposal that oligotrophy stimulates the desiccation resilience of a microbial biofilm was assessed in desiccation-sensitive and desiccation-tolerant species.

All of these questions and hypotheses inform the contribution of microbes in deep geological nutrient cycling within the bentonite interfaces, as well as fundamental surface-air microbial ecology, a field that has received minimal microbiological attention despite dominating the human ecological experience.

6. Contributions of Authors

Chapter 2 was published as Stone, W., Kroukamp, O., Moes, A., McKelvie, J., Korber, D. R., & Wolfaardt, G. M. (2016). Measuring microbial metabolism in atypical environments: Bentonite in used nuclear fuel storage. *Journal of microbiological methods*, 120, 79-90. doi:10.1016/j.mimet.2015.11.006.

Hypotheses and experimental design were carried out by WS, supervised by OK. Experiments, data analyses and manuscript preparation were carried out by WS, and AM assisted with sulphide standard curves and water retention experiments. Manuscript was supervised and edited by OK, JM, DRK and GMW.

Chapter 3 was accepted for publication in the *Journal of Applied Clay Science* as Stone, W., Kroukamp, O., McKelvie, J., Korber, D. R., & Wolfaardt, G. M. Microbial metabolism in bentonite clay: Saturation, desiccation and relative humidity. Hypotheses and experimental design were carried out by WS, supervised by OK. Experiments, data analyses and manuscript preparation were carried out by WS. Manuscript was supervised and edited by OK, JM, DRK and GMW.

Chapter 2

Measuring Microbial Metabolism in Atypical Environments:

Bentonite in Used Nuclear Fuel Storage

Chapter 2 was published as Stone, W., Kroukamp, O., Moes, A., McKelvie, J., Korber, D. R., & Wolfaardt, G. M. (2016). Measuring microbial metabolism in atypical environments: Bentonite in used nuclear fuel storage. *Journal of microbiological methods*, 120, 79-90. doi:10.1016/j.mimet.2015.11.006

2.1 Abstract

Genomics enjoys overwhelming popularity in the study of microbial ecology. However, extreme or atypical environments often limit the use of such well-established tools and consequently demand a novel approach. The bentonite clay matrix proposed for use in Deep Geological Repositories for the long-term storage of used nuclear fuel is one such challenging microbial habitat. Simple, accessible tools were developed for the study of microbial ecology and metabolic processes that occur within this habitat, since the understanding of the microbiota-niche interaction is fundamental to describing microbial impacts on engineered systems such as compacted bentonite barriers. Even when genomic tools are useful for the study of community composition, techniques to describe such microbial impacts and niche interactions should complement these. Tools optimized for assessing localized microbial activity within bentonite included: (a) the qualitative use of the resazurin-resorufin indicator system for redox localization, (b) the use of a $CaCl_2$ buffer for the localization of pH, and (c) fluorometry for the localization of precipitated sulphide. The use of the Carbon Dioxide Evolution Monitoring System was also validated for measuring microbial activity in desiccated and saturated bentonite. Finally, the buffering of highly-basic bentonite at neutral pH improved the success of isolation of microbial populations, but not DNA, from the bentonite matrix. Thus, accessible techniques were optimized for exploring microbial metabolism in the atypical environments of clay matrices and desiccated conditions. These tools have relevance to the applied field of used nuclear fuel management, as well as for examining the fundamental biogeochemical cycles active in sedimentary and deep geological environments.

2.2 Introduction

The rapid advancement in molecular techniques has facilitated a deeper understanding of microbial genetic diversity, metabolism and ecology, but has also achieved a popularity and focus that is somewhat limiting, as these techniques are not suitable for all samples or environments. For instance, genomic techniques are traditionally applied to environmental samples in surface waters and soils with higher biomass, but low-biomass systems introduce amplification bias, although steps have been taken to overcome this limitation (Binga et al., 2008; Barton et al., 2006). Examples of such low-biomass systems include almost any carbon-poor, deep-subsurface environment. However, despite the limited presence of microbial biomass, the potential for microbial metabolism and impact in such environments has been repeatedly demonstrated, for instance in geological cycling (Sherwood Lollar, 2011; Hirsch et al., 1995; Kotelnikova, 2002). Similarly, any extremes (i.e., temperature, pressure or desiccation) will drive biomass down, introducing bias. However, microbial activity in such environments is often of particular interest, both due to practical impact and a human fascination with adaptation to hostile niches (Horneck et al., 2008; Murray and Fritsen, 2011). Notably, most microbes of human concern are at least transiently exposed to desiccation, as our environment is not aquatic, yet microbial studies are overwhelmingly carried out in water/media saturated systems (Ronan et al., 2013). The study of microbial activity, as opposed to identification or quantification, is even more challenging in such low-biomass unsaturated systems, since RNA is less stable than DNA (Fleige and Pfaffl, 2006). This necessitates the development of tools to study microbial activity and impact in low-biomass systems.

An example of such a challenging low-biomass environment is highly compacted Wyoming MX-80 bentonite, selected for use as a buffer in the long-term storage of used nuclear fuel in Deep Geological Repositories (DGR). The need for such repositories is an international priority and a number of countries have been collaboratively exploring plans for the containment of highly-radioactive used nuclear fuel. The Adaptive Phased Management plan of Canada (NWMO, 2005) is one such response to this growing inventory, with multiple barriers for prevention of radionuclide escape (Fig 2.1), having an operational life cycle of 100,000 – 1 million years.

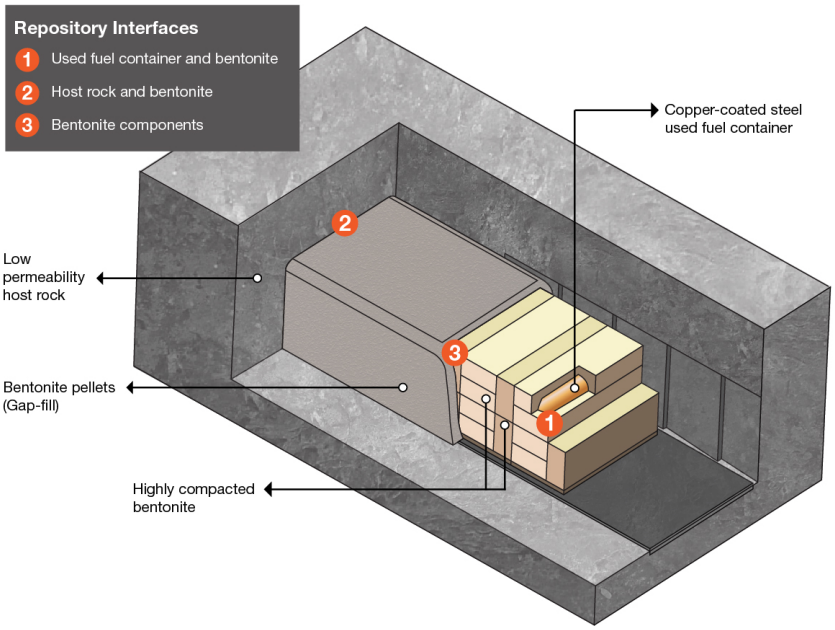

FIG 2.1 The Canadian Engineered Barrier System (EBS) in a deep geological repository for used nuclear fuel storage. The current Canadian design employs copper used fuel containers as a barrier for the prevention of radionuclide escape from CANDU fuel bundles, and highly compacted bentonite (HCB) blocks as a buffer between the used fuel containers and the host rock. The interface between the host rock and HCB is of greatest microbiological interest.

Although repository details differ due to unique geological factors (host rock formation, proximity to underground water sources) and waste parameters (fuel production process, waste size and form), Wyoming MX-80 bentonite has almost unanimously been chosen as the candidate buffer. The swell pressure and consequent limitation of water activity upon saturation of compacted MX-80 prevents microbial growth in the DGR (Masurat et al., 2010; Stroes-Gascoyne et al., 2010), although interfaces may provide transient microenvironments for microbial activity (Pederson, 2010; Stroes-Gascoyne et al., 2011A&B; Wolfaardt and Korber, 2012). Potential microbial processes of interest in this DGR bentonite substrate include: (1) the consumption of oxygen after the closure of the repository, (2) the production of sulphide by sulphur reducing bacteria (SRB), which could cause microbially influenced corrosion (MIC) if diffused to the container, and (3) the formation of cracks or preferential pathways in the bentonite due to gas generation (i.e., by methanogenic bacteria). Groups evaluating MX-80 bentonite barrier performance include the NWMO (Canada: Stroes-Gascoyne and Hamon, 2014), Nagra (Switzerland: Hofstetter et al., 2014), SKB (Sweden: Borgesson and Hernelind, 2014) and Posiva (Finland: Muurinen, 2009). Large-scale collaborative efforts on bentonite shaft seals demonstrate the popularity of the bentonite buffer, and the need to understand this matrix as a microbial environment (Dixon et al., 2014). This work also facilitates the study of fundamental microbiology in extreme environments, with broader application in biogeochemical cycling in subsurface environments.

The interactions between microbes and bentonite are key to understanding microbial DGR impacts, particularly localization of microbial metabolic activity. Wyoming MX-80 bentonite imposes a number of challenges to standard microbiological methods and techniques. Clay

materials have a strong binding capacity due to their inherent ion exchange properties, fundamental to the buffer's performance, which potentially interferes with the extraction of nucleic acids due to charge-based complexing and subsequent interference (Filip, 1973; Paget et al., 1992; Walker et al., 1989). This was the suggested reason for the failure of culture-independent techniques in the identification of Opalinus clay microbiota, and the popularity of culture-based approaches in DGR microbiology. Phospholipid fatty acid analysis has thus been the primary molecular/biochemical method for assessing DGR microbiota (Mauclaire et al., 2007; Stroes-Gascoyne et al., 2007A). Overall, the typical metagenomic toolbox has proven largely unsuitable for identifying bentonite microbiota. Similarly, cell adsorption by clay molecules provides challenges in separating cells from clay, while autofluorescence of bentonite poses challenges for direct microscopy-based observation.

Tools for localizing zones of microbial activity and consequent environmental transformations are also necessary. Reduction-oxidation potential (redox), sulphide precipitation and pH are all indicators of microbial activity, and simple techniques to localize these fluctuations are necessary. These parameters link microbiology and the integrity of the DGR in a number of ways: (1) reduced redox potential is indicative of anaerobic conditions, and sulphide stress cracking of copper is due to hydrogen embrittlement, an anaerobic process (Chen et al., 2011), as are methanogenesis and methane oxidation (using alternate electron acceptors such as nitrate or nitrite), key elements of the deep subsurface carbon cycle (Kotelnikova, 2002), (2) a drop in pH may solubilize metal, leading to metal leaching (Rawlings, 2002), and (3) microbial activity has been linked to the illitization of smectite clays, rendering the clay less swellable (Mulligan, 2009). Another indicator of microbial activity is sulphide production by SRB. Aqueous sulphide

is typically measured with the Methylene Blue technique, but sulphide species are notoriously varied and the quantification of precipitated sulphide would be useful (Meysman, 2005). Tools for studying microbial activity at bentonite-air interfaces are also necessary, due to the previously identified gap in DGR microbiology at bentonite-rock interfaces (Stroes-Gascoyne et al., 2011). This particular niche introduces the added challenge of studying microbial activity in a desiccated environment.

This study therefore aims to evaluate tools for assessing microbial metabolic activity in saturated and unsaturated bentonite. Tools evaluated include:

(1) The localization of microbial activity in saturated bentonite with (a) redox, (b) pH, and (c) precipitated and soluble sulphide measurements,

(2) The measurement of microbial activity at bentonite-air interfaces using CO_2 Evolution Measurement Systems (CEMS), and

(3) The influence of pH on the separation of cells and DNA from the bentonite matrix.

2.3 Materials and Methods

2.3.1 Bentonite Sampling and Microcosms

Uncompacted Wyoming VOLCLAY MX-80 bentonite samples were obtained from American Colloid Company (Lovell, Wyoming), stored in sealed bags outside the laboratory and handled aseptically. As-received, non-sterile but aseptically-handled, uncompacted bentonite (5 g/microcosm) was placed in 10 mL luer-lock sealed syringes, and saturated with sterile tap water. Similar aerobic microcosms were set up in glass vials (height: 58 mm, diameter: 20 mm), and covered with parafilm, which is permeable to both O_2 and CO_2 (150 cc/m^2d and 1200 cc/m^2d, respectively, at 23 °C). Optimal slurry concentrations were determined by consistency and ease of handling. During static incubation, microcosms were monitored for the visible formation of black precipitate, presumed to be the precipitation of iron sulphides such as pyrite, mackinawite and greigite, due to microbial sulphate reduction (Hunger and Benning, 2007; Rickard and Morse, 2005). The concept is similar to Winogradsky columns, employed to study sulphide precipitation in anaerobic regions of environmental sediments (Corner, 1992; Zavarzin, 2006). Visible iron sulphide precipitation was recorded in each microcosm (+++, ++, + or -; representing heavy, average, barely visible or zero precipitate, respectively), and percentages of microbial activity per treatment recorded. In microcosms where microbial activity occurred, black precipitation was visible in 2 – 6 weeks and analysed at 9 weeks. Microbial activity was confirmed with sulphide, redox and pH measurements in black microcosms, as compared to twice-autoclaved control microcosms and microcosms without sulphide precipitation.

2.3.2 Bentonite pH and Redox

Resazurin Sodium Salt solution, modified from Atlas (2004) and Gonzalez-Pinzon et al. (2012), was used to monitor bentonite redox potential in zones of visible iron sulphide precipitation, compared to controls without iron sulphide precipitation. Bentonite microcosms (5g/microcosm) were set up in 10 mL luer-lock syringes and glass vials (height: 58 mm, diameter: 20 mm) as described above, saturated with resazurin solution (0.06 g/L) instead of tap water. The addition of 2.5 mL resazurin solution (0.06 g/L) was assessed pre-incubation and post-incubation (Table 1). The indicator was for visual, real-time localization of microbial activity, in relation to gas production and sulphide precipitation. Thus, resazurin was pre-mixed through the bentonite in aerobic glass vials or forced through the bentonite using syringe pressure in syringes. Due to resazurin's potential influence on sulphide precipitation, resazurin localization was also assessed post-incubation (a) by using syringe pressure to force resazurin into the microcosms at 9 weeks and (b) by removing layers of the microcosm from glass vials and adding 0.5 g (wet weight) to a 3 mL cuvette, followed by addition of 1 mL resazurin (0.006 g/L) solution. The optimal pre-mixed resazurin solution was 10X more concentrated than the optimal post-incubation solution. Six microcosms were set up per pre-treatment, per dilution, for a total of 36 microcosms (Table 2.1). Post-incubation microcosms (36) were set up as described in the 'Sampling and Microcosms' section above. The precipitation of pyrite (+++, ++, + or -; representing heavy, average, barely visible or zero precipitate, respectively) and a colour change from blue to pink to colourless (+ or -) were monitored, and gas bubbles were recorded (+ or -). In all redox studies, twice-autoclaved controls were included.

TABLE 2.1 Bentonite redox measurements. Bentonite microcosms were saturated with dilutions of a 6 g/L resazurin solution pre-incubation by mixing before adding the slurry to the syringe or saturating the dry bentonite using syringe pressure. Redox was measured in bentonite microcosms post-incubation (9 weeks) by (a) syringe saturation and (b) removal of 0.5 g layers and subsequent addition to resazurin in cuvettes.

	Resazurin Dilution (6 g/L)	Pre-Incubation Resazurin Treatment		Post-Incubation Resazurin Treatment	
1	10^{-1}	Mixed	Syringe Saturated	Syringe Saturated	Cuvettes
2	10^{-2}				
3	10^{-3}				

Water was compared to $CaCl_2$ for the measurement of bentonite pH, adapted from Henderson and Bui (2002). This buffer is less sensitive to electrolyte changes and is thus commonly used for monitoring soil pH. Thirty bentonite-tap water microcosms were set up in syringes and glass vials as described above. After 9 weeks, six microcosms with zones of iron sulphide precipitation were selected as 'active', and six microcosms without visible iron sulphide precipitation were selected as controls. Twelve microcosms (six each, from two different clay batches received from American Colloid Company) were mixed on the day of analysis for monitoring the pH of as-received bentonite. The pH of each microcosm was measured with water or $CaCl_2$.

Henderson and Bui (2002) recommend a 5:1 water:soil ratio, but bentonite swelling necessitated using an increased ratio of 15:1 water:bentonite (67 g/L). Bentonite was weighed (1 g) and mixed with 15 mL water or $CaCl_2$ in a 50 mL polyethylene tube, and the pH was measured with

a ROSS Ultra pH/ATC Triode with Refillable Glass Electrode, calibrated before each use with the 3 buffer (pH values of 4.01, 7.00, 10.01) method. Means and standard deviations of triplicate samples were calculated in Excel and compared with independent-sample two-tail t-tests. This statistical analysis was employed for all comparisons of means in this study. Samples from each microcosm (1 g) were also weighed in duplicate and dried overnight to assess dry weight variation.

2.3.3 Sulphide Measurements: Methylene Blue and Fluorometry

Soluble sulphide was measured with Methylene Blue (Truper and Schlegel, 1964; Cline, 1969; Reese et al., 2011). Measurements were made in 3 mL acrylic cuvettes, using a Perkin Elmer Lambda 20 & 40 UV/Vis Spectrometer (Massachusetts, USA). All chemicals and reagents used were of analytical grade, ordered from Sigma Aldrich (Oakville, ON, Canada). Sulphide was trapped by adding 39.5 µl of a sample aliquot to 632 µl zinc acetate (2 % w/v in 0.1 % w/v glacial acetic acid). Thereafter, 789 µl of pPDA reagent (0.2 % w/v of N,N-dimethyl-p-phenylenediamine sulphate (Alfa Aesar, MA, USA) in 20 % w/v H_2SO_4) was added. The mixture was vortexed (5 s), incubated at room temperature (2 min) and centrifuged (2 min; 13,000 g; room temperature). The supernatant was transferred to a clean microcentrifuge tube. A 39.5 µl aliquot of 10 % $FeNH_4(SO_4)_2 \cdot 10\ H_2O$ (in 2 % w/v H_2SO_4) was added to the supernatant, the mixture incubated (20 min) and absorbance measured (670 nm).

Two standard curves (triplicate samples) were prepared using the Methylene Blue method:

(A) 0-5 mM Sulphide (Na_2S) in distilled water

(B) 0-5 mM Sulphide in a 100 g/L solution of uncompacted dry bentonite in distilled water

Standard samples for dilution were anaerobically-prepared under positive nitrogen pressure, after the dH_2O had been sparged with N_2 gas for an hour, and only exposed to oxygen after trapping the sulphide in the zinc sulphate solution. Each sample in the standard curve was vortexed, after mixing bentonite and sulphide for 20 min in a 15 mL polyethylene tube (5 mL per tube), before the 39.5 µl aliquot was measured according to the protocol above.

Fluorometry was assessed for quantifying precipitated sulphide in bentonite. The measurement of the inhibition of bentonite autofluorescence by FeS was modified from Skjerdal et al (2004). Bentonite (1 g) was suspended in 15.0 mL dH_2O (50 mL polyethylene tubes) and vortexed (1 min). A sulphide series was set up in triplicate, with 0-0.5 g FeS/g bentonite. After optimising emission and excitation ranges, the inhibition of the emission peak at 350 nm was measured upon excitation at 300-400 nm using an LS50B Luminescence Spectrometer, and FL Winlab version 4.00.02 software for data analysis. Peak areas (to baseline) were calculated. Arbitrary fluorescence units were reported as a ratio, normalized to the highest fluorescence value per experiment. This was repeated with bentonite suspended in saline tap water (200 g/L NaCl). Long-term bentonite microcosms with visible pyrite precipitation were compared to control samples without FeS precipitation. For microcosms, 1 g (wet weight) was dried overnight, the equivalent of 1 g dry weight approximated (1.8 g wet weight) and added to 15 mL water as above.

2.3.4 Measuring Microbial Metabolism: Bentonite as a Matrix for CO_2 Evolution at Surface-Air Interfaces

Bentonite (50 g/L) was incubated with sterile tap water in 50 mL polyethylene tubes. A sterile control included 50 g/L radiated (2.5 MRad) bentonite in 50 mL sterile tap water. All microcosms were vortexed (3 min) and aerobically incubated in covered Falcon tubes under static conditions (room temperature, 14 days). Microcosms were subsequently vortexed (1 min) and 15 mL injected from each into separate, clean sections of Tygon tubing (1 m long, 1 cm inner diameter). Tubes were secured lengthwise with open ends upwards, so that the bentonite slurry was spread as a film (~1 mm thick) across the bottom (along ~50 cm of the U-shaped section of the tube). Air was passed through each tube at 16-20 L/min for 16 h until visible desiccation, indicated by bentonite flaking and lightness of colour. The tubes were subsequently incubated in chambers controlled at 75 % relative humidity (RH). After 48 h, CO_2 production by the desiccated samples was measured by connecting the tubes to a closed-loop Carbon Dioxide Evolution Monitoring System (CEMS), described by Kroukamp and Wolfaardt (2009) and Bester et al. (2010). The carrier gas was air, equilibrated to ambient levels of CO_2 (~450 ppm), circulated with a peristaltic pump. The accumulation of CO_2 in the system was measured after 3-5 h, disconnecting the sample tubes from the CEMS loop and replacing them at controlled RH between measurements.

RH was maintained using saturated salt solutions in covered 5-L glass chambers (Greenspan, 1997). Slurries of $MgCl_2$ and KCl were made in distilled water at 3 times their solubility limit in 100 mL glass beakers and sealed within the chambers to achieve RH values of 33 % and 85 %, respectively, at room temperature. RH was monitored using 915 MHz Wireless Temperature

Stations (La Crosse Technology, Saint-Laurent, QC, Canada). Bentonite altered the chamber RH, as compared to the results reported by Greenspan (1997), but they stabilized at 23-30 % (further referred to as 30 %) and 75-79 % (further referred to as 75 %), consistently returning to the controlled RH within an hour after opening and resealing the chamber.

Saturated and desiccated bentonite was assessed as a carbon sink. For saturated bentonite, a 10 mL solution of a 50 g/L bentonite slurry (pH 9.5 in $CaCl_2$) was mixed in a glass vial (height: 58 mm, diameter: 20 mm) with 2 ports for tubing connections and sealed with an anaerobic stopper. This vial was connected to the closed-loop CEMS system and the CO_2 was recorded over time, measuring fluctuations from ambient CO_2 (~450 ppm). The CO_2 absorption capacity of the slurry was compared to a sodium tetraborate/sodium hydroxide buffer system (10 mL, pH 9.5) in an identical glass vial.

For the analysis of desiccated bentonite incubated long-term at 30 % RH and 75 % RH, bentonite was weighed (20 g) into glass vials (height: 58 mm, diameter: 20 mm) and incubated at the respective RH values for one year. The bentonite (5 g) was transferred into glass vials (height: 58 mm, diameter: 20 mm) with two ports, sealed with an anaerobic stopper, and connected to the CEMS system for CO_2 monitoring.

The log transformation of the relationship between CO_2 and time was correlated, and the means and standard deviations of gradients of triplicate samples compared with independent-sample t tests.

2.3.5 The Influence of pH: DNA Extraction and Isolate Culturability

The influence of bentonite pH on DNA extraction and microbial isolation was explored by buffering at various stages in the isolate recovery and DNA extraction procedures.

Four DNA extraction methods were tested:

1) ZR Fungal/Bacterial DNA Microprep Kit (Zymo Research, Cedarlane Labs, Burlington, Canada),
2) PowerSoil DNA Isolation Kit (MO BIO Laboratories, VWR, Mississauga, Canada),
3) PowerMax Soil DNA Isolation Kit (MO BIO Laboratories, VWR, Mississauga, Canada), and
4) Protocol of Takada-Hoshino and Matsumoto (2004).

Four bentonite slurries were mixed in sterile 50 mL Schott bottles, in duplicate:

1) 5 g bentonite in 15 mL sterile dH_2O, shaken (room temperature, 300 rpm) for 10 h,
2) 5 g bentonite in 15 mL sterile buffer (pH 7.0), shaken for 10 h,
3) 5 g bentonite in 15 mL *Bacillus simplex* and *Cryptococcus magnus* culture (about 10^6 cells/mL dH_2O), shaken for 10 h, and
4) 5 g bentonite in 15 mL *Bacillus simplex* and *Cryptococcus magnus* culture (about 10^6 cells/mL buffer, pH 7.0), shaken for 10 h.

The *Bacillus simplex* culture (grown overnight in 3 g/L Tryptic Soy Broth) and the *Cryptococcus magnus* culture (grown 36 h in Yeast Malt Broth, 3 g/L Malt Extract, 3 g/L Yeast Extract, 10 g/L Dextrose, 5 g/L Peptone) were washed 3 times with tap water or buffer and diluted to about 10^6

cells/mL using an absorbance value (600 nm) standard curve. The cultures had been originally isolated from MX-80 bentonite. The bacterial culture, *B. simplex*, was chosen for its ubiquity in the bentonite samples, and its heat resistance (Sikorski and Nevo, 2007). The eukaryotic culture, *C. magnus*, was also chosen for its ubiquity in bentonite samples and its resistance to extreme environments (Butinar et al., 2007).

One bottle of each was set aside for pH measurement immediately prior to DNA extraction, with a ROSS Ultra pH Electrode calibrated before each use using the 3 buffer method.

Each of the four slurries were subjected to each of the four extraction procedures, with positive and negative controls for both extractions and PCR amplifications, and the DNA visualized under UV light (Geneflash Syngene Bioimaging Unit, Cambridge, UK) after electrophoresis in a 8 g/L agarose gel with SYBR Safe DNA gel stain (Invitrogen, Burlington, Canada). A GeneRuler 1kb DNA molecular weight ladder (Thermo Fisher Scientific, Waltham, USA) was used to quantify DNA concentration.

For eukaryote-specific PCR, the universal primers ITS1 (5'-TCCGTAGGTGAACCTGCGG-3') and ITS4 (5'-TCCTCCGCTTATTGATATGC-3') were used to amplify the internal transcribed spacer (ITS) region (200-700 bp) of the 18S ribosomal subunit gene cluster (White et al., 1990). The 50 µl PCR reaction mixture contained 0.5 µg of gDNA, 6.875 µg Bovine Serum Albumin, 200 µM of each of the four dNTP's, 25 pmol of each primer oligonucleotide (Centre for Applied Genomics, SickKids, Toronto, ON, Canada) and 2.5 units of Taq DNA polymerase in Taq buffer (10 mM Tris-HCl pH 9.0, 50 mM KCl, 1.5 mM $MgCl_2$) (New England Biolabs, Pickering, ON, Canada). The amplification was performed in a Bio-Rad S1000 thermal cycler. Thermal cycling included an initial denaturation at 95 °C for 4 min, 30 cycles of denaturation at 95 °C for 30 s,

annealing at 57 °C for 40 s and extension at 72 °C for 1 min and a final extension at 72 °C for 4 min. The PCR products were purified with the EZ-10 Spin Column PCR Purification Kit (Bio Basic Inc., Markham, ON, Canada) and visualized as described above.

For prokaryote-specific PCR, the universal primers U341F (5'- CCTACGGGAGGCAGC AG-3') and U758R (5'-CTACCAGGGTATCTAATCC-3') were used (Ronan et al., 2013) to amplify a 418-bp fragment corresponding to the variable V3 and V4 regions of the 16S rRNA gene sequence in *Escherichia coli*. PCR reactions were denatured at 96 °C for 5 min with thermocycling at 94 °C for 1 min. An initial annealing temperature of 65 °C was lowered by 1 °C every cycle for a total of 20 cycles, using an elongation time of 3 min at 72 °C. An additional 15 – 20 cycles were performed with a 55 °C annealing temperature and visualized as described above.

The positive controls for each DNA isolation procedure and PCR reaction were pure cultures of *Bacillus simplex* and *Cryptococcus magnus*.

For the isolation of culturable bentonite microbiota, four similar bentonite slurries were mixed in 50 mL Schott bottles, in triplicate:

1) 1 g as-received, uncompacted bentonite in 15 mL sterile dH_2O, shaken (orbital shaking, room temperature, 300 rpm) for 10 min, 1 h and 10 h,
2) 1 g as-received, uncompacted bentonite in 15 mL buffer (pH 7.0), shaken for 10 min, 1 h and 10 h,
3) 1 g as-received, uncompacted bentonite in 15 mL *Bacillus simplex* and *Cryptococcus magnus* culture (about 10^6 cells/mL dH_2O), shaken for 10 h, and

4) 1 g as-received, uncompacted bentonite in 15 mL *Bacillus simplex* and *Cryptococcus magnus* culture (about 10^6 cells/mL buffer, pH 7.0), shaken for 10 h.

Each slurry was vortexed and 5 mL aliquots transferred to 15 mL Falcon tubes and sonicated for 30 min. Optimization of sonication times for cell removal agreed with the results of Mermillod-Blondin et al. (2001). A dilution series of the various samples were plated (1 mL/plate) on Tryptic Soy Agar and R2A for the isolation of bacteria, and YMA and 10% YMA for the isolation of eukaryotes. Plates were incubated for 2-5 days at room temperature and cell counts were compared between treatments. Yeast Malt Agar (3 g/L Malt Extract, 3 g/L Yeast Extract, 10 g/L Dextrose, 5 g/L Peptone, 15 g/L Agar), Tryptic Soy Agar (3 g/L and 15 g/L Agar) and R2A (18.2 g/L R2A and 15 g/L Agar) media were made in distilled water, according to Atlas (2004), with chemicals purchased from Sigma Aldrich (Oakville, ON, Canada). The potassium dihydrogen orthophosphate/sodium hydroxide buffer system was used to buffer the bentonite to a pH of 7.0.

2.4 Results

2.4.1 Localization of microbiological pH and redox fluctuations in bentonite

Methods were assessed for the localized measurement of bentonite pH and redox. Resazurin was used to monitor site-specific redox fluctuations within bentonite, with the aim of linking it to sulphide precipitation, gas generation and pH fluctuations in long-term (9 week) microcosms. Long-term resazurin incubation was effective for visualizing overall microbial activity within bentonite, since autoclaved controls showed no reduction (Fig 2.2A1); whereas, natural bentonite

microcosms incubated with resazurin were visibly reduced (Fig 2.2A2-3). Similarly, resazurin demonstrated bentonite reduction near sites of obvious gas generation, which was often seen to occur near zones of sulphide precipitation (Fig 2.2B). However, the pre-mixed indicator color faded over time and with depth in the bentonite (e.g., with distance from the air- water interfaces) (Fig 2.2A1-3). Notably, sulphide rarely precipitated in long-term microcosms pre-mixed with resazurin, despite the reduction-oxidation potential being lowered by microbial activity. In bentonite microcosms incubated with sterile tap water, sulphide precipitate was seen in 20% of the samples after 9 weeks (Fig 2.2A4), whereas 80% of the samples showed no sulphide precipitate (Fig 2.2A5). In contrast, in bentonite microcosms incubated with resazurin, sulphide precipitate was evidenced in only 1% of the samples after 9 weeks. This suggests that long-term bentonite incubation with resazurin limits SRB activity, influencing community dynamics. Thus, addition of resazurin post-incubation was assessed for evaluation of localized microbial activity in bentonite.

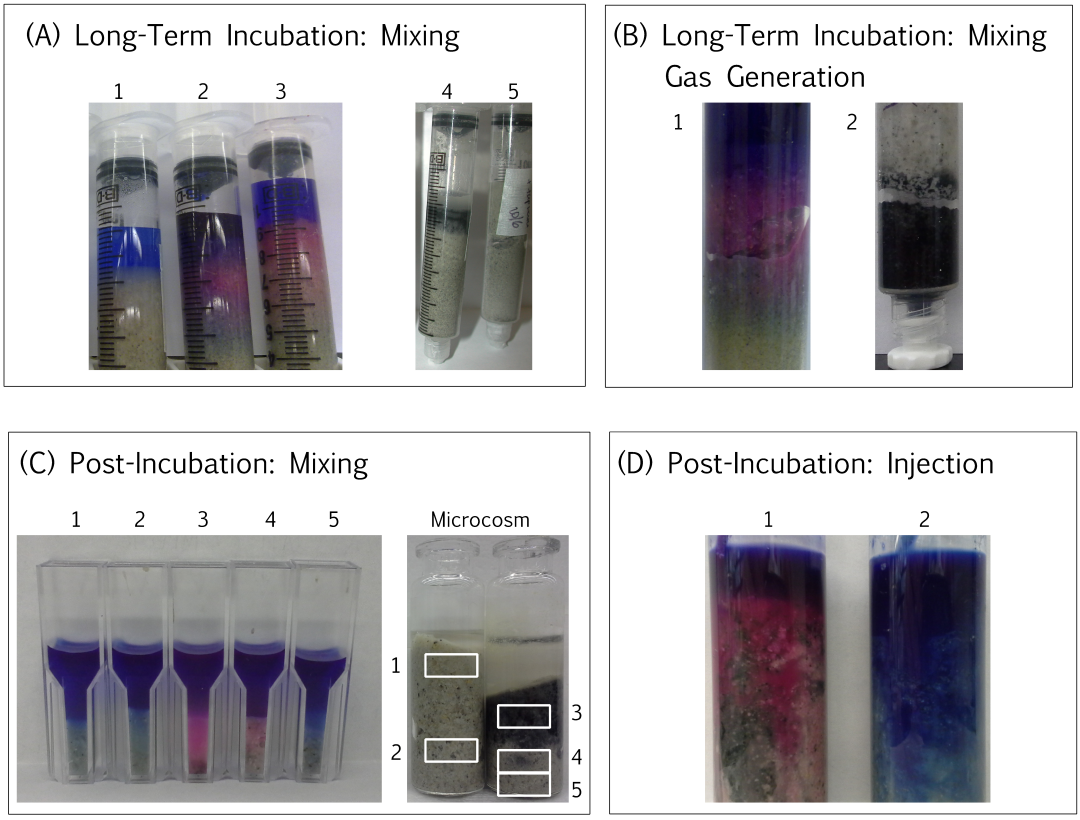

FIG 2.2 Resazurin for the localization of microbial activity in bentonite microcosms. Microbial activity, as detected by sulphide precipitation, took 9-12 weeks to develop (A4 and A5). Resazurin was explored as a tool for localizing microbial activity in relation to sulphide precipitate (A2 and A3), as compared to sterile autoclaved controls (A1). Resazurin was mixed with bentonite prior to incubation (A and B). Post-incubation removal of bentonite layers from the microcosm, and subsequent addition to resazurin was the most effective tool for localization of bentonite reduction (C), as opposed to post-incubation addition to microcosms by syringe pressure (D).

Resazurin was added to the water phase of microcosms incubated for 9 weeks, and forced into the bentonite using syringe pressure. The colorless state, which had progressed through blue and

pink, of the injected resazurin (compared to the pink or blue color in other regions) indicated that a redox potential of lower than <-111 mV had been attained in zones of sulphide precipitate, as opposed to bentonite microcosms without sulphide precipitate (Fig 2.2D). However, precise localization was somewhat compromised, as mixing and diffusion occurred due to the syringe pressure. The final, most successful, attempt at localization involved the removal of consecutive bentonite layers using a fine spatula, and adding them to separate cuvettes with resazurin (0.006 g/L). This allowed for the relative, localized association of precipitated sulphide and reduction within bentonite microcosms (Fig 2.2C).

The localization of zones of different pH was similarly performed via the consecutive, layered removal of bentonite from microcosms followed by addition to water or a buffer. Distilled water or $CaCl_2$ is commonly used for soil pH measurements (Henderson and Bui, 2002). A $CaCl_2$ buffer is often preferred, since soil solution electrolyte concentration influences pH measurements. The optimal $CaCl_2$ concentration has been shown to be 0.01 M. However, the critical consequence of these studies is that standardization is necessary, and an optimal method needs to be selected for individual soil types. These two solutions were compared for as-received bentonite, as well as active (+ sulphide precipitate) and inactive (- sulphide precipitate) long-term bentonite microcosms (9 weeks, Table 2). The use of a $CaCl_2$ solution influences the measurement of soil pH, and the difference between measurements in dH_2O and $CaCl_2$ is not linear (Henderson and Bui, 2002). This work also suggested that the methods were significantly different, more so in the as-received bentonite at higher pH than in long-term microcosms with lower pH (Table 2). Lower standard deviation was associated with $CaCl_2$, chosen for further studies.

TABLE 2.2 Bentonite pH measurements. Water and a 0.01 M solution of $CaCl_2$ were compared for the measurement of bentonite pH (means and standard deviations of triplicate samples) in saturated microcosms. 'Active' and 'Inactive Zones' refer to the respective regions of long-term (9 week) microcosms with and without iron sulphide precipitate, 'Control' refers to long-term microcosms without any pyrite precipitate, and 'As-Received' refers to two different batches of Wyoming MX-80 bentonite mixed immediately prior to pH measurement.

	Active Zone Microcosms	Inactive Zone Microcosms	Control Microcosms	As-received Bentonite (Batch 1)	As-received Bentonite (Batch 2)
dH_2O	8.00 ± 0.10	9.00 ± 0.11	9.01 ± 0.10	9.90 ± 0.11	9.94 ± 0.12
$CaCl_2$	7.82 ± 0.08	8.92 ± 0.09	8.80 ± 0.10	9.42 ± 0.10	9.65 ± 0.09

Thus, for localization studies, consecutive, layered removal of bentonite, with subsequent measurement of redox and pH, was optimal. Reduction zones were best visualized with post-incubation addition of bentonite to resazurin (0.006 g/L). A $CaCl_2$ buffer was selected as the method of choice for the localization of pH fluctuations in bentonite (67g/L).

2.4.2 Sulphide Measurements: Methylene Blue and Fluorometry

The Methylene Blue technique quantified soluble sulphides in the phases in which precipitated sulphide, redox and pH were measured (active and inactive zones of long-term bentonite microcosms). The addition of bentonite to a sulphide standard curve decreased the slope (m =

0.0006; m= 0.059, where m is the slope of sulphide absorbance against concentration with and without bentonite, respectively) within the range of 0-5 mM NaS (Fig 2.3), suggesting that bentonite adsorbs sulphides. Soluble sulphide measurements in experimental bentonite microcosms were compared to a standard curve without bentonite, since any soluble sulphide measured within microcosms would be equilibrated in solution and not bound to bentonite.

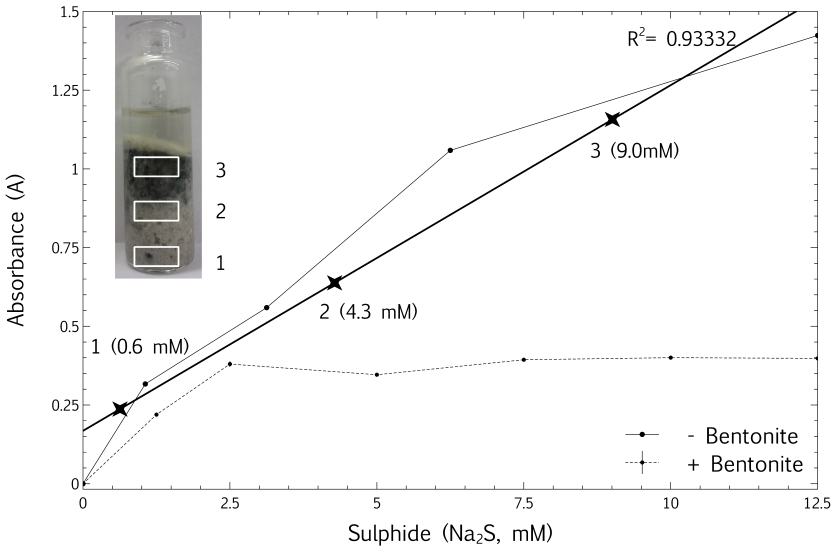

FIG 2.3 Methylene Blue for the localization of soluble sulphide in bentonite microcosms: standard curves and microcosm localization. A standard curve for the colorimetric measurement of soluble sulphide (NaS) was compared to a standard curve with the addition of 100 g/L bentonite. Points represent the mean of triplicate samples and bars represent the standard deviation. Samples (1) 0 precipitate, (2) + precipitate and (3) +++ precipitate, were removed in layers from an active, long-term (9 week) bentonite microcosm and plotted on the standard curve for comparison.

Fluorometry was investigated as a technique for measuring precipitated sulphide in bentonite. It was shown that FeS diminished the natural autofluorescence of bentonite, with increasing FeS concentrations leading to decreasing fluorescence emission at 350 nm, when excited at 300-400 nm (Fig 2.4.1). The log transformation of this data showed a strong negative correlation (Fig 2.4.2, A: $R^2 = 0.908$; B: $R^2 = 0.901$). However, the standard deviation was high, more so if the experiment was repeated on different days (Fig 2.4.2A), as opposed to triplicate samples conducted on one day (Fig 2.4.2B). This was attributed to the sedimentation tendency of bentonite. Mixed bentonite settles quickly, with increasing sedimentation occurring at higher FeS concentrations. Thus, the bias of mixing prior to fluorometric assessment inevitably leads to measurement bias.

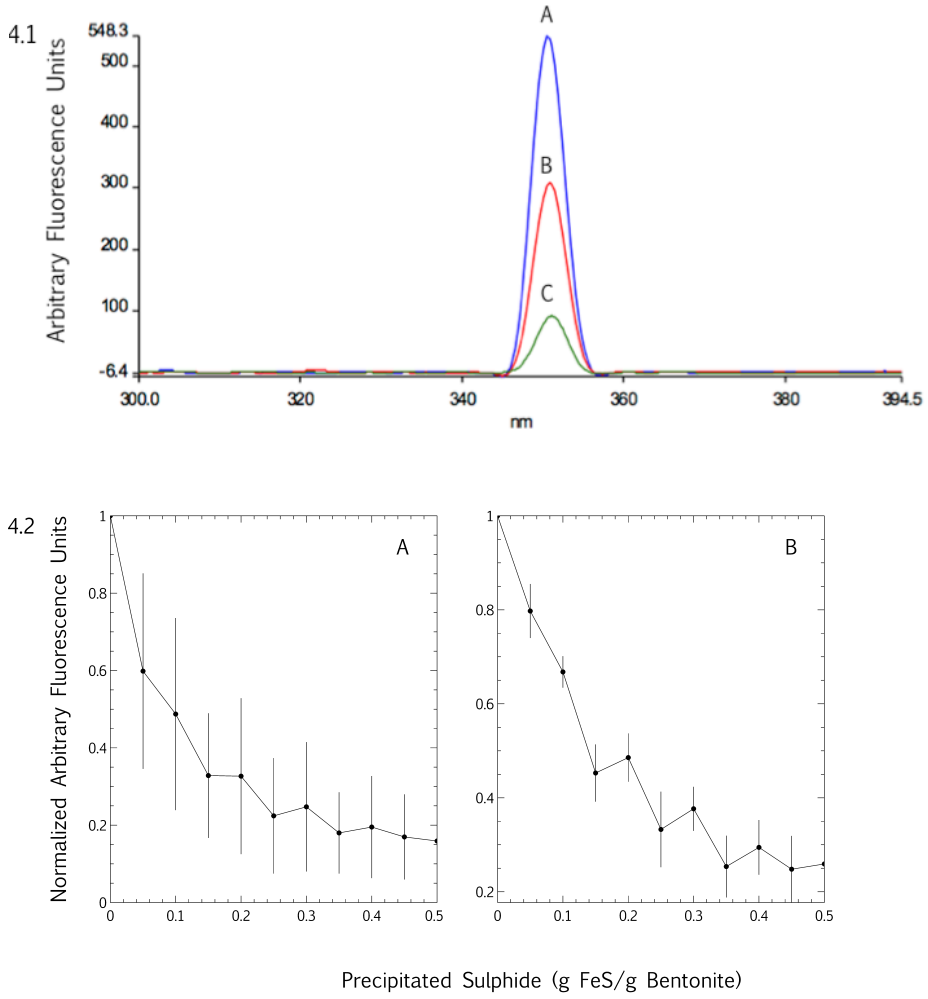

FIG 2.4 Fluorometry for the localization of sulphide precipitation in bentonite microcosms: standard curves. Bentonite is autofluorescent, and thus emits fluorescence over a wide range of excitation wavelengths. (2.4.1) The autofluorescent emission peak of bentonite at 350 nm excitation was compared at (A) 0, (B) 2.5 and (C) 5 g FeS/g bentonite. (2) The log transformation of this data showed a strong negative correlation (2.4.2, A: $R^2 = 0.908$; B: $R^2 = 0.901$). The standard deviation of the means of measurements taken on different days (2.4.2A) was compared to the means of measurements taken on the same day (2.4.2B). Points represent means of triplicate samples, with bars indicating the standard deviation.

Salinity also influences sedimentation of saturated bentonite (Fig 2.5), and is pivotal as natural groundwater in some DGR host rock environments is highly saline (Vilks, 2009). If mixing is consistent and thorough, salinity does not influence the correlation between the log transformation of autofluorescence emission vs sulphide concentration (R^2 = 0.9078), but the slope of the fluorescence units against sulphide concentration is decreased (Saline: m= -0.27; Non-saline: m= -1.95). Thus, a saline standard curve is necessary for the measurement of sulphides in saline bentonite environments. Samples from active zones of long-term (9 week) microcosms were significantly (t statistic=32.706, df=6, $p<0.05$) lower than samples from inactive zones of the same microcosms, and inactive microcosms (Fig 2.6).

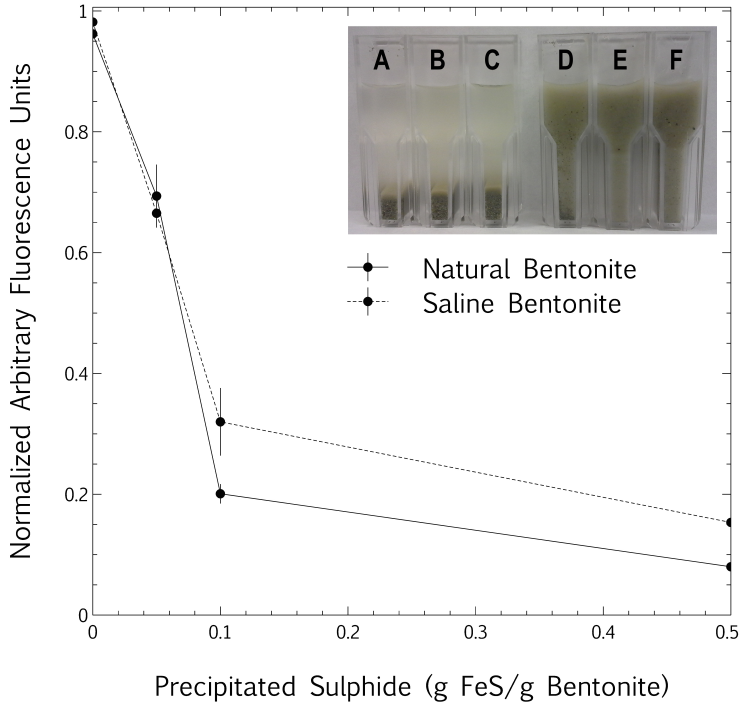

FIG 2.5 The influence of salinity on the measurement of FeS inhibition of bentonite autofluorescence. Although salinity increased the sedimentation of saturated bentonite (insert A-C: bentonite suspended in saline (200 g/L NaCl) water; insert D-F: bentonite suspended in non-saline (0 g/L NaCl) water), upon thorough mixing directly prior to absorbance measurement, it did not influence the correlation between the log transformation of this graph (R^2 = 0.908). However, the line describing autofluorescence versus FeS concentration had a larger negative gradient under non-saline conditions (Saline: m= -0.27; Non-saline: m= -1.95). Points represent means of triplicate samples, with bars representing the standard deviation.

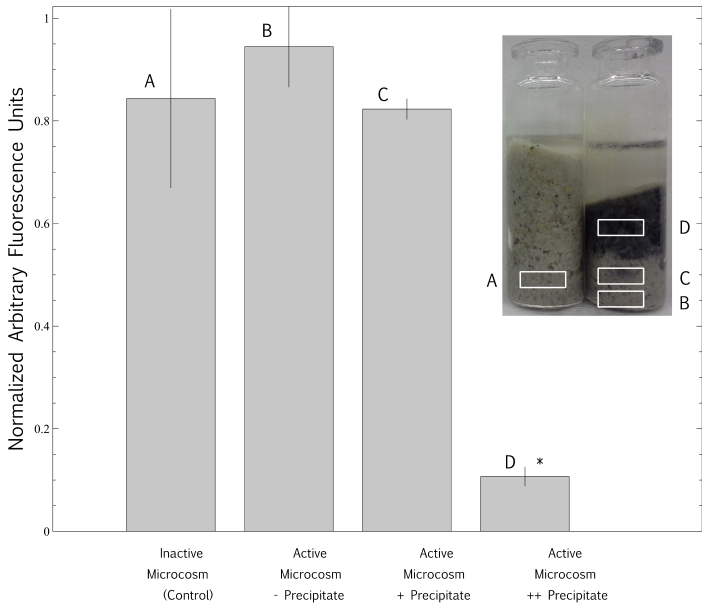

FIG 2.6 Fluorometry for the localization of sulphide precipitation in bentonite microcosms. Fluorometry was used to compare the sulphide concentrations in different zones in long-term (9 week) bentonite microcosms. 'Active Microcosm' refers to a microcosm in which visible sulphide precipitate was evident, confirmed with pH and redox decreases. 'Inactive Microcosm' refers to a bentonite microcosm incubated for the same period of time, in which no precipitated sulphide was visible, confirmed with pH and redox stability. The qualitative, visible amount of precipitate in the layers of active microcosms is relatively represented by – (0), + and ++. Columns represent means of triplicate samples and bars represent standard deviation.

Fluorometry was an effective tool for relative measurements of localized precipitated sulphides within the bentonite matrix. Bias and variation due to sedimentation of bentonite suggests that the value of this tool lies in relative assessments, rather than absolute sulphide measurements and necessitates thorough mixing and standard curves designed for each experiment.

2.4.3 Metabolic Measurements in a Desiccated Bentonite Environment: Bentonite as a CO_2 Sink

The rate of CO_2 production by a microbial community is an indicator of metabolic activity, and may be measured *in vitro* using CEMS (Kroukamp and Wolfaardt, 2009). By operating CEMS in a closed-loop design (Bester et al., 2010), CO_2 accumulation may be measured rather than single-pass CO_2 production, significantly lowering the detection limit for CO_2 and permitting studies of even slowly-metabolizing microbial communities.

CEMS was assessed for the measurement of microbial activity at bentonite-air interfaces for discrete conditions of desiccation (i.e., an RH value of 75 %; Fig 2.7.1). Upon desiccation of active bentonite microcosms, and subsequent 48 h incubation at 75 % RH, slopes of the CO_2 accumulation graphs were higher in active microcosms than in sterile controls. The negative gradient in sterile controls demanded an investigation of bentonite as a CO_2 sink. Thus, CEMS was used to evaluate the basic bentonite matrix as a CO_2 sink, before utilizing the system to understand microbial CO_2 generation and complex carbon cycles in this matrix.

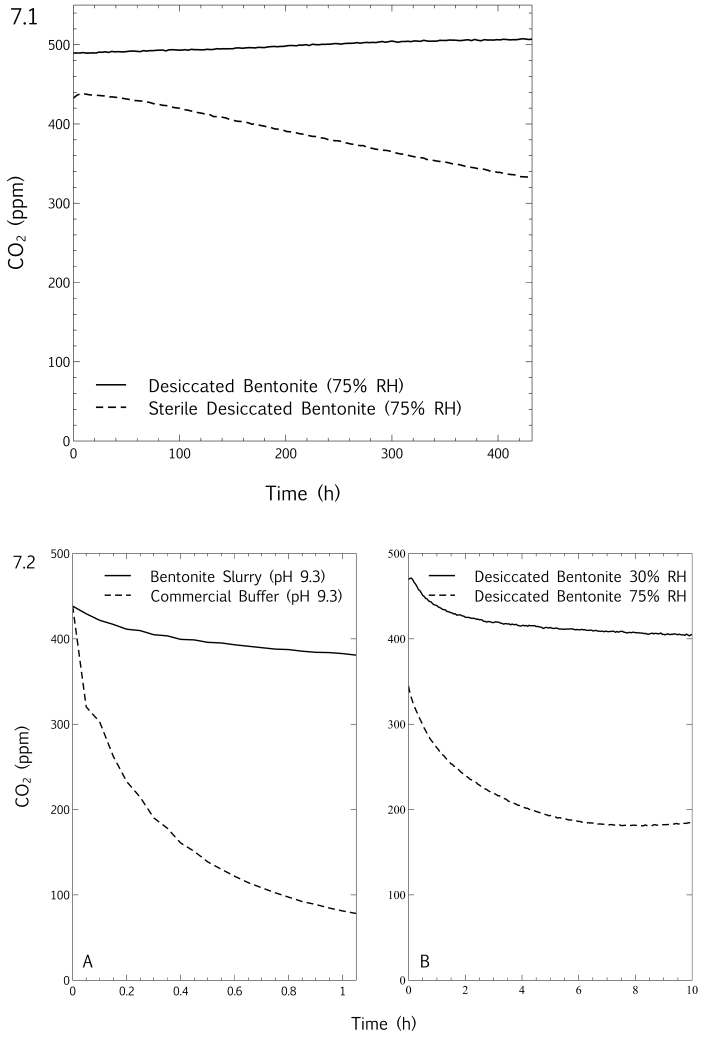

FIG 2.7 CEMS for the measurement of microbial metabolic activity in a saturated and desiccated bentonite matrix. Bentonite saturated with sterile tap water was incubated for 2 weeks, and desiccated. Metabolic activity after 48 h of desiccation, quantified as CO_2 accumulation in a closed-loop system, was compared to sterile controls (7.1). Based on the negative gradient of the sterile control (a decrease in the atmospheric CO_2 levels in the system over time), the CO_2 adsorption capacity of bentonite was assessed (7.2). The CO_2 equilibration in a natural bentonite slurry (pH 9.5) was compared to a commercial buffer solution of pH 9.5 (sodium bicarbonate/sodium hydroxide). Similarly, the CO_2 equilibration in the CEMS system

was compared between 20 g of as-received, dry bentonite incubated for 1 year at 30 % RH and 75 % RH, respectively.

Adding a basic buffer (pH 9.5) to a closed-loop CEMS system, pre-equilibrated to atmospheric CO_2 levels (440 ppm) caused a drop in CO_2 levels as the carbon re-equilibrated as CO_3^- in solution (Fig 2.7.2A). The same volume of bentonite, with the same natural pH, demonstrated a similar capacity as a CO_2 sink; however, equilibrium was reached at a higher CO_2 concentration (390 ppm, as opposed to 100 ppm in the commercial buffer). The CO_2 concentrations were negatively-correlated with time after log transformation (Buffer: $R^2 = 0.95 \pm 0.020$; Bentonite: $R^2 = 0.94 \pm 0.005$) and the buffer slope ($\log[CO_2(ppm)]$ vs time) mean ($m = -0.54 \pm 0.03$, where m is the mean of triplicate slopes) was significantly steeper than the bentonite slope ($\log[CO_2(ppm)]$ vs time) mean ($m = -0.07 \pm 0.006$, $p < 0.05$, t statistic = -37,2, df=4), suggesting a greater capacity as a CO_2 sink.

Similarly, desiccated bentonite incubated for 1 year at 75 % RH had a greater capacity as a CO_2 sink compared with the same volume of bentonite similarly incubated at 30 % RH (Fig 2.7.2B). Bentonite is hygroscopic, suggesting that ambient gaseous CO_2 is soluble in the water bound hygroscopically to the bentonite.

Thus, CEMS is useful for measuring microbial activity in desiccated bentonite; however, the capacity of bentonite as a CO_2 sink needs to be taken into account when assessing carbon cycles in a bentonite environment. Even in desiccated bentonite, relative humidity had an impact on CO_2-CO_3^- equilibration at bentonite-air interfaces. Therefore, controls are essential to normalize

for such effects when investigating microbial contributions to CO_2 cycles in bentonite environments.

2.4.4 The influence of pH on the separation of cells and DNA from bentonite

Bentonite is a notoriously challenging matrix for molecular studies, as DNA has not been successfully removed from Wyoming MX80 bentonite (Mauclaire et al., 2007; Stroes-Gascoyne et al., 2007A). The influence of basic bentonite pH on cell and DNA removal from the matrix was assessed by comparing natural bentonite (pH 9.5) and bentonite buffered at pH 7.0.

After 1h and 10 h of shaking in tap water and buffer (pH 7.0), the final pH of bentonite microcosms was significantly different in both natural and inoculated bentonite, with buffered bentonite remaining stable at around pH 7 and natural bentonite above pH 9. The mean pH of natural bentonite in tap water was 9.28 ± 0.015, whereas the pH of buffered (pH 7.0) natural bentonite stabilized at 7.12 ± 0.025. The mean pH of inoculated bentonite in tap water stabilized at 9.11 ± 0.035 and inoculated bentonite in a buffer (pH 7.0) at pH 7.07 ± 0.012.

After 10 min and 1 h of buffering, there was trend of higher cell numbers recovered from natural bentonite than in tap water, but the differences in means were not statistically significant (Fig 2.8.1). In natural and inoculated microcosms after 10 h of mixing, both the eukaryotic and prokaryotic cell numbers were significantly lower (up to 75 %) in tap water than in buffer (Fig 2.8.2A). Thus, neutral buffering of the basic bentonite facilitates the isolation of higher cell numbers from bentonite. It is not clear from this study whether that is due to planktonic growth

at neutral pH, or clay-cell complexing. However, even with high cell numbers (up to approximately 10^6 cells/mL) and neutral pH, no DNA extractions were successful (Fig 2.8.2B). Single DNA copies can be amplified by PCR; thus, PCR confirmed that no DNA was present below the visible detection limits of the UV stain. Since all DNA extraction and PCR attempts were unsuccessful, despite pH changes and cell number changes, only one sample image of a DNA extraction was included (Fig 2.8.2B).

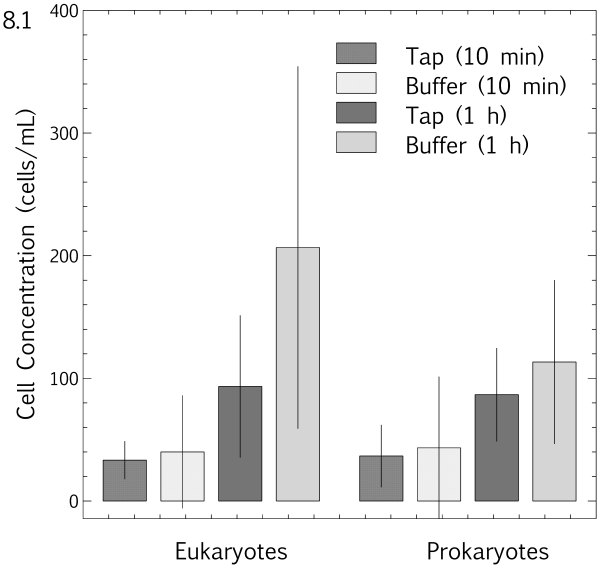

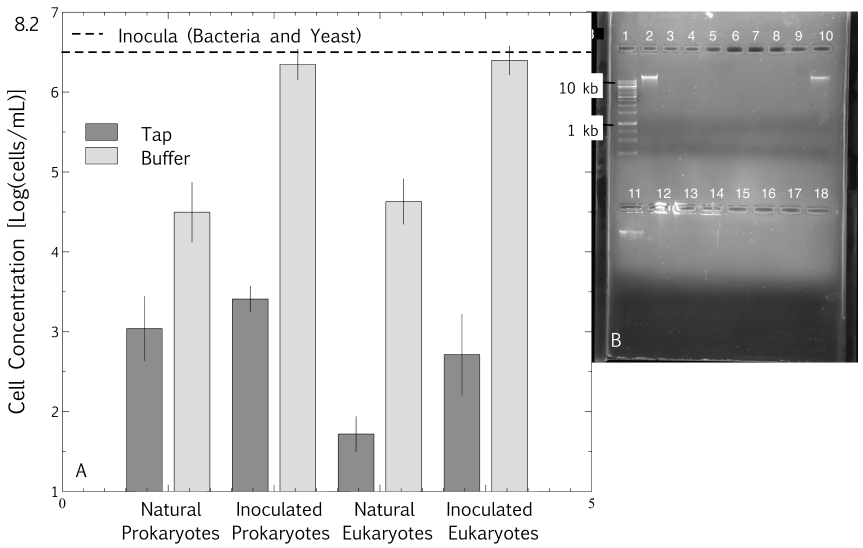

FIG 2.8 The influence of pH on cell recovery and DNA extraction from bentonite microbial populations. Saturated natural bentonite was incubated with sterile tap water and buffer (pH 7.0, sodium tetraborate/sodium hydroxide) for 10 min and 1 h, and cell concentration compared (8.1). Columns represent means of triplicate samples, and bars represent standard deviation. Saturated natural (bentonite) and inoculated (bentonite + approximately 10^6 CFU/mL) microcosms were incubated for 10 h in sterile tap water and buffer (pH 7.0, sodium tetraborate/sodium hydroxide). Prokaryotic and eukaryotic cell numbers were significantly lower after plating bentonite saturated with tap water than in bentonite buffered at pH 7.0, for both inoculated and natural microcosms (8.2A). No DNA was successfully isolated from any bentonite microcosms (8.2B). The gel is representative of some of the DNA extractions performed on bentonite. Lanes include (1) DNA ladder, (2, 10, 11) positive controls, (4, 9) negative controls, (3, 5-8, 12-18) bentonite DNA extractions.

2.5 Discussion

The study of microbial ecology in extreme environments and atypical matrices demands a toolbox outside the traditional genomics, proteomics and metabolomics that have found overwhelming popularity in microbiology. Highly-compacted bentonite proposed for use in a DGR provides a number of such challenges to the study of microbial ecology. Thus, alternative methods with novel twists were evaluated to expand the range of tools available to measure potential microbial processes in a DGR.

Repository interfaces were identified as regions of potential microbial activity warranting further study. The reduction of sulphur by SRB, and consequent production of corrosive species that can diffuse through the bentonite and cause corrosion of the copper canisters surrounding the CANDU bundles, is the primary microbiological concern within a DGR. The swelling of compacted bentonite upon saturation limits water activity and space sufficiently for microbial suppression within a DGR (Masurat et al., 2010; Stores-Gascoyne et al., 2010). However, compaction any lower than 1.6 g/cm^3 at pore water salinities <50 g/L may lead to an increase in microbial numbers upon saturation (Stroes-Gascoyne et al., 2010). A nearly-sterile zone is expected to form at the container-bentonite interface due to high temperature and radiation. However, the heat of used nuclear fuel emplacement may lead to moisture cycles, with the non-uniform drying of the bentonite barrier potentially introducing transient microenvironments of non-uniform pressure at bentonite-rock interfaces, possibly allowing for microbial activity and growth (Pedersen 2010; Stroes-Gascoyne et al., 2011). Thus, tools are needed to study: (1) the potential for microbial activity at bentonite-air interfaces during moisture cycles, and (2)

localization of microbial activity, specifically, the potential for any activity to compromise bentonite-suppressive parameters such as swell pressure, possibly facilitating a more conducive environment to microbial growth upon re-swelling.

In this study, techniques to address such questions were proposed and evaluated. These included: (1) the localization of microbial activity in saturated bentonite with (a) redox, (b) pH, and (c) sulphide measurements, (2) the measurement of microbial activity at bentonite-air interfaces using CO_2 Evolution Measurement Systems (CEMS), and (3) the influence of pH on the separation of cells and DNA from the bentonite matrix.

Ideally, minimally invasive methods for the localization of pH and redox potential in bentonite microenvironments would involve the use of probes, particularly microelectrodes (Babauta et al., 2012), commercially-available down to tip sizes of 2.5 μm (Unisense, Denmark; World Precision Instruments, Sarasota, FL, USA). However, there are two major obstacles to the use of microelectrodes for microbial studies in bentonite: the physical fragility and cost of the instrument. The fragility of costly microelectrodes would likely not withstand the pressures generated by the swelling of highly compacted bentonite upon saturation (>2 MPa). Thus, alternative robust and accessible methods were investigated for the localization of microbial activity within the bentonite matrix.

The layered removal of bentonite and subsequent addition to resazurin was most efficient for local measurement of redox potentials within microcosms (Fig 2.2C). Color change from blue to pink indicates the first, irreversible stage of reduction, whilst further development of the pink to colorless state indicates the second, reversible stage of reduction. The endpoint analysis of this

color change was selected over the more attractive *in situ*, real-time use of pre-mixed indicator, as long-term incubation with resazurin influenced community dynamics within the bentonite. The precipitation of FeS, a visible indicator of SRB activity, occurred in 20 % of bentonite microcosms incubated long-term (9 weeks) in tap water (Fig 2.2A4, 5). In contrast, sulphide precipitation only occurred in 1 % of the bentonite microcosms incubated long-term with resazurin (Fig 2.2A1-3, 2B). Despite the absence of sulphide precipitate, resazurin reduction did occur during long-term incubation in bentonite microcosms, often localized around sites of gas generation (Fig 2.2A2, 2B); whereas, resazurin was not reduced in sterile controls (Fig 2.2A1). This suggests that resazurin was not inhibitory to bentonite microbial activity, but did cause a shift in community composition away from SRB. Since communities are driven by energy flow and thermodynamic competition for available electron donors and acceptors (North et al., 2004), and the resazurin-resorufin indicator functions on the key property of electron transfer (Gonzalez-Pinzon et al., 2012), it is not surprising that it influences long-term microbial community dynamics. Similarly, due to interference in the electron transfer chain, resazurin is typically avoided in microbial energy transfer studies (Mathis et al., 2008; Bond et al., 2002). In addition to its influence on the electron transfer chain in a microbial community, resazurin has been shown to be bactericidal against some pathogens via unknown mechanisms, potentially including intercalation of DNA similar to acridine (Schmitt et al., 2013). Resazurin end-point analysis (Fig 2.2A) was performed aerobically, since the aim was to hone techniques that were simple and accessible. However, upon removal of microcosm layers, the anaerobic clay is exposed to atmospheric oxygen, which would influence the redox potential. Thus, this technique would be even more efficient within an anaerobic chamber.

Similarly, layered bentonite removal and subsequent addition to $CaCl_2$ was most efficient for the localization of pH within the bentonite matrix, using an unusually high 15:1 buffer:soil ratio (67 g/L) due to the clay swell capacity of bentonite. $CaCl_2$ buffers are popular for soil pH measurement, as they reduce the impact of electrolytes (positive and negative ions other than H^+/OH^-) on the measurement of the pH. This is relevant in soils with a charged surface, supported here with lower variation in the buffered solution (Schofield and Taylor, 1955).

Methylene Blue is common for sulphide measurement, quantifying aqueous sulphide by comparing samples to a colorimetric standard curve of Na_2S. However, the addition of bentonite to a standard curve (and subsequent removal by centrifugation prior to the last step) lowers the gradient of the curve tenfold, below 5 mM (m = 0.0006; m= 0.059, with and without bentonite, respectively), suggesting that bentonite adsorbs sulphide (Fig 2.3). Experimental microcosm sulphide was quantified against a standard curve without bentonite, as the sulphide quantified with this technique is in the aqueous phase, already in equilibrium with the bentonite.

Sulphides are also precipitated as a wide variety of compounds including pyrite, mackinawite and greigite (Hunger and Benning, 2007; Rickard and Morse, 2005). These species are important in sulphur cycling, providing useful localization information of phase transformation of clay minerals in the bentonite matrix. Thus, a tool was evaluated for the quantification of precipitated sulphide in bentonite. The inhibition of background fluorescence by the production of FeS has been modelled as a tool for the rapid quantification of SRB in the cold storage of fish. A similar principle was investigated for the relative quantification of precipitated sulphide species due to SRB activity in bentonite. The inhibition of bentonite autofluorescence at 350 nm excitation (Fig

2.4.1) was plotted as a function of FeS in a bentonite solution (Fig 2.4.2). The log transformation showed a strong negative correlation (A: $R^2 = 0.908$; B: $R^2 = 0.901$). Bentonite sedimentation in solution is influenced by sulphide concentrations and salinity, introducing bias and variation in this technique, as indicated by the high standard deviation (Fig 2.4.2 and 2.5). A fluorometer equipped with a stirrer may decrease this variation. Salinity had little influence on the negative correlation of the log of this data ($R^2 = 0.9078$), but decreased the fluorescence vs sulphide concentration slope by almost ten-fold. Thus, a saline standard curve is necessary for the measurement of sulphides in saline bentonite environments. Samples from active zones of long-term (9 week) microcosms demonstrated significantly greater precipitated sulphide concentrations with this technique (t statistic=32.706, df=6, $p<0.05$), proving the usefulness of the tool (Fig 2.6). It is recommended that it be employed for relative studies and standard curves are set up immediately prior to the experiment, tailored for specific experimental normalization (i.e., salinity, concentration of bentonite and length of microcosm incubation).

In contrast to saturated bentonite, microbial activity at bentonite-air interfaces demands unique techniques. The measurement of CO_2 accumulation as an indicator of microbial activity is effective (Fig 2.7.1) if the capacity of bentonite as a CO_2 sink is considered, as suggested by the negative gradient of the sterile control. In solution, high pH causes the speciation of CO_2 to carbonates via bicarbonates, shifting the CO_2 equilibrium in solution and stimulating the transfer of CO_2 (air) to CO_2 (aq) (Fig 2.7.2A; Mulder, 1996). Saturated bentonite (pH 9.5) shows a similar shift from CO_2 in the gaseous phase to the aqueous phase, although the equilibrium was 300 ppm lower than a buffer at the same pH (9.5). This suggests that other physico-chemical parameters influence the CO_2 sorption capacity of saturated bentonite, such as dilution and

diffusion. Desiccated bentonite incubated at both 30 % RH and 75 % RH absorbed CO_2, with equilibrium approximately 2 times lower at 75 % RH (Fig 2.7.2B). Thus, CO_2 is likely solubilized in the liquid adsorbed to the hygroscopic clay during incubation at higher RH, a parameter that needs to be considered when measuring microbial activity at bentonite-air interfaces.

Although the development of metabolic tools is useful, the additional use of genomics in the bentonite matrix would be desirable for linking community composition and functionality. Thus, the influence of pH on the complexing of cells and DNA to the Na/Ca-montmorillonite clay matrix was investigated. DNA is highly-adsorbed to smectite, dependent on the concentration and valency of the montmorillonite cations (Paget et al., 1992). Similarly, cell walls and cell envelopes are adsorbed to smectite and kaolinite clays, likely due to multivalent metal cation bridging (Walker et al., 1989). It was investigated whether buffering the bentonite would influence such multivalent cation bridging by increasing the positive ionic strength of the solution. The buffering of bentonite at pH 7.0, as opposed to natural bentonite pH (9.5), showed an increasing trend in the isolation of natural bentonite microbiota within the first hour of incubation (Fig 2.8.1), and significantly increased the cell concentration of both prokaryotes and eukaryotes recovered from the natural bentonite matrix by up to 75 % after 10 h of shaking (Fig 2.8.2A). Similarly, the prokaryotic and eukaryotic populations isolated from inoculated bentonite were also over 50 % higher if buffered at pH 7.0 for 10 h. It was unclear whether these higher cell numbers were due to planktonic growth alone, or release of cells from cell-clay complexes. Although the buffer stabilized the bentonite at pH 7.0 within an hour, potential exchange with clay-cell complexes may be time-dependent. Nevertheless, neither the physical buffering of

bentonite at pH 7.0 nor higher cell concentrations resulted in successful isolation of DNA from the bentonite matrix (Fig 2.8.2B). Thus, there may be elements within the clay matrix that prevent the successful isolation of intact DNA, such a DNases that degrade isolated DNA, or more tightly-complexed DNA-clay compounds that negatively affect the extraction protocol.

A number of tools were optimized for the quantification and localization of microbial activity in the bentonite matrix. Such tools could be applied to analyze bentonite samples from laboratory experiments that simulate the repository environment and from underground demonstration experiments. These metabolic tools are useful for relative measurements of redox, pH, sulphide and CO_2 metabolism, rather than absolute measurements. It must be considered that microbes could change the properties of clay (dry weight:wet weight ratio) through the conversion of smectite to illite (Liu et al., 2012; Mulligan et al., 2009). Thus, careful controls and experimental design are necessary to employ these techniques. However, these tools are cost-effective and simple, and should facilitate the exploration of microbial activity within the low-biomass bentonite environment for applications in nuclear waste management, as well as the broader fundamental fields of extreme desiccated microbiology and biogeochemical cycling.

2.6 Acknowledgments

The authors would like to acknowledge the Nuclear Waste Management Organization and the Natural Sciences and Engineering Research Council of Canada for funding the research. WS received scholarships from the Ontario Trillium Foundation of Canada and the National Research Foundation of South Africa. All funding sources had no role in the collection and

interpretation of data, or writing of the manuscript. The NWMO reviewed the manuscript in support of submission for publication. Dr. Alexander Grigoryan and Daphne Jalique (University of Saskatchewan) are thanked for discussions and collaborative advice regarding the methylene blue sulphide protocol and DNA extractions.

CHAPTER 3

Microbial Metabolism in Bentonite Clay:

Saturation, Desiccation and Relative Humidity

Chapter 3 has been accepted for publication in the *Journal of Applied Clay Science* as Stone, W., Kroukamp, O., McKelvie, J., Korber, D. R., & Wolfaardt, G. M. Microbial metabolism in bentonite clay: Saturation, desiccation and relative humidity.

3.1 Abstract

Within a Deep Geological Repository for used nuclear fuel storage, compacted bentonite clays are the candidate buffer due to their physical and rheological properties, and their ability to suppress microorganisms. This study focused on the potential for microbial metabolism at bentonite-air interfaces, the influence of relative humidity (RH) and the consequences of metabolic activity on bentonite. Microbial activity, determined by monitoring the concentration of evolved CO_2, was sustained at desiccated bentonite-air interfaces at 75% RH (0.6 ppm CO_2/min after 5 days of dessication) but was completely suppressed at 30% RH. Conversely, microbial survival was promoted in dry bentonite, with culturable cell survival up to 3 times higher at lower RH (30%) than higher RH (75%). It was also shown that, under water-saturated conditions, microbial sulphur reduction decreased the clay swell index of uncompacted bentonite, swelling approximately 2.7 cm/(g dry weight) less than controls. Notably, natural groundwater salinities were shown adequate to suppress all microbial activity under both saturated and desiccated conditions, confirming that a combination of high bentonite dry density and high salinity inhibits microbial activity, even in microenvironments like surface-air interfaces where swelling pressure limitations may be transiently compromised. Along with the applied need for this knowledge, this study also provided a fundamental opportunity to explore microbial activity in desiccated environments, and suggests that lower RH may promote rapid entry into a dormant cell state and thus more effective long-term adaptation.

3.2 Introduction

Many countries are actively developing deep geological repositories (DGR) for the long-term storage of used nuclear fuel. In Canada, the Nuclear Waste Management Organization (NWMO), mandated by the *Nuclear Fuel Waste Act* (2002), has implemented a site-selection program to develop a DGR in a willing, informed host community (NWMO, 2005; NWMO, 2010). As of 2014, Canada had accumulated approximately 2.5 million CANDU fuel bundles (ca. 50,000 tonnes of heavy metal, t-hm) in reactor site storage, projected to increase to more than 3.4 million fuel bundles (ca. 69,000 t-hm) prior to DGR emplacement (Garamszeghy, 2010). DGR designs rely on engineered and natural barriers to isolate radionuclides. The Canadian engineered barrier system (Fig. 3.1) consists of copper-coated steel used fuel containers (UFC's), containing 48 CANDU bundles each, surrounded by highly-compacted bentonite (HCB) clay. The natural barrier system will be 500 m of overlying low-permeability sedimentary or crystalline host rock. The UFC is designed to provide containment for at least 100,000 years; whereas, the HCB clay and host rock will be relied upon for isolation of radionuclides to one million years.

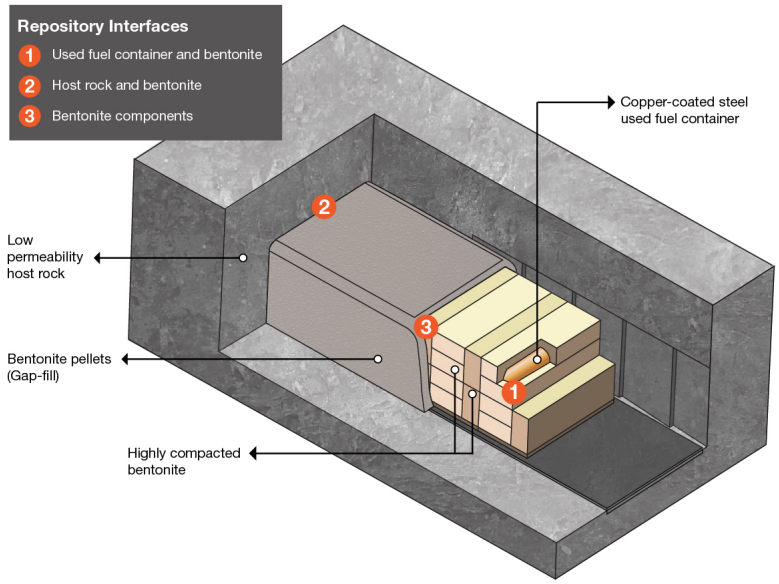

FIG 3.1 The Canadian Engineered Barrier System in a Deep Geological Repository for used nuclear fuel storage. The current Canadian design employs copper used fuel containers as a first barrier for the prevention of radionuclide escape from CANDU fuel bundles, and highly-compacted bentonite (HCB) blocks as a buffer between the used fuel containers and the host rock. The interface between the host rock and HCB is of greatest microbiological interest.

The primary microbiological concern in the DGR is that metabolic sulphide production could cause microbiologically influenced corrosion (MIC) of the UFC's. Highly compacted Wyoming bentonite (MX-80) was the buffer initially selected and designed to physically and chemically protect the UFC's. The fact that the HCB can suppress microbial activity was discovered through research, and the HCB requirements in the NWMO design are now such that the HCB will suppress microbial activity (Fig 3.1; NWMO, 2005). Water activity (a_w) is the key parameter limiting microbial survival in a DGR environment (Stroes-Gascoyne et al., 2010). The HCB compaction and resultant swelling pressure, combined with the natural salinity of groundwater,

are relied upon to limit a_w and prevent MIC (Stroes-Gascoyne et al., 2010; Masurat et al., 2010). Low bentonite porosity and permeability limit transport of metabolites and microbes from the host rock (Sherwood Lollar, 2011) through the bentonite buffer by creating a diffusion-dominated environment (Stroes-Gascoyne et al., 1997; Pedersen, 2010; Hallbeck and Pedersen, 2012).

Saturated, compacted bentonite microbiology has been assessed in terms of aerobic culturable numbers and migration (Stroes-Gascoyne et al., 2010). Compaction of bentonite to a dry density of 1.6 g/cm^3, with a corresponding saturation swelling pressure of >2 MPa and a_w of <0.96, limited culturable microbial numbers to background levels in as-received, powdered bentonite. These limiting parameters, combined with used nuclear fuel heat and radiation, are expected to create a virtually sterile zone in the UFC-HCB buffer interface and its immediate vicinity (Fig. 3.1). However, limiting parameters may not be maintained at HCB buffer-host rock interfaces due to non-homogenous swelling. This warrants further study to determine if these interfaces could provide transient microenvironments conducive to microbial activity (Pedersen, 2010; Stroes-Gascoyne et al., 2011A; Wolfaardt and Korber, 2012).

Although anaerobic Sulphate Reducing Bacteria (SRB) have received the most attention, other potential microbial DGR impacts include weathering of bentonite and gas production (Mulligan et al., 2009). Biofilm formation at HCB-host rock interfaces may affect the transport of radionuclides and metabolites or provide microenvironments that promote microbial survival and activity. Stroes-Gascoyne et al. (2010, 2011A) postulated the occurrence of DGR moisture gradients that would influence microbial activity. Heat from radioactive waste would drive water out of the repository, with subsequent cooling resulting in increased moisture levels. Desiccation would be expected to limit microbial activity, whereas upon saturation, clay swell pressure

would additionally limit a_w and microbial metabolism. During the transition between the dry and wet phase, microbes may have access to water or water vapor without sufficient clay swell pressures to limit activity. Microbial activity in non-uniform microenvironments could lead to the production of extracellular polymeric substances (EPS) and metabolites, changing the properties of the clay matrix.

It is accepted that microbes survive desiccation due to dormancy, a cessation of metabolic processes. DGR microbiology has thus focused on characterizing microbial survival under desiccation, and metabolic impacts within saturated HCB. However, biofilms provide alternative survival strategies during desiccation (Chang et al., 2007) that may sustain metabolism at repository interfaces. As such, the overall objective of this study was to explore the potential for microbial activity at bentonite-air interfaces. The three main questions posed are:

(i) Can microbial biofilms at bentonite-air interfaces metabolize during desiccation under saline and non-saline conditions?

(ii) Does relative humidity (RH) have an effect on microbial metabolism at bentonite-air interfaces?

(iii) Does microbial activity influence the swelling ability of bentonite, a key suppressive attribute?

These questions evaluate potential impacts of microbial activity in DGR interface microenvironments, when limiting parameters may not be maintained during the heat-shrinking and moisture-swelling bentonite gradient.

3.3 Materials and Methods

Microbes: Activity and Survival in Desiccated Bentonite

3.3.1 Isolation and Identification of the Aerobic Culturable Bentonite Microbial Community

Uncompacted Wyoming VOLCLAY MX-80 bentonite powder (American Colloid Company, Wyoming, USA) and compacted bentonite blocks (14.4% water, 1.61 g/cm³ dry density, 1.88 g/cm³ bulk density, 5x5x5 cm, crushed with a spatula for isolations) were stored in sealed bags and handled aseptically. Enrichments involved (1) direct scattering of bentonite powder (0.5 g/plate) on agar media and (2) detaching microbiota from bentonite using sonication. For detachment, 2 g bentonite (100 g/L) was suspended in 20 mL NaCl (8.9 g/L) in 50 mL Falcon tubes, and the resultant slurry sonicated (Branson B3510 Ultrasonic Bath, Danbury, CT, USA; 335 W, 40 kHz, 45 min) according to Mermillod-Blondin et al. (2001). The undiluted slurry (500 µL) was plated on agar media. Eukaryotes were enriched on full- and 10% strength Yeast Malt Agar and ¼ strength Cornmeal Agar. Prokaryotes were enriched on Tryptic Soy Agar (3 g/L) and R2A Agar (18 g/L), all at natural bentonite pH (9.0). Media recipes were according to Atlas (2010) and chemicals purchased from Sigma-Aldrich (Oakville, ON, Canada). Colonies were selected for isolation based on distinctive morphology. Eukaryotes were identified with the universal primers ITS1 (5'-TCCGTAGGTGAACCTGCGG-3') and ITS4 (5'-TCCTCCGCTTATTGATATGC-3') according to White et al. (1990) and Vreulink et al. (2010). Prokayotes were identified with the universal primers U341F (5'- CCTACGGGAGGCAGC AG-3') and U758R (5'-CTACCAGGGTATCTAATCC-3') according to Ronan et al. (2013).

PCR products were sequenced (Centre for Applied Genomics, SickKids, Toronto, ON, Canada) and the online Basic Local Alignment Search Tool (BLAST) was used to detect homology with CBS (Centraalbureau voor Schimmelcultures) and ATCC (American Type Strain Culture Collection) reference and type strains on the NCBI (National Centre for Biotechnology Information) database (http://www.ncbi.nlm.nih.gov/BLAST/). Bacterial, yeast and fungal species of particular interest were selected based on morphology and extremotolerance as described in literature (Table 3.1).

3.3.2 Phylogenetic Identification of Culturable Bentonite Microbiota.

The resulting eukaryotic DNA sequences were manually edited with 4Peaks for Macintosh, Version 1.7.2 (Nucleobytes, Amsterdam, Holland). Consensus sequences were generated by alignment in Mega for Macintosh, Version 5.2.2. The online Basic Local Alignment Search Tool (BLAST) was used to detect homology with species on the NCBI (National Centre for Biotechnology Information) database (http://www.ncbi.nlm.nih.gov/BLAST/). Isolate sequences were aligned with CBS (Centraalbureau voor Schimmelcultures) and ATCC (American Type Strain Culture Collection) reference and type strains obtained from the NCBI database. A neighbour-joining tree was constructed in Mega 5.2.2 using the Jukes-Cantor distance model. Branching pattern quality was assessed by bootstrap resampling of the data sets with 1,000 replications. For tree rooting, *Drosophila melanogaster* was selected as the eukaryote outgroup. Prokaryotes were listed in a table, as the isolation and identification of prokaryotes was the focus of another branch of the project.

3.3.3 Relative humidity and microbial activity in desiccated bentonite

Microbial respiration at bentonite-air interfaces during desiccation was assessed in triplicate samples of four distinct microcosms, as described below:

1) Inoculated bentonite microcosms

Uncompacted non-sterile bentonite (50 g/L) microcosms in 50 mL Falcon tubes were inoculated with a cocktail of bentonite prokaryotic and eukaryotic strains (Table 3.1). Bacterial and yeast strains were grown to stationary phase in liquid culture (2 and 4 days, respectively) and diluted to 10^6 cells/mL. Each culture was washed three times with sterile tap water, and 2.5 mL per culture was added aseptically to 2.5 g non-sterile bentonite. Fungal spores (2 mL per strain, 10^2 spores/mL) from the two isolates were added, and the culture topped up to 50 mL with sterile tap water.

2) Natural bentonite microcosms

Uncompacted non-sterile (uninoculated) bentonite (50 g/L) was added to 50 mL sterile tap water.

3) Inoculated saline bentonite microcosms

As per inoculated microcosms, but re-suspended and topped up with sterile saline (50 g/L NaCl) tap water.

4) Sterile bentonite microcosms

Twice-autoclaved bentonite (50 g/L) was suspended in 50 mL sterile tap water.

Inoculated (1) and sterile (4) microcosms were repeated with a total of 10 replicates each, for stronger statistical analyses. All microcosms were vortexed (3 min) and aerobically incubated in

capped Falcon tubes under static conditions at room temperature for 10 days. Microcosms were subsequently vortexed (1 min) and 15 mL of the bentonite slurry injected from each microcosm into two clean sections of Tygon tubing (80 cm long, 1 cm inner diameter) for incubation at 30% and 75% RH (15 mL/tube). Tubes were secured lengthwise with open ends upwards, so that the bentonite slurry was spread as a film (~1 mm thick) across the bottom (along ~40 cm of the U-shaped section of the tube, Fig. 3.2). Air was passed through each tube at 15-20 L/min for 16 hours until visible desiccation, indicated by bentonite flaking and lightness of colour. The tubes were subsequently incubated in chambers controlled at 30% and 75% RH, respectively.

TABLE 3.1 Strains selected for microcosm inoculation in this study. One desiccation-tolerant bacterial indoor air isolate (Ronan et al., 2013) was used. All other prokaryotic and eukaryotic strains were selected from bentonite isolates. Genbank accession numbers are included for species isolated in this study.

Indoor Air Isolate[a]	Bentonite Bacteria		Bentonite Yeasts		Bentonite Fungi	
Arthrobacter spp. (desiccation tolerant[a])	*Bacillus simplex* KX229705	*Arthrobacter globiformis* KX229706	*Cryptococcus magnus* (extremotolerant[b]) KX229704	*Cryptococcus antarcticus* (extremotolerant[c]) KX229704	*Penicillium chrysogenum* (Melanized spore-former) KX229702	*Fusarium solani* (Filamentous spreading hyphal mat) KX229703

[a]Ronan et al. (2012) [b]Butinar et al. (2007) [c]Vishniac and Onofri (2003)

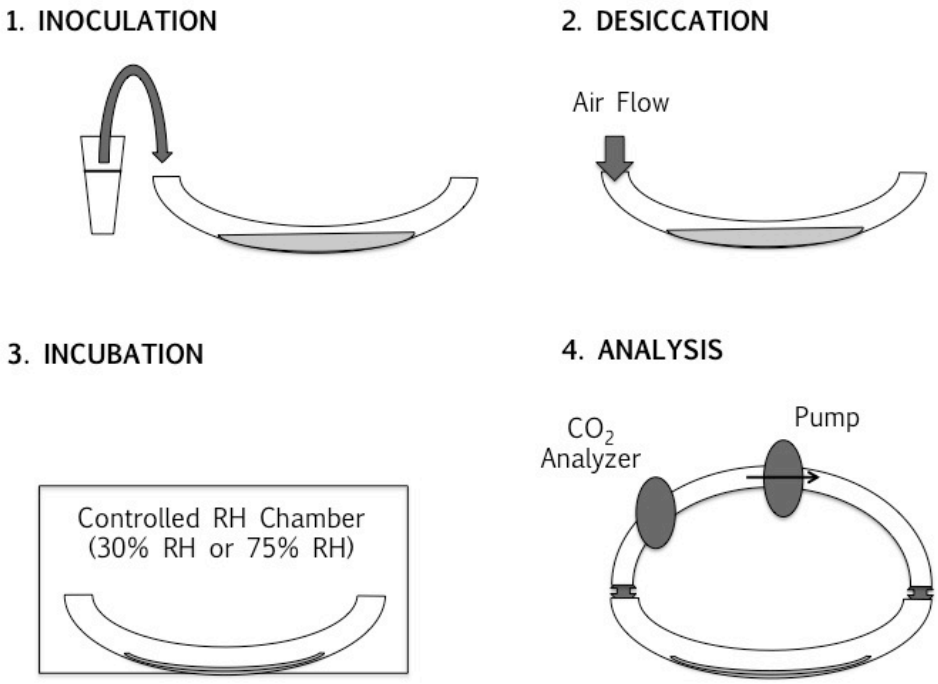

FIG 3.2 Experimental setup for the measurement of microbial metabolism at bentonite-air interfaces. Microcosms in 50 mL Falcon tubes (natural bentonite + tap water, inoculated bentonite + tap water, saline and sterile controls) were incubated under static conditions and inoculated into tubes (1). The samples were desiccated overnight (2) and subsequently incubated at low (30%) and high (75%) RH (3). Microbial respiration at bentonite-air interfaces was analyzed at 5 days and 20 days incubation, by connecting the tubes to a CO_2 analyzer and measuring CO_2 accumulation within a closed-loop system (4).

RH was maintained using $MgCl_2$ (33%) and KCl (85%) saturated salt solutions (100 mL/chamber) in covered 5-L glass chambers, according to Greenspan (1977). RH was monitored with 915 MHz Wireless Temperature Stations (La Crosse Technology, Saint-Laurent, QC, Canada). Bentonite-altered chamber RH, as compared to those reported by Greenspan (1977), stabilized at 23-30% (hereafter referred to as 30%) and 75-79% (hereafter referred to as 75%), consistently returning to the controlled RH within an hour after opening and resealing.

After 5-7 and 17-20 days, CO_2 production by the desiccated samples was measured by connecting the tubes to a closed-loop Carbon Dioxide Evolution Monitoring System (CEMS), described by Kroukamp and Wolfaardt (2009) and Bester et al. (2010). The carrier gas was air equilibrated to ambient levels of CO_2, circulated with a peristaltic pump. The accumulation of CO_2 in the system (3-5 hours) was measured, disconnecting the sample tubes from the CEMS loop and replacing them at controlled RH between measurements.

The evolution of CO_2 was plotted over time, and the gradients (ppm CO_2/min) at different RH, under different conditions were compared. Means and standard deviations of gradients of triplicate samples were calculated in Excel and compared with independent-sample two-tail t-tests. This statistical analysis was employed for all comparisons of means in this study.

3.3.4 Relative humidity and microbial survival in desiccated bentonite

The survival of bentonite microbiota was assessed after incubation of triplicate samples of 10 g uncompacted bentonite (1 year) and HCB blocks (2 months) at 30% and 75% RH. Aerobic colony forming units (CFU's) were assessed with sonication (2.1.1), on TSA and R2A (prokaryotes), and full- and 10% strength YMA (eukaryotes). For uncompacted bentonite

samples, the top 2 g was aseptically removed and discarded, and the next 1 g suspended in diluent, sonicated for 30 minutes, and appropriate dilutions plated on the respective media. For compacted bricks, the outer layer (~2 mm) was aseptically removed via scraping and a further 1 cm crumbled and homogenized. From this bentonite, 1 g was used for sonication and plating.

Bentonite as a Microbial Habitat

3.3.5 Desiccated bentonite as a water sink

Uncompacted bentonite-air water exchange capacity was assessed at 30% and 75% RH. Precisely 20.00 g of uncompacted bentonite was dispensed into pre-weighed glass vials (height: 58 mm, diameter: 20 mm; ten vials per treatment group). The samples were divided into four treatment groups: autoclaved (121 °C, 100 kPa), irradiated (2.5 MRad), dry heat (120 °C, overnight), and untreated. Five jars per treatment group were incubated per RH chamber (30% and 75%) at 30 °C. The bulk mass was monitored over 2 years.

Similarly, three pre-weighed HCB blocks were incubated at 30% and 75% RH (30 °C), respectively. After two months, the external physical appearance (total thresholded brightness and dark spots) was compared using ImageJ Particle Analysis of 700x580 pixel RGB snapshots, with a brightness maximum threshold of 160 and saturation threshold of 7 (hue un-thresholded). For standardization, single images of HCB block pairs (30% and 75% RH) were digitally split for analysis. Bulk mass and a_w (Novasina ms1 Water Activity Meter, linear offset calculated with distilled water and saturated $MgCl_2$ and KCl solutions) of the crushed blocks were compared. Internal measurements were 1 cm deep.

3.3.6 Metabolites and biomass: bentonite sedimentation phases

Clay sedimentation is the inverse of clay swelling, and thus indicative of one of the key suppressive properties of bentonite on microbial activity. Thus, the influence of salinity, FeS, lactate, and heat-killed biomass on sedimentation zone heights (mm) was assessed in bentonite slurries. Each 20 mL glass vial (height: 58 mm, diameter: 20 mm) had 10 mL NaCl, FeS, or lactate, respectively (see concentrations below). Non-sterile bentonite (1 g in 10 mL; 100 g/L) was added to each solution (FeS remained precipitated and settled with the bentonite), mixed, and allowed to settle for 36 hours. A heat-killed cell culture range was similarly assessed, but scaled down to 0.2 g bentonite in 2 mL (4.5 mL cuvettes). Heat-killed cells (5 mL) were collected from 3 day-old liquid cultures of *Cryptococcus magnus* (Table 1, YMB, 10^5 cells/mL) and *Arthrobacter* spp (TSB, 10^6 cells/mL). Cells were centrifuged together in 15 mL Falcon tubes at 10,000 g, washed twice, and re-suspended in 5 mL sterile tap water. The suspension and tap water for dilution were boiled (30 minutes) and cooled before dilution ranges were set up and bentonite (100 g/L) added.

Salinity range: 0, 10, 25, 50, 100, 150 and 200 (g/L)

Sulphide range: 0, 0.025, 0.05, 0.1, 0.2 and 0.4 (% w/w bentonite)

Lactate range: 0, 10, 25, 50, 100, 200 (g/L)

Heat-killed cell culture range: 0, 12.5, 25, 50,100 (% v/v)

The mean phase heights and standard deviations of triplicate samples were plotted against concentration (salinity, sulphide, lactate or cells). Phases included (a) water, (b) sedimentary bentonite, and (c) a light, cloudy interphase.

3.3.7 Microbial activity: clay swell index and water retention capacity

Bentonite clay swell index and water retention capacity were measured in (1) 12-week natural microcosms with microbial sulphur reduction, compared to non-sterile controls without microbial sulphur reduction and (2) 3-week inoculated microcosms, compared to sterile controls.

(1) Natural microcosms were set up and the clay swell index and water retention capacity were analyzed at 12 weeks:

Non-sterile, aseptically-handled uncompacted bentonite (5 g/microcosm) was weighed into 10 mL sealed syringes. Subsequently, 4 mL of treatment solution was added and forced through the bentonite with the syringe. Treatment solutions included sterile tap water, 20 g/L lactate, NaCl in sterile tap water (0, 50, 100, 150, 200 g/L), and the same range of saline solutions in 20 g/L lactate. Microcosms were monitored for visible formation of black precipitate, presumed to be microbial sulphate reduction to iron sulphides such as pyrite (FeS_2), mackinawite [$(Fe,Ni)_{1+x}S$ (x = 0-0.11)], and greigite (Fe_3S_4) (Rickard and Morse, 2005; Hunger and Benning, 2007). Microbial activity was confirmed with soluble sulphide, redox, and pH measurements in black microcosms, as compared to (1) twice-autoclaved microcosms and (2) non-sterile bentonite microcosms where visible sulphide precipitation was not evident.

The Methylene Blue method was used to measure soluble sulphide, according to Truper and Schlegel (1964). Bentonite redox was compared in zones with and without sulphide precipitation, using a 0.006% (w/v) Resazurin Sodium Salt solution, modified from Gonzalez-Pinzon et al. (2012). Bentonite pH was compared in zones with and without sulphide precipitation, using 0.01 M $CaCl_2$ according to Henderson and Bui (2002). For more detail, refer to Stone et al. (2015).

Visible sulphide precipitation was recorded in each microcosm (+ or -), and percentages of microbial activity per treatment recorded (percentage of total vials evidencing sulphur reducing microbial activity). In microcosms where microbial activity occurred, black precipitate was visible in 2 – 6 weeks and the clay swell index and water retention capacity analyzed at 12 weeks.

(2) Inoculated, natural and sterile microcosms were set up in 50 mL Falcon tubes, as described in section 2.1.2. The clay swell index and water retention capacity were analyzed at 3 weeks, well before sulphide precipitate formed.

The clay swell index of bentonite was measured according to ASTM Standard D5890 (ASTM D5890-11, 2011), scaled down to 1 g dry weight in 50 mL dH_2O, measured in a burette for 3-week inoculated microcosms, and 0.015 g dry weight in 3 mL cuvettes for 12-week natural microcosms. The water retention capacity of bentonite was measured with the general principle of ASTM Standard D5891 (ASTM D5890-02, 2009.). The method was scaled down to 5 g wet weight, and the water loss rate due to pressure was substituted with water loss rate due to heat (60 °C, dry heat). The method was as described, but instead of squeezing water off the bentonite, it was incubated at 60 °C and weighed every hour until a consistent dry weight, with samples cooled (desiccation chambers, 5 min) before weighing. Bulk mass as a percentage of the final dry weight was plotted over time, the gradients (decrease in weight (g/g dry weight)/hour) were calculated, and means and standard deviations (4 replicate samples) were compared with independent t-tests.

3.4 Results

Microbes: Activity and survival in desiccated bentonite

3.4.1 High RH extends short-term microbial metabolism at bentonite-air interfaces, but limits long-term desiccation survival

After 5 days of desiccation under sterile (control) and saline conditions, the rate of CO_2 production at bentonite-air interfaces was lower at 75% RH than at 30% RH (sterile: p= 0.005, t= 4.23, df= 6; saline: p= 0.061, t= 1.46, df = 6; Fig. 3.3A). The sterile bentonite CO_2 production rate of -0.13 ppm/min at 75% RH, in contrast to 0.07 ppm/min at 30% RH, suggests that bentonite absorbs CO_2 at high RH, likely due to a high natural pH (9.5; Stone et al., 2015). There was no significant difference between the mean CO_2 production rate at 30% and 75% RH in natural desiccated bentonite at surface-air interfaces (p=0.622, t=0.518, df=6), suggesting low levels of microbial respiration, or a change in the bentonite CO_2 absorption capacity. However, microcosms inoculated with bentonite isolates consistently respired CO_2 at 75% RH after 5 days of desiccation (p=0.0045, t=3.242, df=18; Fig. 3.3A and B). Standard deviation was high, since some inoculated microcosms ceased to metabolize at day 5 at 75% RH, despite the overall trend of continued metabolism (Fig. 3.3C). However, even inoculated bentonite samples that showed no activity (zero gradient) at 5 days of desiccation had higher levels of CO_2 in the equilibrated system at 75% RH than at 30% RH (Fig. 3.3C). This higher concentration of CO_2 in the desiccated tubes at 75% RH, despite a zero gradient, suggests that CO_2 had accumulated in the tubes during desiccation at high RH, even in tubes that were no longer metabolizing at day 5. This further confirmed that metabolism continued longer at 75% RH than 30% RH. By day 20, the mean inoculated microcosm metabolic rate at 75% RH had only decreased by 10%, from 0.6

ppm CO_2/min to 0.52 ppm CO_2/min. However, the standard deviation was greater and the difference between respiration at 30% and 75% RH was less distinct (p=0.26 t=1.31, df=6).

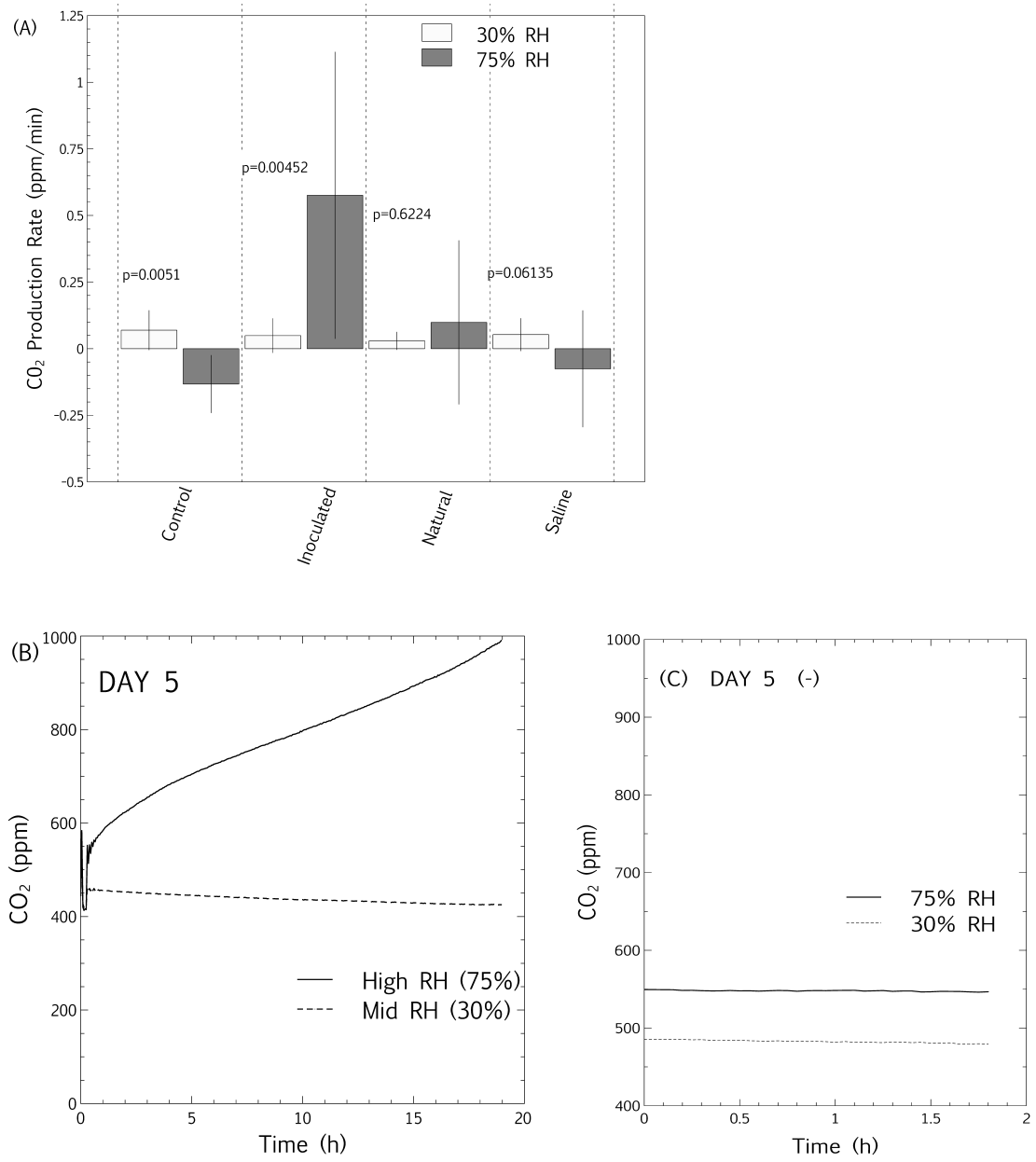

FIG 3.3 Microbial CO_2 production on dry bentonite-air interfaces at 30% and 75% RH. Of all inoculated samples, 30% RH did not show CO_2 production, whereas 75% RH showed persistent aerobic respiration (A). CO_2 accumulation at 75% RH in a single sample, after 5 days

of desiccation, connected to a closed-loop system is represented in (B) and (C). Some inoculated samples did not show respiration at 75% RH (A and C). Boxes (A) represent the means of the CO_2 accumulation gradients (ppm CO_2/min) of a minimum of triplicate samples after 5 days of desiccation under sterile control, inoculated, natural and saline conditions; and error bars standard deviation. P values represent the probability the there is a significant difference in mean pairs, based on an independent t-test.

In contrast, after desiccated incubation for one year, bentonite culturable prokaryotic and eukaryotic populations (quantified in CFU's/mL) were 2 to 3 times higher at 30% RH than at 75% RH (prokaryotes: p=0.0032, t=6.35, df=4; eukaryotes: p=0.0056, t=5.44, df=4; Fig. 3.4). Bentonite compaction suppressed background community levels up to tenfold; however, a lower survival trend at higher RH was still evident.

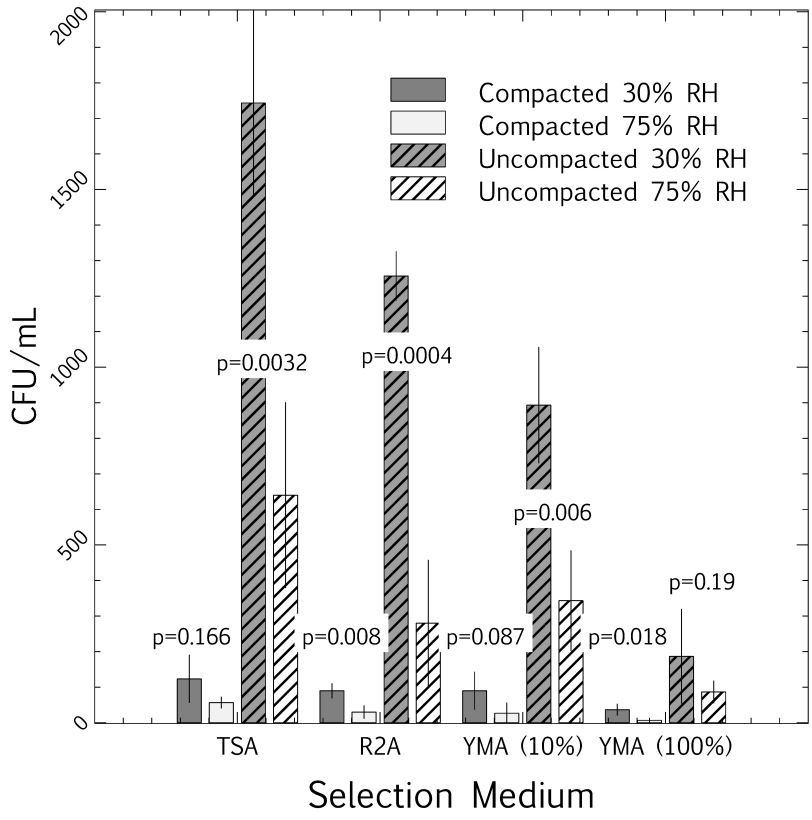

FIG 3.4 Survival of aerobic, culturable bentonite microbiota at 30% and 75% RH. In both as-received, dry compacted blocks (incubated at 30% and 75% RH for two months) and as-received, dry loose bentonite (incubated at 30% and 75% RH for one year), survival of aerobic culturable pro- and eukaryotic communities was greater at 30% RH. Boxes represent means of triplicate samples, and error bars standard deviation. P values represent the probability that there is a significant difference in mean pairs due to RH, based on an independent t-test.

3.4.2 Bentonite-air water exchange is influenced by humidity, heat and irradiation, and is non-homogenous upon compaction

Heat and irradiation increased bentonite's hygroscopic capacity (Fig. 3.5). Autoclaving (20 min), dry heat (120 °C), and irradiation (2.5 MRad) all forced water out of the as-received bentonite. During incubation at 30% RH, the untreated bentonite mass decreased over time, losing water to the gaseous phase; whereas, bentonite that had lost water due to treatment gained bulk mass until equilibrium, suggesting a hygroscopic tendency to bind water from the air. This hygroscopic trend was observed for all bentonite treatments at 75% RH. At both 30% and 75% RH, irradiated bentonite increased in bulk mass faster and reached a higher equilibrium than bentonite treated with heat and pressure, suggesting that irradiated bentonite has a greater hygroscopic capacity.

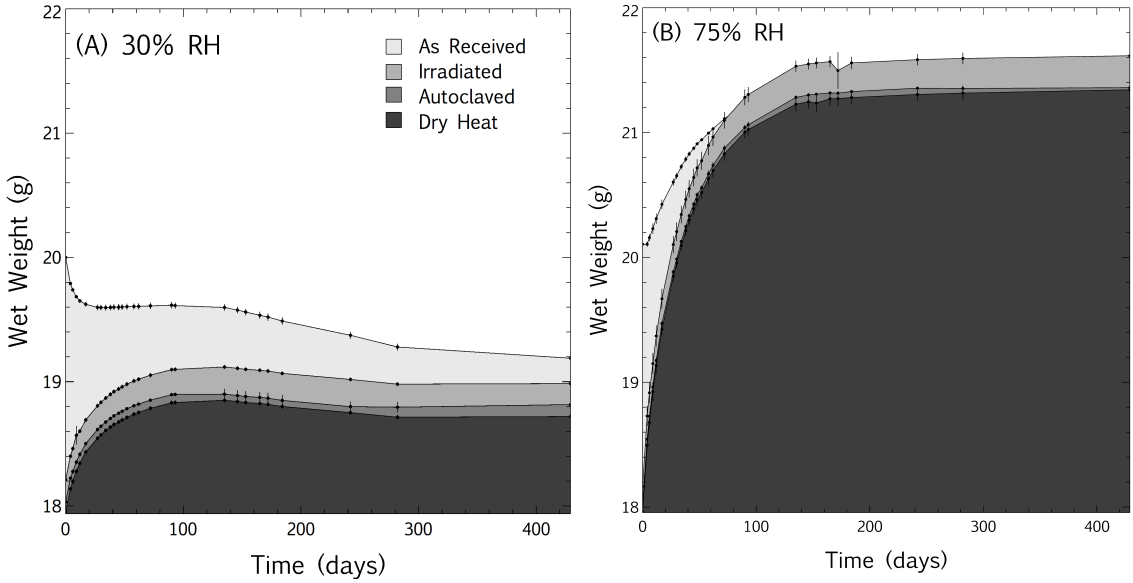

FIG 3.5 Bentonite-air water exchange in uncompacted bentonite. Initial 20 g (as-received, wet weight) samples of uncompacted Wyoming MX-80 bentonite powder were divided into 4 categories: untreated (as received), irradiated (2.5 MRad), autoclaved, and heated (dry, 120 °C). These were treated in jars, exposed to air at (A) 30% RH and (B) 75% RH, and mass increase was monitored. Error bars represent standard deviation of five replicate samples per time point.

HCB blocks were also hygroscopic, with higher bulk mass and a_w after incubation at higher RH (Fig. 3.6). Image J analyses of 700x580 pixel RGB images of HCB blocks (saturation threshold = 7, brightness threshold = 160) demonstrated that the color of bentonite bricks incubated at 75% RH was darker (% total area over 160 threshold) than at 30% RH ($p=0.0001$, $t=6.95$), suggesting that color correlated with bound water. The higher mean particle size ($p=0.0221$, $t=2.83$) at high RH suggests concentrated localization of hygroscopically-bound water.

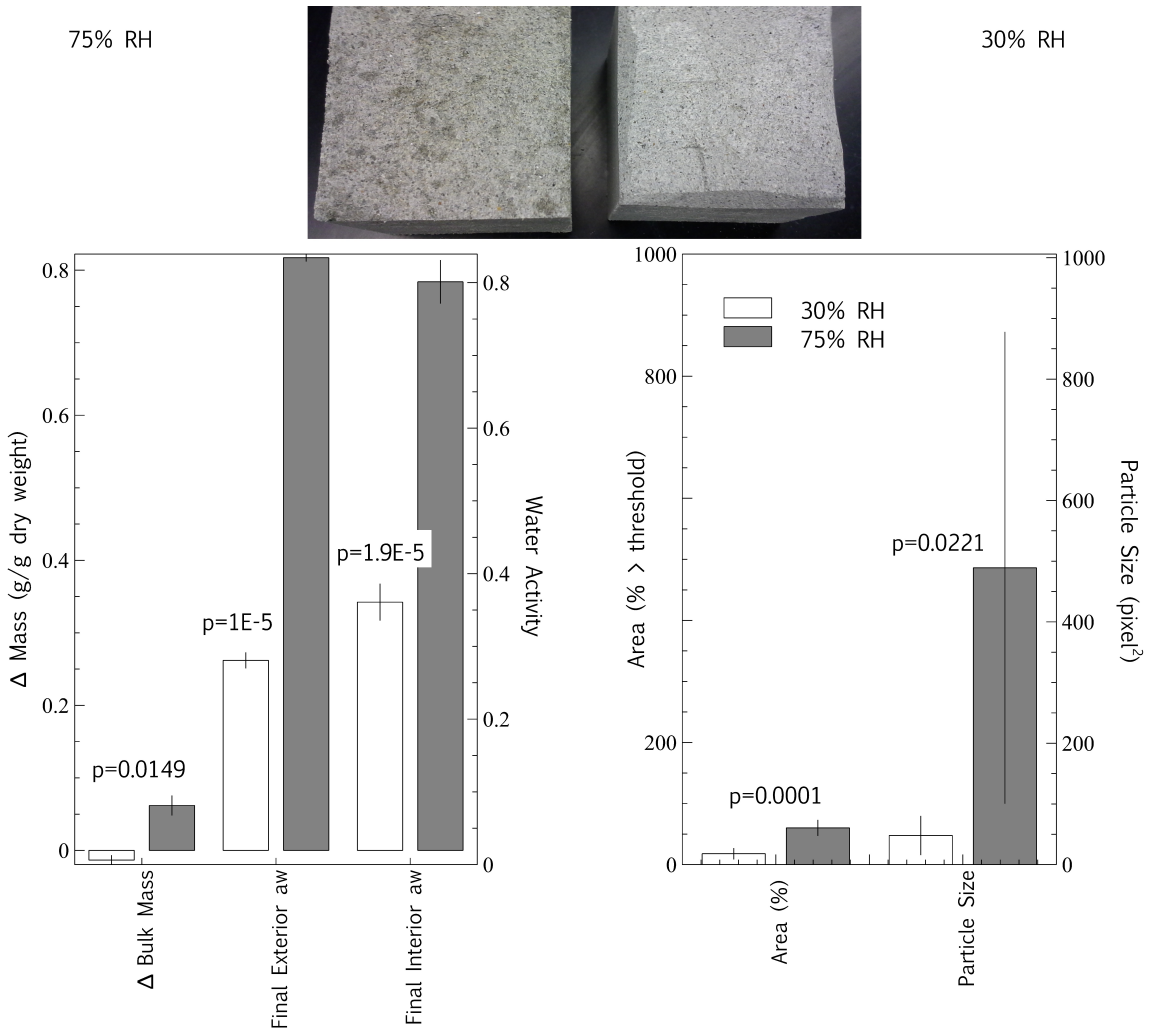

FIG 3.6 Bentonite-air water exchange in compacted bentonite. Cross-sections of compacted Wyoming MX-80 bentonite bricks incubated at 75% RH and 30% RH for 2 months. Qualitative parameters such as size, weight and hue (which were initially uniform) are noticeably distinct after 2 months incubation at the respective RH's. Image analysis quantification of these qualitative parameters, comparing total darker hue (area) and concentrated localization of water retention as a dark hue (average particle size), were recorded after 2 months, along with bulk mass and a_w. Boxes represent means of triplicate samples, and error bars standard deviation. P values represent the probability the there is a significant difference in means, based on an independent t-test.

3.4.3 Salinity, precipitated sulphides, lactate, and heat-killed microbial biomass influence the sedimentation of saturated bentonite

Microcosms were set up for monitoring SRB activity with tap water, NaCl (200 g/L, simulating porewater salinities; Vilks, 2009), and lactate (20 g/L, source of electrons and carbon). Similarly, bentonite was mixed with commercial FeS for evaluating the Methylene Blue protocol. These compounds influenced the sedimentation of saturated bentonite slurries, suggesting that clay-water interactions were influenced by salt, precipitated sulphide, and lactic acid. Since a key bentonite parameter for microbial suppression is its tendency to swell upon saturation (the inverse of sedimentation), this sedimentation was quantified as an indicator of clay-water interactions. An increase in concentration of NaCl, FeS, and Na-lactate (Fig. 3.7A-C) all lead to greater clay sedimentation (i.e., a larger water phase and smaller, more-compacted bentonite phase). Consequently, a concentration range of heat-killed cells was mixed with bentonite to assess whether extracellular microbial compounds had a similar influence on bentonite sedimentation. In contrast to the trends described above, bentonite sedimentation decreased slightly with an increase in cell-extract concentration (Fig. 3.7D).

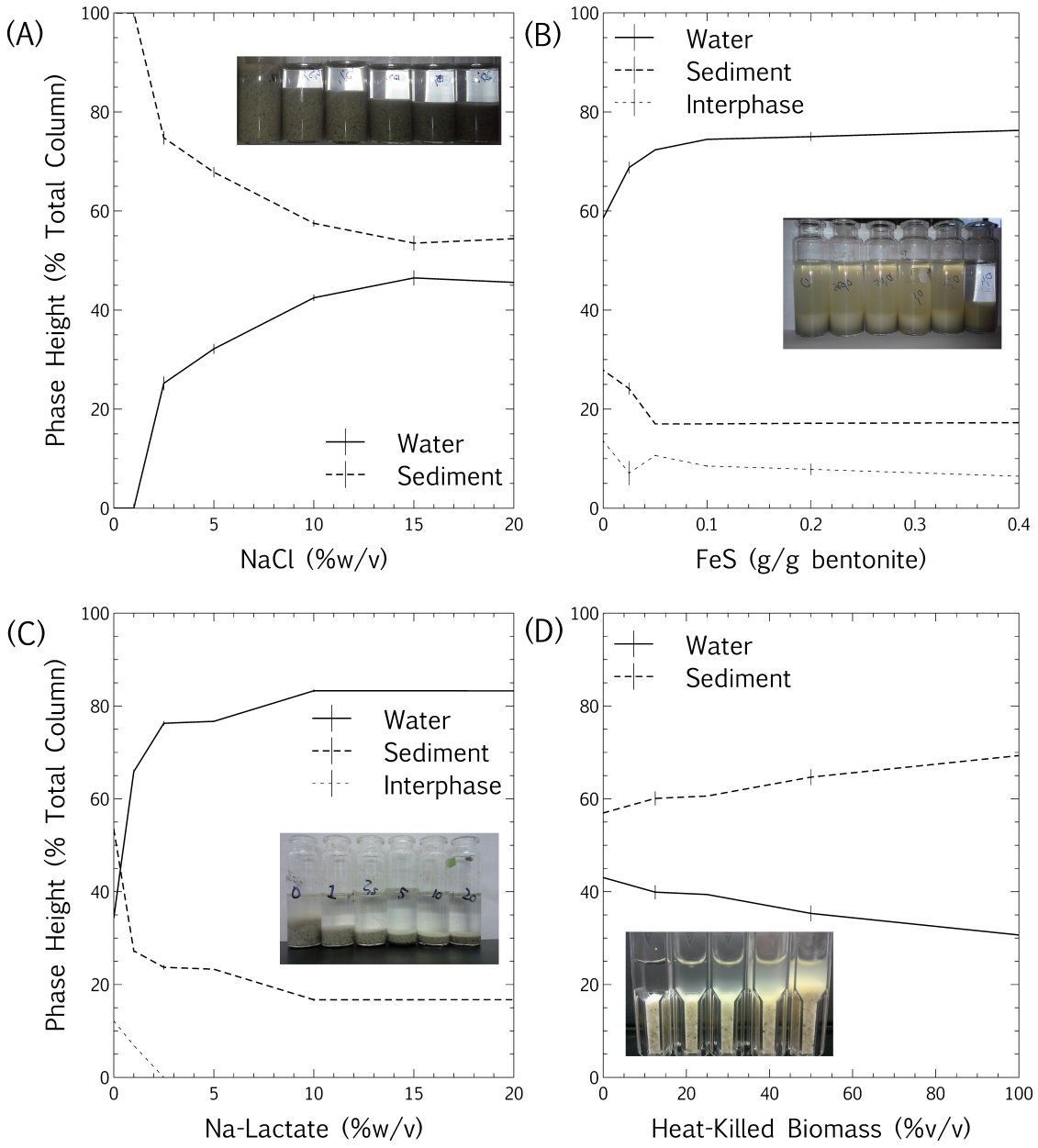

FIG 3.7 Bentonite sedimentation. Sedimentation phases (solid bentonite, interphase and water phase) were measured after mixing bentonite (10% w/v) with a range of concentrations of (A) NaCl [0-20% w/v], (B) sulphide [0-0.4 g/g bentonite], (C) Na-lactate [0-20% w/v] and (D) heat-killed biomass [0-100% v/v] and allowing it to settle. Error bars represent standard deviation of triplicate samples per concentration point.

3.4.4 Natural microbial activity in saturated bentonite has an influence on clay-water interactions

Iron sulphide precipitation was used as a simple visual indicator of microbial metabolism in saturated bentonite microcosms. Redox and pH always decreased and soluble sulphide increased concurrently with sulphide precipitation, while remaining constant in all controls, confirming that the sulphide precipitation was due to microbial activity. A resazurin color change from blue to pink to colorless, accompanied by a drop in pH from 9.8 ± 0.15 to 7.8 ± 0.2, likely due to organic carbon oxidation, only occurred in microcosms where visible sulphide precipitated. Autoclaved and irradiated controls, and saline microcosms showed no microbial activity over 2 years, indicated by stable redox and pH and zero precipitated and soluble sulphide.

Microbial activity, determined with precipitated and soluble sulphide and pH and redox decreases, was evident in 20% of microcosms saturated with tap water and 3% of microcosms saturated with lactate. These precipitates took 1-3 months to develop. The carbon source was expected to increase the frequency of sulphur reduction, but did not.

Twelve-week natural microcosms with FeS precipitate, hereafter referred to as microbially-active microcosms, were selected for assessment of bentonite swell index and water retention capacity, as compared to non-sterile controls in which microbial activity did not occur. Similarly, the clay swell index and water retention of bentonite in 3-week inoculated, natural, and autoclaved microcosms were compared. In twelve-week, natural microcosms, clay from microbially-active microcosms with precipitated sulphide swelled approximately 2.7 cm/(g dry weight) less than controls ($p=0.001$, $t=4.343$, $df=10$; Fig. 3.8A). The rate of water loss [g.(g dry weight)$^{-1}$.h^{-1}) upon incubation at 60 °C] had a higher trend in microbially-active microcosms

than in controls, although the difference was not significant at $p<0.05$ ($p=0.140$, $t=1.70$, $df=6$; Fig. 3.8C). Inoculated short-term microbial activity of aerobic bentonite microbiota had no influence on bentonite swell index or water retention (Fig. 3.8B and D).

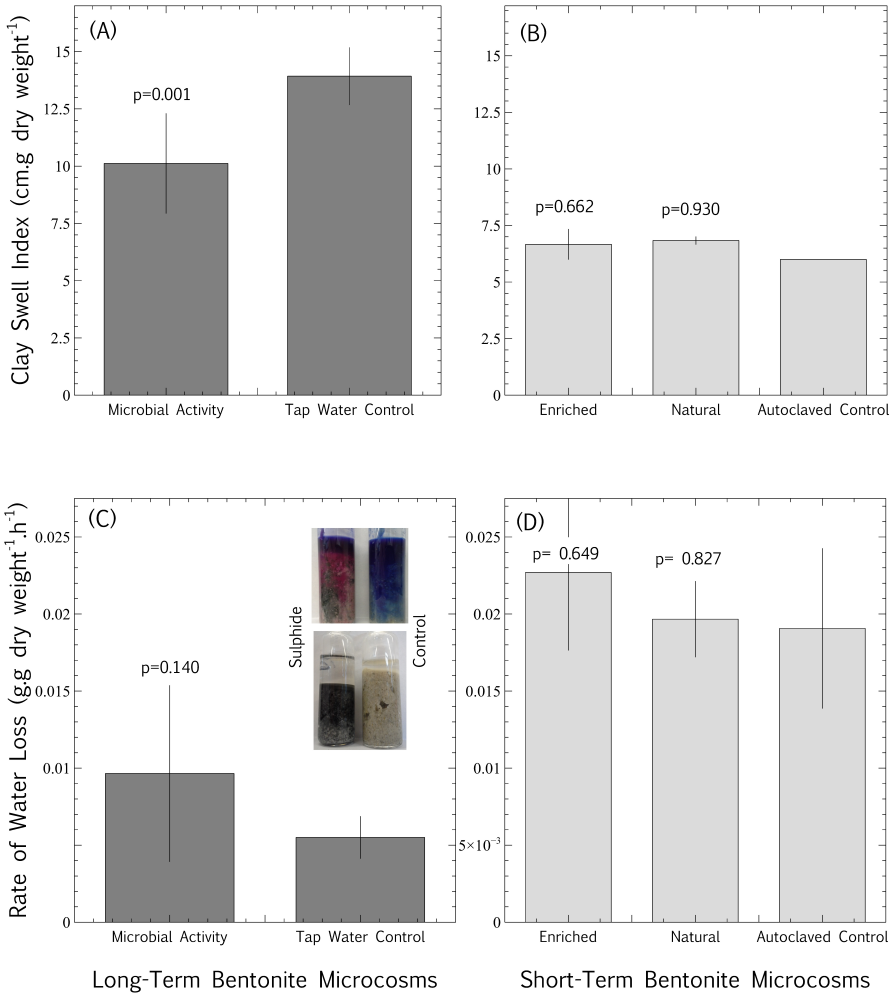

FIG 3.8 The influence of microbial activity on the clay swell index and water retention capacity of saturated bentonite. The clay swell index (A and B) and water retention capacity (C and D) of bentonite was compared in twelve-week microcosms (natural bentonite microbial activity, indicated by sulphide precipitate, redox and pH decrease; and tap water controls)

incubated for 3 months (A and C), and in short-term microcosms (inoculated, inoculated saline and sterile controls) incubated for 3 weeks (B and D), and. Boxes represent means of triplicate samples, and error bars standard deviation. P values represent the probability that there is a significant difference in means, based on an independent t-test.

3.5 Discussion

Water limitation is considered the primary microbial suppressive property of the HCB barrier in a DGR (Stroes-Gascoyne et al., 2010). Desiccation limits a_w when the barrier is unsaturated whereas upon saturation, high swelling pressures, the natural salinity of bentonite and small pore size limit a_w. However, microbial culturability has been documented in saturated HCB with dry densities lower than 1.6 g/cm^3 (Stroes-Gascoyne et al., 2010; Stroes-Gascoyne et al., 2011A). This suggests the potential for microbial activity if these suppressive conditions aren't consistently imposed. Thus, during transient desiccation in moisture gradients, two parameters are key: (1) the homogeneity of bentonite swelling and a_w, and (2) potential microbial access to water at surface-air interfaces for continuing metabolism. Most DGR microbiology studies have explored the kinetics of microbial sulphide generation and diffusion in saturated HCB; whereas this work explored the potential for microbial activity during desiccation, when swelling pressure is least likely to be homogenous and these suppressive conditions are least likely to be met. Micro-pockets of aerobic microbial activity could persist during desiccation and impact the bentonite physico-chemical properties responsible for SRB limitation during saturation.

Thus, the central questions were: (i) Does microbial activity occur at bentonite-air interfaces? (ii) Does RH (e.g., in a DGR) influence microbial activity at bentonite-air interfaces? (iii) Do microbes affect the swell index and water retention capacity of Wyoming MX-80 bentonite?

The evolution of CO_2 in closed-loop systems demonstrated that microbial activity could persist at desiccated bentonite-air interfaces, and that RH does play a role. After 5 days of desiccation at 30% RH, mean CO_2 production rates of inoculated bentonite samples were the same as the control, suggesting that metabolic activity ceases at bentonite-air interfaces at low RH (Fig. 3.3). However, CO_2 respiration of inoculated bentonite at 75% RH was significantly higher ($p=0.0045$, $t=3.242$, $df=18$; Fig. 3.3) than at 30% RH, suggesting that higher RH stimulates microbial metabolic persistence at bentonite-air interfaces under desiccation. This trend was still evident by Day 20, but with much greater variation ($p=0.26$). Organic matter is necessary for such metabolic persistence, but is largely limited to recalcitrant carbon in bentonite (Marshall and Simpson, 2014). This is a potential explanation for the lower metabolic rates in natural bentonite, as opposed to inoculated bentonite. It is likely that the degradation and recycling of biomass carbon provided most of the organic matter for respiration in this experimental setup. A pertinent continuation of this work would involve exploring the influence of substrates with higher carbon content on microbial metabolism at surface-air interfaces, as well as the potential regulation of metabolic rates in adaptation to lower water and carbon availability at surface-air interfaces.

In contrast to metabolic persistence, low RH (30%) improved the survival of aerobic culturable eukaryotes (2.6 times, $p=0.0056$, $t=5.44$, $df=4$) and prokaryotes (2.7 times, $p=0.0032$, $t=6.35$, $df=4$) in desiccated bentonite (Fig. 3.4). This survival trend was also evident in HCB blocks, although populations were smaller and variation greater. Thus, persistent metabolism during

desiccation might not be beneficial to the adaptation and survival of a microbial community over extended periods, since vegetative cells are more sensitive to stress than dormant cells. Ronan et al. (2013) demonstrated that high RH suppressed the survival of desiccation-tolerant indoor air isolates at surface-air interfaces. This is relevant to a DGR, since the aerobic culturable community of commercial bentonite included a diversity of spore-formers and desiccation-tolerant species (Table 3.1). Previous studies confirmed the predominance of spore-formers in analyses of compacted bentonite microbiota (Stroes-Gascoyne et al., 2010; Pedersen et al., 2000) and an increase in aerobic culturable numbers at bentonite interfaces, as compared to internal regions of the compacted clay buffer (Stroes-Gascoyne et al., 2007B). This study adds to this knowledge by demonstrating that desiccation may extend the survival of the aerobic culturable community at DGR interfaces. Potentially, extended metabolism at surface-air interfaces due to high relative humidity may suppress desiccation adaptation responses such as spore-formation, lowering survival capacity.

Although high RH (75%) suppressed survival of the aerobic bentonite microbiota, the persistence of microbial metabolic activity at surface-air interfaces at high RH may impact the physical parameters of the Na/Ca-montmorillonite clay matrix. The clay swell index is an important property responsible for limiting microbial activity in saturated HCB. Previous studies demonstrated the microbial role in smectite-illite conversion and concurrent decrease in swelling capacity (Mulligan et al., 2009; Liu et al., 2012). Since swelling pressure limits microbial activity, non-homogenous swelling may create microenvironments conducive to microbial growth, although this would occur rarely and transiently. However, if these microenvironments were exposed to air during desiccation, the potential for continued metabolism would exist, providing that microbes could access water (a) from the air, (b) from the hygroscopic clay

surface or (c) during exchange of water between the air and the surface. Higher water vapor in the air leads to sustained metabolism (Fig. 3.3). However, whether it is accessed from the air, the clay surface or during exchange with the hygroscopic matrix needs further investigation. The present study also showed that irradiation increases the capacity of the bentonite surface for holding water (Fig. 3.5) and thus may influence the potential of microbes to access water on irradiated bentonite. The distinct influence of gamma irradiation, heat and autoclaving on soil properties has been explored, with conflicting evidence on the effects of different energy sources on the aggregation or disaggregation of clay particles (Berns et al., 2008). It was suggested that irradiation often causes less of a disruption to soil matter than other sterilization techniques. Greater disruption, for instance the pressure of autoclaving, was posited to cause the collapse of pores, decreasing the surfaces area, which may have contributed to the decrease in clay accessibility to water vapor evidenced in this work. Similarly, the mean area of concentrated spots of dark hue, quantified with Image J analyses, was approximately 10 times greater on HCB bricks incubated at 75% RH than at 30% RH ($p=0.0221$, $t=2.831$, $df=8$; Fig. 3.6). Thus, if microbes do access matrix-bound water during desiccation, concentrated hygroscopic localization of water vapor could cause non-uniform swelling and form compromised microenvironments conducive to microbial activity.

Microbial communities in clay complexes in any transient microenvironments could modify solute concentrations (Kempf and Bremer, 1998), deposit carbohydrates (Wolfaardt et al., 1999), deposit iron sulphide (greigite, mackinawite, and pyrite) and catalyze the illitization of smectite (Hunger and Benning, 2007; Liu et al., 2012). Since the study of microbiology at surface-air interfaces presents limitations in terms of reaction rates, the microbial impact on bentonite-water interactions was further explored in this study in saturated microcosms, although similar

principles should apply to slower reactions rates at surface-air interfaces. Although salt, FeS, and lactate all increased bentonite sedimentation (the inverse of swelling), concentrated heat-killed cells did not (Fig. 3.7). It was shown that 12-week activity of the natural bentonite microbiota, leading to sulphide precipitation, decreased the mean bentonite swell index by 27% ($p=0.001$, $t=4.343$, $df=10$; Fig. 3.8A), although the impact on the rate of water loss by 43% was more variable ($p=0.140$, $t=1.70$, $df=6$; Fig. 3.8C). Short-term (3 week) bentonite microcosms, inoculated with high cell concentrations of aerobic prokaryotic and eukaryotic bentonite isolates, showed no decrease in bentonite swell index and water retention (Fig. 3.8B and D). This suggests that natural bentonite microbial activity, with sulphide precipitation, has an influence on bentonite-water interactions, but microbial biomass and short-term aerobic microbial activity do not. The carbon and salts attributed directly to biomass did not influence sedimentation, bentonite swell index or water retention within this timespan. This reflects classic colloid theory, which suggests that salt ions compress the diffuse negatively charged montmorillonite double-layer, influencing the potential of mean force and allowing Van der Waals forces to precipitate the clay (Tavares et al., 2004). In contrast, complex organic molecules will stabilize the clay suspension. In 12-week, natural microcosms, the swell index and water retention changes may be due to sulphide precipitation or illite-smectite conversion, both slow processes. An interesting investigation would be into the structural changes of the molecular clay sheets and complexes, using x-ray diffraction or electron diffraction. Conceptual models of interface microbial activity suggest bentonite corrosion depths of less than 5.3 mm in 100,000 years (Nakano and Kawamura, 2010). It is also worth noting that laboratory mineral dissolution rates are generally exaggerated, due to higher clay-surface reactive sites (Maher et al., 2006) and interface:bulk HCB ratios are very low, thus any interface microbial activity should have small DGR-scale

impacts. Similar long-term *in situ* studies would confirm the observations in this study and the postulations of such conceptual models. In addition to man-made environments like a DGR, this would also inform studies in microbial geochemical evolution.

Thus, the first two questions, (i) whether microbial activity can persist at bentonite-air interfaces, and (ii) whether RH influences this metabolism, were both confirmed. The third, (iii) addressing whether microbial activity has an influence on the bentonite swell index and water retention capacity, was confirmed in natural, saturated bentonite microcosms with visible precipitated sulphide. Under saline conditions, all microbial activity was completely suppressed, in both saturated and desiccated conditions. This supports the conclusions of Stroes-Gascoyne et al. (2010), that high salinity suppresses microbial activity, even with bentonite dry densities below 1.6 g/cm^3. The crystalline and sedimentary host rocks being characterized through the Canadian site selection program have salinities on the order of 50 g/L and 250 g/L, respectively (Vilks, 2009). These conclusions would be further strengthened by studying the metabolic capacity and influence of halophiles sourced from groundwater at bentonite-air interfaces.

This study suggests that high RH may prolong the activity of microbes at interfacial regions in subsurface environments within the engineered barrier system of a DGR, but simultaneously reduces survival of the aerobic microbiota. Long-term microbial activity and sulphide deposition may also influence bentonite-water interactions, decreasing the swell index and water retention capacity. However, even if swelling is compromised in transient microenvironments during desiccation, microbial activity will likely be limited by groundwater salinity in potential Canadian host rocks, thereby preventing weathering of the highly compacted bentonite and MIC of used fuel containers.

3.6 Acknowledgments. The authors would like to acknowledge Dr. James Noel (University of Western Ontario) for supplying compacted bentonite bricks according to NWMO specifications. In addition, thanks go to Evan Ronan and Roshanak Pashang (Ryerson University) for their role in bacterial isolations from the bentonite buffer, as well as Dr. Alexander Grigoryan and Daphne Jalique (University of Saskatchewan) for their assistance with soluble sulphide measurements.

CHAPTER 4

The Interaction of Microbial Metabolism and Survival at Surface-Air Interfaces:

Relative Humidity and Hygroscopic Surfaces

4.1 Abstract

The human environment is predominantly not aqueous, and microbes are ubiquitous at the surface-air interfaces with which we interact. Yet microbial studies at surface-air interfaces are largely survival-oriented, whilst microbial metabolism is overwhelmingly investigated from the perspective of liquid saturation. This study explored the interaction between microbial survival and metabolism under desiccation, particularly the influence of surface hygroscopicity on the capacity of microbial communities to access water vapor at surface-air interfaces. It was shown that the combination of a hygroscopic matrix and high relative humidity results in persistent microbial metabolism during desiccation, in both clay and polyethylene glycol (PEG, MW4,000). In contrast, neutral interfaces like sand and plastic/glass, and hygroscopic interfaces at low relative humidity stimulated no measurable CO_2 production of microbial communities at surface-air interfaces. ATP was evaluated as a tool for corroborating this metabolic profile, but was shown to be uncoupled from CO_2 production during desiccation. Finally, a potential link between the inhibition of microbial survival at high relative humidity and metabolic persistence at high relative humidity was explored. The idea of population resilience as a result of metabolic pacing informed a hypothesis, proposing that an oligotrophic water-saturated biofilm would recover from desiccation more robustly than a carbon-fed, metabolically active biofilm, mirroring the dual observation of metabolic persistence and survival inhibition at high relative humidity. This hypothesis was supported in desiccation-tolerant *Arthrobacter* biofilms, but not in desiccation-sensitive *Pseudomonas* biofilms. The interactive influence of surface hygroscopicity and relative humidity on microbial metabolism and survival has the potential to inform industrial, nosocomial and architectural built environments.

4.2 Introduction

Water is widely considered the determining element of the metabolic network that constitutes life on earth (Zolensky, 2005). In the microbial context, one of the earlier fundamental reviews on water activity in soil underscored this by calling single-cellular microbes "[regardless of their habitat…] aquatic creatures" (Stotzky and Pramer, 1972). Similarly, Brown articulated that, since prokaryotes predominantly obtain nutrients from solution, even a desiccated environment is essentially just a "concentrated solution with which the microbial cell must come directly to thermodynamic terms" in order to persist (Brown, 1976). These observations highlight a bias towards liquid systems that pervades microbiological research. However, despite the methodological challenges of studying microbial activity under desiccation, the environments with which humans interact are primarily not aquatic. Also, microbes are renowned for their ubiquity in terrestrial niches and flexibility in response to diverse stressors, many of which are often simultaneously associated with desiccation (Bauermeister et al., 2011; de Goffau et al., 2011; Chang and Halverson, 2003; Ramirez et al., 2004; Ritchie et al., 2006). Thus, although it is true that microbial activity and survival at surface-air interfaces must be explored in relation to the essential element of water, their activity in these inherently slower desiccated conditions is not anomalous, but rather a truer exploration of how microbes persist and influence many industrial, agricultural and medical settings relevant to humans. Examples of such "slow" surface-air microbiome consequences include the weathering of rock (de Goffau et al., 2011; Gorbushina and Broughton, 2009), structural architecture (Mottershead et al., 2003; Cheng et al., 2015) and artwork (Garg et al., 1995; Guglielminetti et al., 1994), hospital pathogen persistence (Kramer et al., 2006), risk-assessment models for the International Space Station (de Goffau, 2011), solid food contamination (Brown, 1976) and agricultural soil ecology (Stotzky and

Pramer, 1972; Ramirez et al., 2004; Ritchie et al., 2006). Ecologically, microbial diversity has been demonstrated in dust storms (Katra et al., 2014) and microbes can travel great distances whilst maintaining metabolic viability (Meola et al., 2015).

Spore-formation, and the accompanying metabolic pause, is arguably the best-studied response of microbes to desiccation (de Goffau et al., 2011; Feofilova et al., 2012). However, a full understanding of microbial impact at surface-air interfaces demands creative responses to the challenge of studying the inherently slow microbial *activity* in non-saturated environments, in addition to the more popular field of microbial *survival* in non-saturated environments. The observations of Chapter 3 suggest that the combination of high RH and hygroscopic clay surfaces promotes the metabolic activity of microbial communities at surface-air interfaces. Reminiscent of Brown's suggestion that microbes at surface-air interfaces essentially exist in a concentrated solution (Brown, 1976), the first proposal built in the present study on this observation is that microbial communities at surface-air interfaces can access water (a) from a hygroscopic surface, (b) from the air or (c) from water transfer between the air and the hygroscopic surface. The hypothesis constructed to test this notion essentially broadens the observation on bentonite clay, and states that if microorganisms can access water bound to hygroscopic surfaces, then the combination of high relative humidity and hygroscopic surfaces will increase the metabolic activity of a microbial community at surface-air interfaces, in comparison to low relative humidity and neutral surfaces. This was tested by assessing microbial community activity in (a) desiccated clay versus sand at 30% RH and 75% RH and (b) PEG-4,000 versus plastic at 30% RH and 75 % RH. Clay (Fisher, 1923) and PEG-4,000 (Donatula, 1998) were selected as hygroscopic matrices, with sand (Fisher, 1923) and glass/plastic

(Donatula, 1998; Harbers, 2007) selected as less hygroscopic surfaces. Within the construct of this hypothesis, the limits of measurement at surface-air interfaces was addressed and ATP swabs, typically employed to assess microbial load on dry surfaces, were considered as a tool to corroborate CO_2 production as a metabolic indicator in desiccated environments.

In addition, Chapter 3 supported previous claims that high relative humidity limits viable cell survival at surface-air interfaces (Ronan et al., 2013), extending this observation to a hygroscopic interface. The observations that (a) metabolic persistence was stimulated short-term at high RH, and (b) viable cell survival was limited long-term at high RH, led to the second hypothesis, that higher initial metabolism correlates with lower long-term survival because higher metabolic rates render the community more sensitive to the stressors accompanying desiccation. Expounding on this idea of metabolic slowness in relation to resilience, a ground-breaking tool to measure *in situ* microbial growth rates at a single-cell level recently demonstrated the vast discrepancy between the typical laboratory and true *in situ* growth rates of *Staphyloccus aureus*, one of the go-to models of opportunistic microbial biofilms (Kopf, 2015). Similarly, microfluidics has made it volumetrically feasible to explore the growth of dental pathogens in sputum, as opposed to the synthetic media that has predominated microbiology for decades (Samarian et al., 2014). This type of work bodes a shift in focus to include microbiological studies more representative of natural habitats, despite the slower metabolic rates and the associated experimental challenges. Such ubiquitous natural "slowness" could suggest that there is physiological, morphological and adaptive strength in microbial metabolic pacing, and thus merit to studying organisms at more challenging natural growth conditions, and thus lower growth rates.

The research hypothesis designed to explore this notion states that a microbial biofilm continually exposed to an easily accessible carbon source, with an associated increased metabolic rate, will recover from desiccation at a slower rate than a biofilm growing under oligotrophic conditions. The experimental design that was used to test these hypotheses focused on the exploration of microbial metabolic persistence and adaptation under desiccation, and involved (1) the validation and use of CO_2 as a metabolic indicator at surface-air interfaces, (2) searching for further support of the notion that hygroscopic surfaces and high relative humidity promote microbial communities' access to water, and (3) probing the notion that persistent metabolism at surface-air interfaces limits the desiccation resilience of a microbial biofilm in desiccation-sensitive and desiccation-tolerant species.

4.3 Materials and Methods

4.3.1 Relative Humidity and Pure Culture Cell Viability at Surface-Air Interfaces: Glass and Clay

Pure culture cell survival at surface-air interfaces of desiccation-tolerant eukaryotes and prokaryotes was assessed using the large droplet method, according to Jawad et al. (1996) and Ronan et al. (2013). *Arthrobacter* sp., an indoor air prokaryote isolated by Ronan et al. (2013), and *Cryptococcus magnus*, a bentonite eukaryote isolated in this study, were grown separately overnight in broth with agitation at room temperature. Bacteria were grown in Tryptic Soy Broth (3 g/L) and yeasts were grown in Yeast Malt Broth (10g/L dextrose, 5 g/L peptone, 3 g/L malt extract, 3 g/L yeast extract). Media was according to Atlas (2010) and chemicals purchased from Sigma-Aldrich (Oakville, ON, Canada). Both cultures were washed with sterile tap water 3 times

(7,000 g; 5 min) and diluted in sterile tap water to a cell concentration of 10^4 cells/mL (yeast) and 10^6 cells/mL (bacteria). Clean glass coverslips were placed in sterile petridishes (6 per dish, 1 mm x 18 mm x 18 mm, VWR International, Mississauga, ON, Canada), 50 µL inoculated per coverslip and allowed to dry in a laminar flow hood for 3 hours. For *Arthrobacter* and *Cryptococcus*, respectively, 75 coverslips were inoculated for incubation at 30 % RH, and 75 inoculated for incubation at 75 % RH. This procedure was replicated, but the glass coverslips were pre-inoculated with a 50 µL droplet of bentonite (100 g/L) solution which was dried in a laminar flow hood for 3 hours before inoculation with *Arthrobacter* or *Cryptococcus* and subsequent drying and incubation.

Prior to incubation at low and high RH, the cell viability after drying was assessed in triplicate (T_0). Coverslips, inoculated with *Arthrobacter* or *Cryptococcus* on glass or bentonite, were placed in separate 50 mL Falcon tubes containing 5 mL NaCl (8.9 g/L), vortexed for 1 min and dilutions plated on Tryptic Soy Agar (3 g/L) or Yeast Malt Agar, respectively, for determination of viable cell concentrations per coverslip. This was repeated at 3h, 24 h, 48 h and 3, 11, 15, 43, 65 and 234 days. At each time point, triplicate coverslips were assessed for (1) *Arthrobacter* at 30 % RH and 75 % RH, on glass and bentonite, and (2) *Cryptococcus* at 30 % RH and 75 % RH, on glass and bentonite. Viable cell concentrations were represented as a percentage of the cell concentration at T_0 (desiccated inoculum). Means and standard deviations of triplicate coverslips were calculated in Microsoft Excel and plotted in the Vuesz online plotting package (http://home.gna.org/veusz/) against time.

Throughout the study, RH was maintained using $MgCl_2$ (33%) and KCl (85%) saturated salt solutions (100 mL/chamber) in covered 5-L glass chambers, according to Greenspan (1977). RH was monitored with 915 MHz Wireless Temperature Stations (La Crosse Technology, Saint-Laurent, QC, Canada). Bentonite-altered chamber RH, as compared to those reported by Greenspan (1977), stabilized at 23-30% (hereafter referred to as 30%) and 75-79% (hereafter referred to as 75%), consistently returning to the controlled RH within an hour after opening and resealing.

4.3.2 Mixed-Culture Community Carbon Dioxide and ATP Measurements during Desiccation: Relative Humidity and Surface Hygroscopicity

The CO_2 generation, ATP generation and viable cell concentrations were compared, for a mixed culture of bentonite origin, desiccated at 30% RH and 75% RH on (1) clay and sand and (2) polyethylene glycol (PEG-4,000) and plastic/glass. Clay (Fisher, 1923) and PEG (Dontula, 1998) were chosen as hygroscopic substrates, whereas sand (Fisher, 1923) and glass/plastic were chosen as less hygroscopic substrates (Harbers et al., 2007). All references to PEG in this work refer to crystalline PEG, with a molecular weight of 4,000 (Sigma Aldrich, Oakville, ON, Canada).

Cultures were selected based on Chapter 3 (Table 3.1), including both eukaryotic and prokaryotic desiccation-tolerant and -sensitive species, of bentonite and air origin. Bacteria were grown in TSB and yeasts were grown in YMB. Cultures were incubated at 25 °C with agitation well into stationary phase (2 days, bacteria, 10^7 CFU/mL; 4 days, yeast, 10^5 CFU/mL) and 2.5 mL of each culture combined in four 50 mL conical tubes. Each mixed culture was washed 3 times with sterile tap water (centrifugation, 7500 x g) prior to microcosm setup. Tap water was

selected as the diluent over physiological saline solution (8.9 g/L NaCl) for more natural precipitated salt concentration upon desiccation. The final culture was mixed together, diluted 1:3 in tap water and divided between 4 microcosms: (1) 100 g/L Wyoming VOLCLAY MX-80 bentonite powder (American Colloid Company, Wyoming, USA), (2) 250 g/L sand (VWR, I think), (3) 100 g/L PEG and (4) pure tap water in 250 mL Schott bottles, and incubated without agitation at room temperature for 2-3 days. Controls included the same four microcosms, suspended in sterile tap water without cells.

At day 3, each microcosm was used as an inoculum to assess CO_2, ATP and viable cell survival profiles during desiccation at 30% and 75% RH. Prior to inoculation and desiccation, prokaryotic and eukaryotic viable cell concentrations were determined by serial dilution (8.9 g/L NaCl) and plating of triplicate samples of each inoculum on Tryptic Soy Agar and Yeast Malt Agar respectively.

4.3.2.1 CO_2 Generation

Modified from Section 3.3.3, 15 mL of each aged (Day 3) inoculum was injected separately into 6 clean sections of Tygon tubing (30 cm long, 1 cm inner diameter) and air passed through at 15-20 L/min (Matheson Stainless Steel air rotameter) for 12 h. PEG-4,000 was dried for 18-20 h. The air was not sterilized, as potential air contaminants were considered (a) representative of most natural environments, (b) insignificant, in terms of cell numbers, in comparison to the concentrated mixed-culture inoculum and (c) irrelevant, since the study drew community conclusions, rather than pure-culture conclusions. Tubes were secured lengthwise with open ends upwards, so that the bentonite slurry was spread as a film (~1 mm thick) across the bottom

(along ~20 cm of the U-shaped section of the tube; Fig. 3.2, Section 3.3.3). Visible desiccation of bentonite and PEG was indicated with the lightness of the substrate and flaking from the surface. Per inoculum, 3 tubes were incubated at 30% RH, and 3 incubated at 75% RH. Sand settled quickly upon mixing, and was not easily transferred into the tubes via syringe. Thus, after mixing of the microcosm, 15 mL of the liquid phase was transferred to each tube, followed by the sterile transfer of approximately 4 g of sand per tube with a sterile spatula. PEG added to the microcosms was solubilized and potentially metabolized. Therefore, prior to inoculating the tubes, an additional 1.5 g PEG crystals were scattered at the base of each tube as an attachment surface during desiccation.

After 2 days of incubation at the relevant relative humidity, CO_2 production by the desiccated samples was measured by connecting the tubes to a closed-loop Carbon Dioxide Evolution Monitoring System (CEMS, Fig 3.2), described by Kroukamp and Wolfaardt (2009) and Bester et al. (2010). The carrier gas was air equilibrated to ambient levels of CO_2, circulated with a peristaltic pump. The accumulation of CO_2 in the system (3-5 hours) was measured, disconnecting the sample tubes from the CEMS loop and replacing them at controlled RH between measurements.

The evolution of CO_2 was plotted over time, and the gradients (ppm CO_2/min) were compared. Means and standard deviations of gradients of a minimum of 5 samples per microcosm were calculated in Excel and compared with independent-sample Student's two-tail t-tests. This statistical analysis was employed for all comparisons of means in this study.

To strengthen the assumption that CO_2 gradients were due to microbial metabolism, a number of controls were included:

(1) One set of inoculated bentonite tubes, incubated for 7 days at 30 % RH and 75 % RH respectively, were connected to the closed-loop CEMS system directly after wetting with 3 mL sterile tap water per tube.

(2) One set of inoculated PEG tubes, incubated for 7 days at 30 % RH and 75 % RH respectively, were connected to the closed-loop CEMS system directly after wetting with 3 mL sterile tap water per tube.

(3) One set of bentonite tubes, one inoculated and one sterile control incubated at 75 % RH, were connected to the closed-loop CEMS system directly after rewetting with 3 mL sterile TSB (3g/L) per tube.

The gradients were compared to those recorded during desiccation, with the expectation that water would increase the CO_2 accumulation gradient in inoculated tubes, TSB would increase the gradient even more markedly, and sterile controls would show zero CO_2 accumulation.

4.3.2.2 ATP Generation and Cell Counts

From each aged (3 Day) inoculum, 50 µL was also inoculated with the droplet-method (Jawad et al., 1996; Ronan et al., 2013) onto clean borosilicate glass coverslips (1 mm x 18 mm x 18 mm, VWR International, Mississauga, ON, Canada) after mixing (1 min). Fifty coverslips were inoculated per microcosm (bentonite, sand, PEG, tap water) and dried in sterile petridishes, 6

coverslips per plate. Sand did not remain in suspension and settled prior to inoculation. Thus, after inoculating the droplets, a sterile spatula was used to transfer approximately 0.2 g (wet weight) sand from the microcosm into the centre of each droplet as a drying substrate. Similarly, since PEG was dissolved and potentially metabolized, 0.01 g (dry weight) PEG was deposited into the centre of each droplet as a drying substrate. The droplets were dried in a laminar flow ventilation hood for 3 hours at ambient temperature and relative humidity. The petridishes were then transferred to RH chambers controlled at 30 and 75% relative humidity.

For assessment of viable colony forming units (CFU's), coverslips were suspended in 50 mL conical tubes containing 5 mL physiological saline solution (8.9 g NaCl/L), vortexed for 1 min and dilution series plated on TSA. For bentonite, sand, PEG and glass; CFU's were assessed with triplicate coverslips after 3 h of drying (T_0), and after incubation at the respective RH's (in triplicate at 30% RH and 75% RH, respectively) for 2 hours (T_1), 8 hours (T_2), 24 hours (T_3), 48 hours (T_4) and 3 days (T_5).

For assessment of droplet community ATP levels, coverslips dried on PEG-4,000 and plastic were swabbed clean with Hygenia (Fischer Scientific, Ottawa, Canada) Ultrasnap ATP surface swabs and assessed in an Hygenia EnSURE luminometer. This commercial product is typically employed to assess microbial sanitation levels on dry surfaces, and measures ATP with the bioluminescence of the luciferin/luciferase system. Coverslips were swabbed gently for 15 s (until PEG was completely soluble), whilst rotating the swab. After replacement in the bulb, each swab was shaken 30 times in 15 s before measurement. Standard curves of active cell culture

droplets suspended in sterile tap water and dried on coverslips with bentonite, sand, PEG and tap water were used to assess the measurement of ATP on the respective substrates using bioluminescence (Appendix B). The technique was effective with PEG and tap water, however bentonite and sand interfered with bioluminescence monitoring. Thus, for PEG and plastic, ATP was assessed with triplicate coverslips after 3 h of drying (T_0), and after incubation at the respective RH's (in triplicate at 30% RH and 75% RH) for 2 hours (T_1), 8 hours (T_2), 24 hours (T_3), 48 hours (T_4) and 3 days (T_5), corresponding to the viable cell concentration curve.

Data (means and standard deviation of triplicate samples) were plotted as ATP (RLU)/CFU(cells/mL), and hygroscopic and neutral surfaces incubated at high and low RH were compared.

4.3.3 Biofilm Resilience after Desiccation: Carbon, Metabolic Rates and Biofilm Recovery

Pseudomonas aeruginosa PAO1 (desiccation sensitive; Ronan et al., 2013) and *Arthrobacter* (desiccation tolerant; Ronan et al., 2013) biofilms were grown in continuous systems and open-loop carbon dioxide generation was monitored as an indicator of biofilm activity. Continuous flow systems were assembled according to Bester et al. (2010). Briefly, two biofilm flow systems were sterilized with ethanol (1 h) and a commercial 5% Na-hypochloride solution (3 h). The system was washed (37.5 mL/h) with sterile tap water overnight (10 h), equilibrated with 0.3 g/L TSB in sterile tap water (1 h) and inoculated with cells upon stopping the flow of media (0.5

mL, ~10^6 cells/mL, grown in TSB for 14 h). After a 45 min (*Pseudomonas*) or 6 h (*Arthrobacter*) attachment period, medium flow was restarted. At 50 h (well into the stationary phase of the CO_2 profile), the medium of one biofilm was changed to sterile tap water. The two identical biofilms were continuously exposed to (a) tap water [oligotrophic] or (b) 0.3 g/L TSB in tap water [carbon-rich], respectively, for 24 h and subsequently run dry. Before running dry, 1 mL of sterile tap water was run through both biofilms at a higher rate (1 mL/min) to wash the TSB biofilm. Both biofilms had sterile air (5 L/min), passed through a filter and a chamber controlled at 40% RH, blown through for 2 days. The desiccated biofilms were then re-exposed to TSB (0.3 g/L), with a 30 min attachment period, and the recovery lag phase and exponential rate of CO_2 production were used as indicators of post-desiccation biofilm resilience. The experiment was repeated in triplicate, for each pair of *Pseudomonas* and *Arthrobacter* biofilms.

This experiment was repeated with *Pseudomonas*, making a few experimental amendments to test different extremes: (1) shortening the biofilm establishment phase to 24 h (as opposed to 50 h), (2) increasing the TSB concentration in the carbon-rich biofilm to 3 g/L during the media switch and (3) increasing the desiccation phase to 3 days (as opposed to 2 days).

4.4 Results

4.4.1 Relative Humidity and Desiccation Viability

After a year of incubation at 30% RH and 75% RH, the natural microbiota of as-received uncompacted bentonite was consistently significantly less viable at high (75%) RH than at low (30 %) RH (Fig 3.4). Both eukaryotic and prokaryotic populations isolated on low-carbon and high-carbon media demonstrated this trend of inhibited viability at high relative humidity.

Further exploring the influence of relative humidity on the survival of microbes at surface-air interfaces, the work of Ronan et al. (2013) was repeated with the same desiccation-tolerant *Arthrobacter* sp. air isolate and a eukaryotic bentonite isolate, *Cryptococcus magnus*, on both glass coverslips and on glass coverslips coated with hygroscopic bentonite clay. Following inoculation with the large-droplet technique, the survival of both eukaryotes and prokaryotes was extended at bentonite-air interfaces in comparison to glass-air interfaces at high and low relative humidity (Fig 4.1). Bentonite both provides a hygroscopic matrix as well as more carbon and trace elements than clean glass (Karnland et al., 2006). Also, the eukaryotic isolate, *Cryptococcus magnus*, demonstrated better viability under desiccation than the prokaryote, which was an indoor air isolate selected for its reported desiccation-resistance (Ronan et al., 2013). However, the survival of both the eukaryote and prokaryote was inhibited at 75% RH in comparison to 30% RH at both glass- and clay-air interfaces. Thus, the conclusions of Ronan et al. (2013) were confirmed and extended to include a desiccation-tolerant eukaryote and hygroscopic clay surfaces. This also supported the long-term survival trends of natural prokaryotic and eukaryotic populations in bentonite (Fig 3.4).

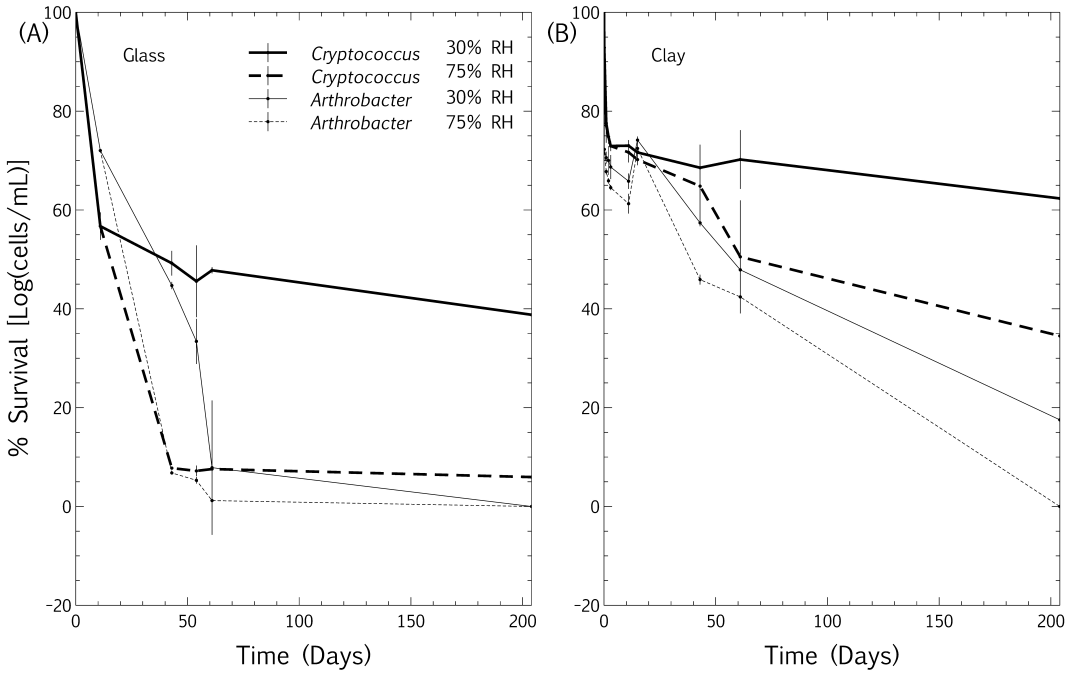

FIG 4.1 Relative humidity, hygroscopicity and the survival of pure-culture prokaryotes and eukaryotes at surface-air interfaces. The survival of cells inoculated onto (A) glass coverslips and (B) glass coverslips pre-inoculated with a coat of desiccated bentonite was evaluated over a period of months. Survival was expressed as a percentage of the desiccated inoculum evaluated after a 3 h drying period. A desiccation-tolerant yeast (*Cryptococcus magnus*) was compared to a desiccation-tolerant prokaryote (*Arthrobacter* sp.), and survival was contrasted at low (30%) RH and high (75%) RH. Plots represent means of triplicate samples and error bars the standard deviation.

4.4.2 Relative Humidity and Desiccation Metabolism

In contrast to survival inhibition, Figure 2 of Chapter 3 suggests that the hygroscopic clay matrix stimulates the CO_2 production of a desiccated microbial community at high (75%) RH, whereas

microbial metabolic CO_2 production was below the closed-loop CEMS detection limit at low (30%) RH. This observation led to the notion that hygroscopic surfaces improve the access of microbial communities to water vapor at surface-air interfaces. The hypothesis designed to test this states that if a hygroscopic matrix improves microbial access to water vapor at surface-air interfaces, then both clay and PEG-4,000 at high (75%) RH will stimulate higher CO_2 production in microbial communities at surface-air interfaces than sand and plastic. Of the 8 combinations of neutral (sand and plastic) and hygroscopic (clay and PEG) surfaces (Fisher, 1923, Harbers et al., 2007, Dontula et al., 1998) at high and low RH, the accumulation of CO_2 in a closed-loop CEMS was only observable for microbial communities on clay at 75% RH and PEG at 75% RH (Fig 4.2). For all uninoculated controls, the production of CO_2 was approximately zero and all inoculated microcosm tubes incubated at 30% RH were not significantly higher than the controls, according to the Student's t-test of independent means (Fig 4.2.2). Any slightly negative CO_2 production rates are likely due to the chemical equilibration of CO_2 in a basic environment, which has been demonstrated at surface-air interfaces (Stone et al., 2016). On both sand and plastic surfaces, there was no significant difference between the means of CO_2 production (ppm/min) between samples incubated at 30% RH and 75% RH. Microbial communities desiccated on a bentonite surface and incubated at high (75%) RH exhibited a mean CO_2 production rate of 0.45 ppm/min, significantly higher than a sterile control sample ($p=0.05$, $t=2.729$; $df=4$; $p=0.026$). The mean CO_2 production rate of the same microbial community on PEG was lower than bentonite (0.13 ppm/min), but still significantly higher than the mean sterile PEG control ($t=3.129$; $df=4$; $p=0.007$). Thus, the hypothesis was supported, and the combination of hygroscopic surface and high RH was shown to improve the metabolic persistence of a microbial community at surface-air interfaces.

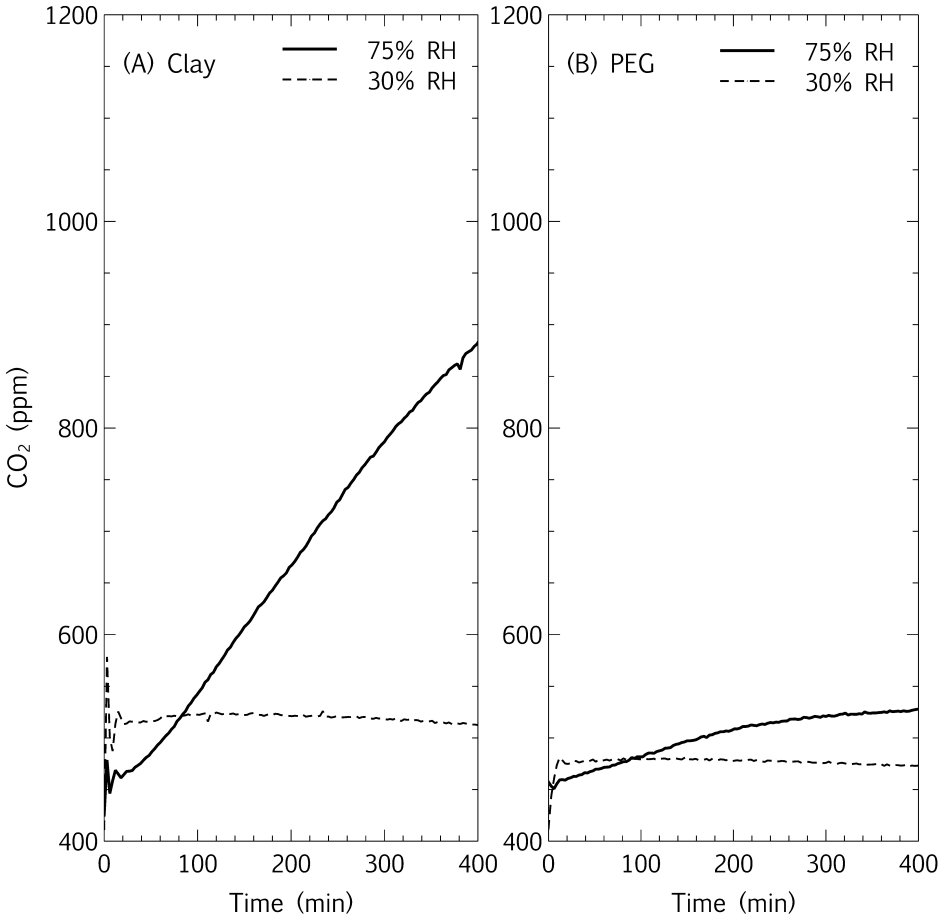

FIG 4.2.1 Interface microbial metabolism in hygroscopic matrices. Carbon dioxide production at (A) bentonite-air interfaces and (B) PEG-air interfaces, measured in a closed-loop CEMS system. Samples were inoculated with microbial biomass that had been pre-incubated under static conditions for 2 days on the respective substrate (bentonite and PEG), desiccated overnight and incubated at low (30%) RH and high (75% RH) for 48 hours before connecting to the CEMS system for measurement of CO_2 accumulation.

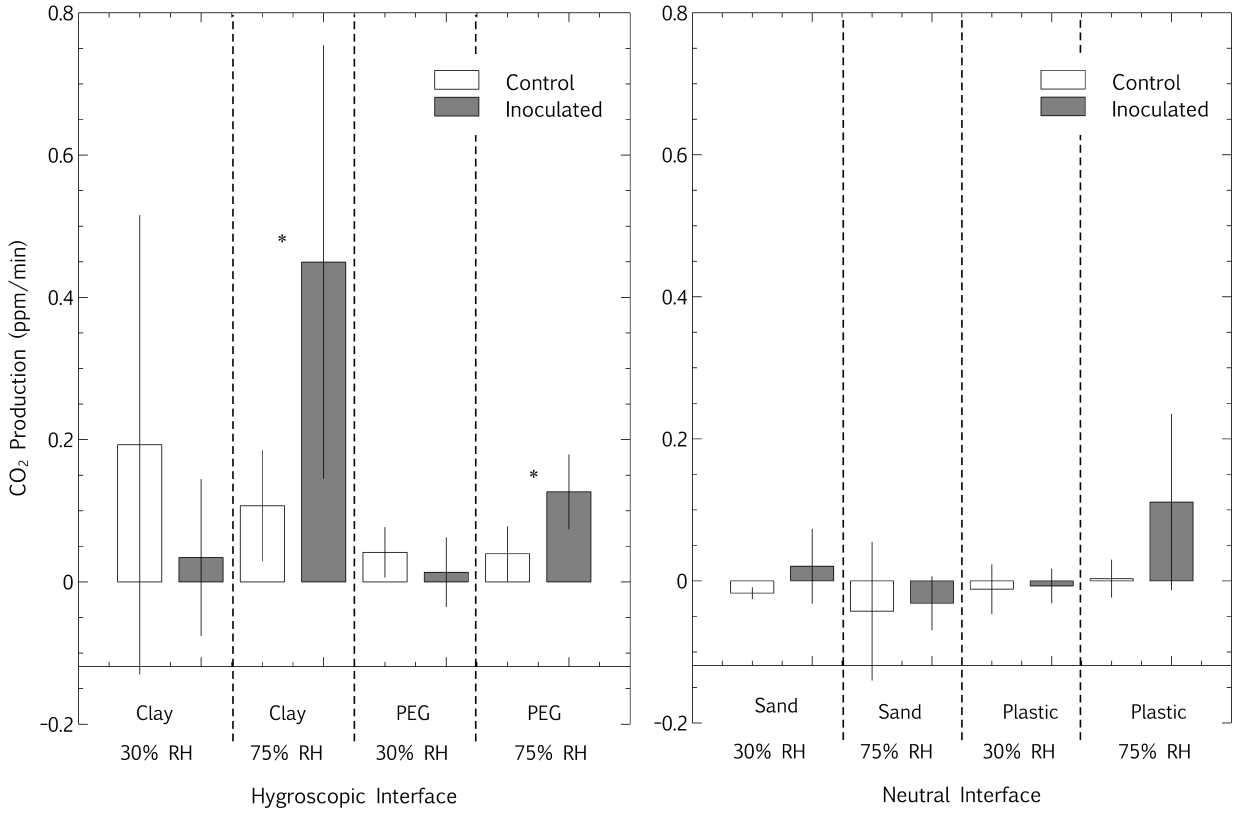

FIG 4.2.2 Microbial metabolism at surface-air interfaces: investigating the interaction of relative humidity and hygroscopicity. Enriched microbial biomass was inoculated in suspension with the 2 hygroscopic substrates (Clay and PEG) and 2 neutral substrates (Sand and Plastic/Tap Water), along with sterile controls. The inocula were statically incubated for 2 days, transferred to tubes, desiccated overnight and incubated at low (30%) RH and high (75%) RH for 2 days. The rate (gradient, Fig 4.2.1) of carbon dioxide accumulation was compared between samples. Bars represent means of a minimum of 4 samples, and error bars represent the standard deviation. The difference between the means of inoculated and sterile controls were statistically calculated with a Student's independent t-test, and significant differences are indicated* ($p<0.05$).

Due to the relative novelty of the CEMS measurement technique, particularly in the closed-loop conformation at low metabolic rates, ATP was explored as a second metabolic indicator and thus a potential tool to confirm the persistence of microbial metabolism at surface-air interfaces at high RH. The hypothesis was that if microbial cell ATP reservoirs fluctuated in tandem with CO_2 production, with higher aerobic respiration rates leading to higher ATP production and higher CO_2 generation, then ATP/cell profiles during desiccation would reflect a similar trend to CO_2 profiles. Commercial ATP hygiene-monitoring swabs, designed to assess microbial load on nosocomial and industrial surfaces, were employed to quantify ATP on coverslips inoculated with desiccated microbial communities, using a photomultiplier to capture bioluminescence generated with the luciferin-luciferase system. Sand and bentonite inhibited the reaction, but controls demonstrated that the system is effective in a liquid system, as well as for at least a relative quantification of organisms dried directly on coverslips using the large-droplet method (Appendix B). PEG influences the ATP quantification by consistently lowering the Relative Light Units (RLU) recorded per cell, however it is still useful for studies of relative comparisons and trends (Appendix B). The ATP trends demonstrated with this system during desiccation did not reflect the CO_2 trends evident in Fig 4.2. On both glass and PEG surface-air interfaces, the ATP levels of the microbial communities were inhibited within hours at high (75%) RH, in comparison to ATP levels at low (30%) RH, whereas RH did not have a similarly immediate and dramatic effect on viable cell numbers at high RH (Fig 4.3A-D). Thus, the ATP/CFU levels were notably reduced within hours on both glass and PEG at high (75%) RH as compared to low (30%) RH (Fig 4.3E and F), although much more dramatically so on glass than on PEG. Within hours of incubation at glass-air interfaces, high RH evidenced RLU/CFU levels that were consistently approximately 10% that of low RH samples. On PEG, the mean ATP/CFU levels at

high RH were also consistently inhibited, but ranged from 6% to 80% of those at low RH. This variation could be attributed to the interference of PEG with bioluminescence detection, or due to PEG stimulating metabolism at high RH. However, in both cases of desiccation, the microbial CO_2 trends are not clearly reflected with ATP. Irrespective of the surface properties, ATP/CFU levels are significantly higher at 30% RH, whereas CO_2 is significantly higher at 75% RH on hygroscopic surfaces. Also, PEG narrowed the difference between ATP/CFU at low and high RH, but the trend was still similar to that on the glass surface, whereas the CO_2 profiles on hygroscopic surfaces are significantly different to that of neutral surfaces at high RH.

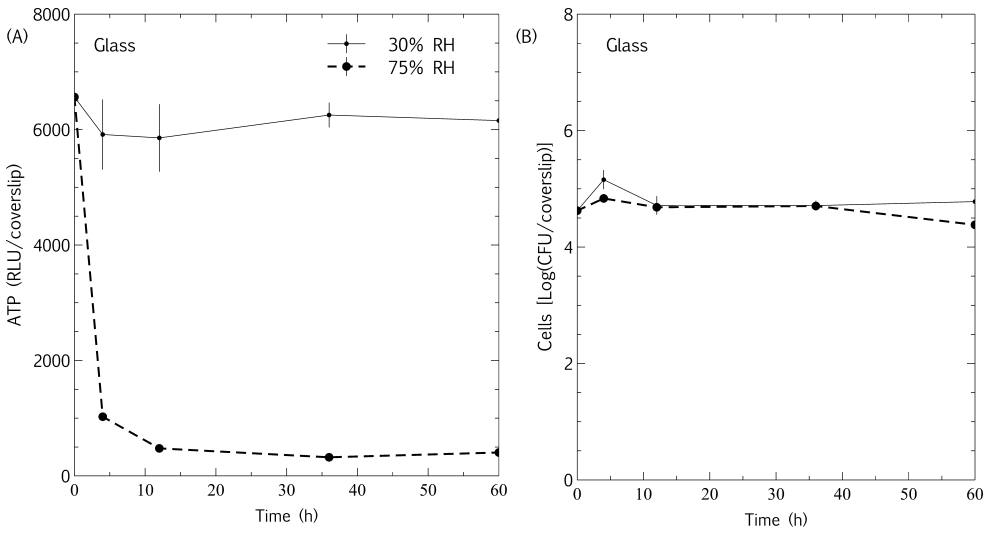

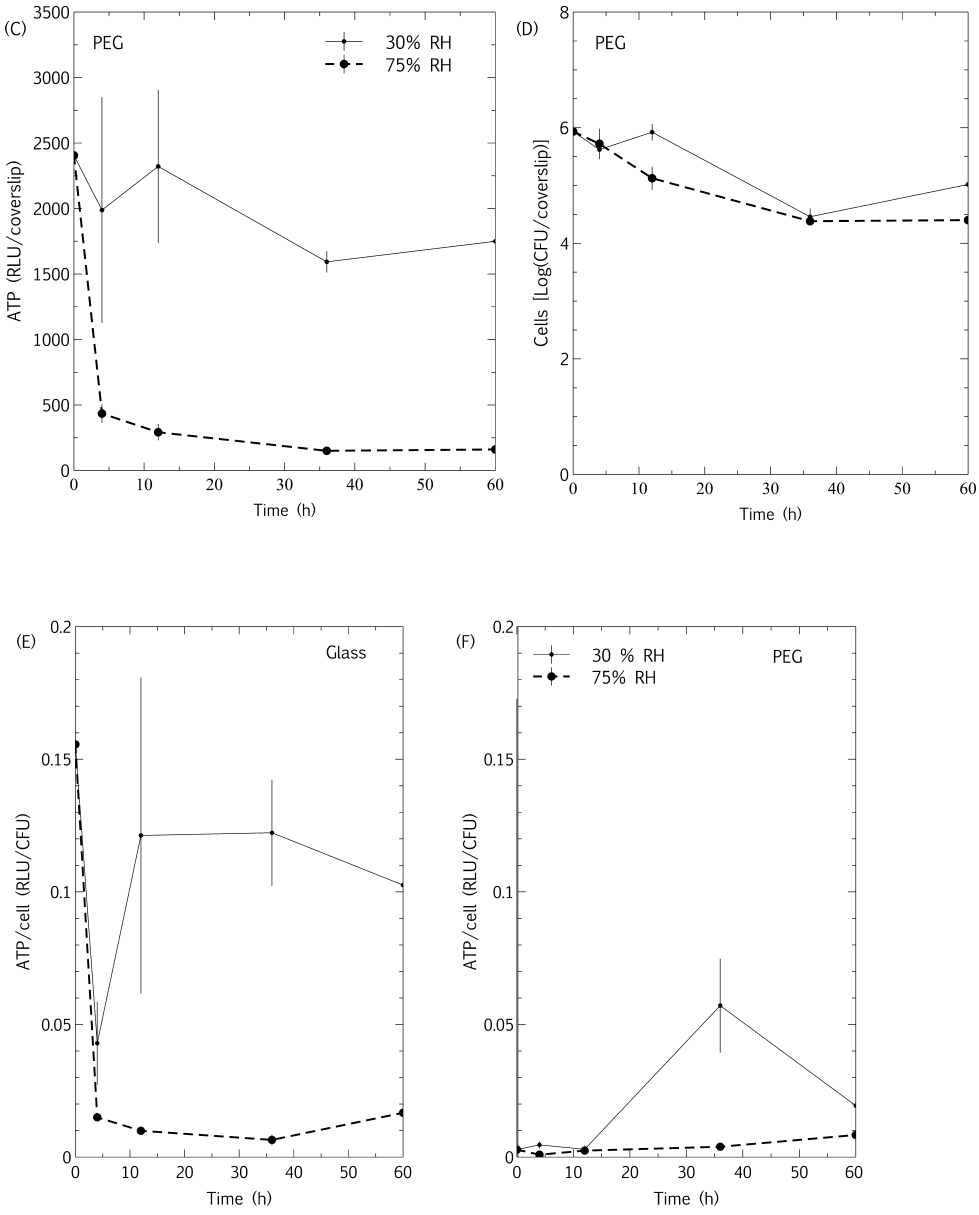

FIG 4.3 The interactive influence of relative humidity and surface hygroscopicity on community ATP levels during desiccation. Mixed microbial communities were inoculated using the large-droplet technique directly onto coverslips (A, B and E) and onto coverslips coated in pre-desiccated PEG (C, D and F). Inoculated coverslips were dried in a laminar flow hood (3-6 h) and incubated at low (30%) RH and high (75%) RH. ATP (A and C) and cell counts

(B and D) were measured over a period of 4 days and ATP/CFU (E and F) was compared. Plots represent the means of triplicate samples and error bars the standard deviation.

As ATP levels did not mirror CO_2 production rates at surface-air interfaces, a number of experiments were performed to corroborate the assumption that CO_2 gradients within a closed-loop system were due to microbial metabolism, rather than purely chemical reactions. The hypothesis was that if the CO_2 gradients measured within the closed-loop system were representative of microbial metabolism during desiccation, then (1) the addition of water would increase the gradient at both 30% RH and 75% RH, (2) the addition of a rich carbon source (3 g/L TSB) would increase the gradient even more markedly, and (3) sterile controls would show no increase in metabolism upon rewetting with water or sugar. The addition of tap water to inoculated samples incubated at 30% and 75% RH at PEG and clay interfaces increased the gradient which had effectively dropped to zero under desiccated conditions by day 7 (Fig 4.4A and B), although in both matrices the lag phase was approximately twice as long (4 h versus 2 h, respectively) for samples incubated at high (75%) RH than at low (30%) RH. An initial negative CO_2 gradient was due to chemical CO_2 equilibration, with the highly basic bentonite slurry acting as a CO_2 sink (Stone et al., 2016). The equilibration was markedly greater in microcosms incubated at 30% RH than at 75% RH, likely due to some pre-equilibration of clay-bound water in hygroscopic matrices incubated at high RH. Similarly, the addition of TSB to microbial communities desiccated at both bentonite and PEG interfaces led to an even more dramatic increase in CO_2 production rate than the addition of tap water, with zero CO_2 production in sterile controls (Fig 4.4C).

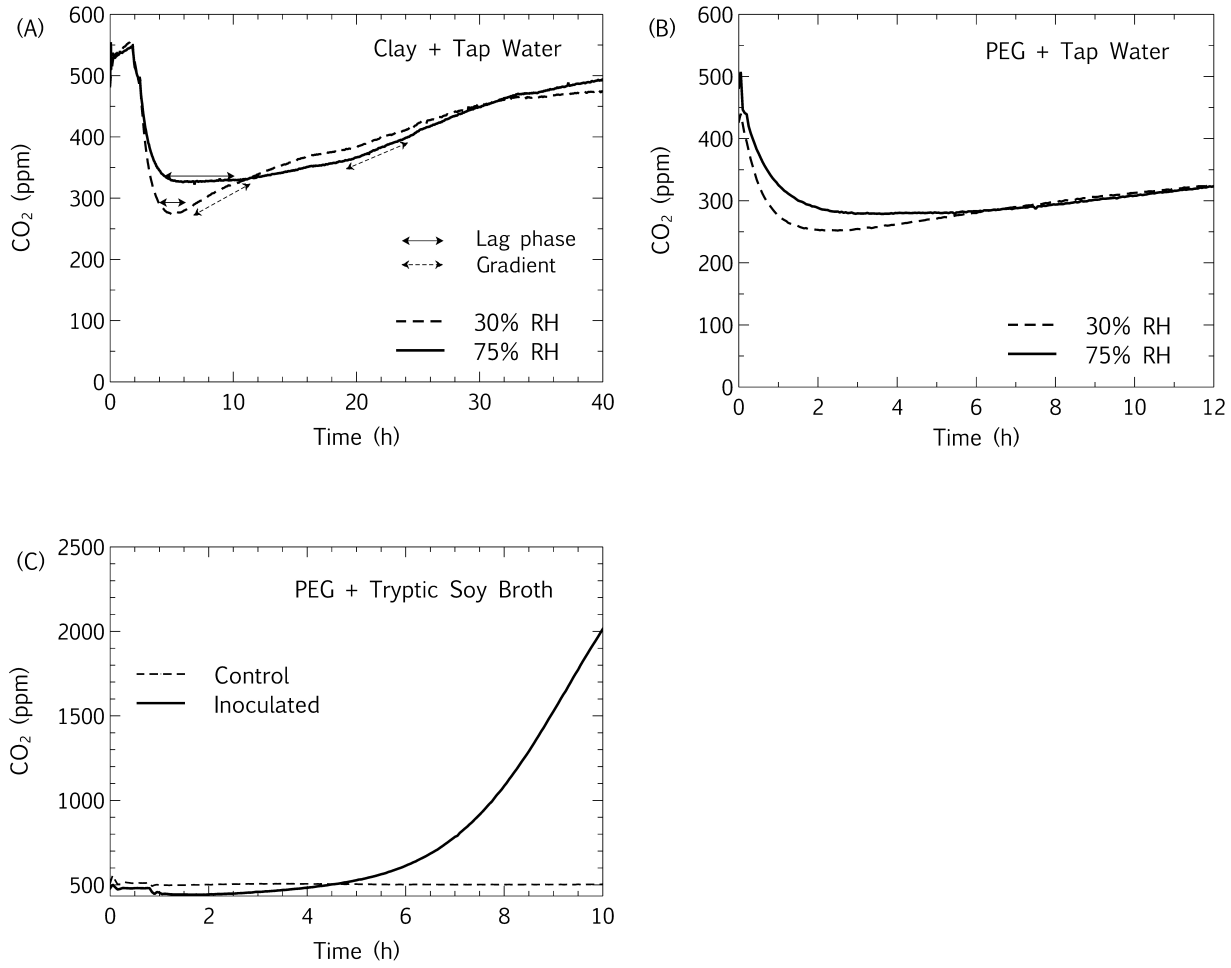

FIG 4.4 Metabolic CO_2 profiles upon rewetting of desiccated samples. Desiccated microbial communities at bentonite and PEG interfaces were incubated at low and high RH for 7 days, rewet (T0) with tap water (A and B) and CO_2 accumulation was measured in a closed-loop system. An inoculated PEG sample was compared to a sterile PEG sample by rewetting (T0) with a rich carbon source (C).

4.4.3 Metabolic Rates and Desiccation Resilience

The final hypothesis expounded on the apparently conflicting observations that microbial survival is inhibited at high RH, whereas short-term metabolic persistence is improved at high RH. The hypothesis suggests that if increased metabolic persistence lowers the adaptive strength or resilience of a desiccated microbial community at surface-air interfaces, then an oligotrophic biofilm will demonstrate a shorter lag phase and/or higher metabolic recovery rate after desiccation than a metabolically active biofilm. In *P. aeruginosa* and *Arthrobacter* biofilms, initial growth for 2 days, starvation for one day and desiccation for 2 days allowed for a full recovery of both starved and metabolically-active biofilms (Fig 4.5). The mean lag phase and CO_2 production rate of duplicated starved and active *P. aeruginosa* biofilms were not significantly different (Fig 4.5A), suggesting that within these experimental parameters, metabolic activity prior to desiccation has no influence on the resilience of a desiccated biofilm. For *P. aeruginosa* biofilms with longer desiccation periods (grown for 1 day, starved or enriched for 1 day and desiccated for 3 days), only the enriched biofilm recovered (Fig 4.6). The starved biofilm did not recover from desiccation. However, for desiccation-tolerant *Arthrobacter* biofilms (4.5B), CO_2 generation seemed to persist during desiccation of a carbon-rich biofilm, but not an oligotrophic biofilm, whereas the oligotrophic biofilm had a higher respiration peak and steady state during recovery, supporting the hypothesis.

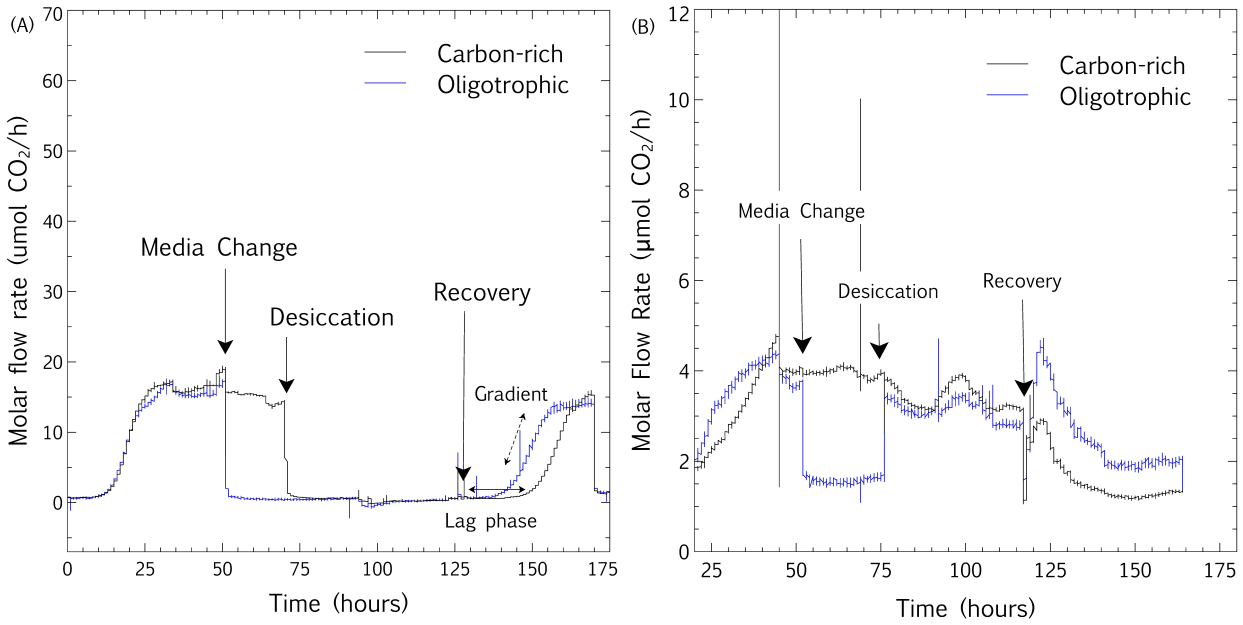

FIG 4.5 The effect of metabolic rate on the recovery of desiccated pure culture biofilms. (A) Desiccation-sensitive *Pseudomonas aeruginosa* PAO1 and (B) Desiccation-tolerant *Arthrobacter* biofilms were grown in duplicate on continuous TSB (0.3 g/L). At 2 days, one biofilm was switched to a continuous feed of tap water for 24 hours and both biofilms were run dry and desiccated for a further 2 days before re-starting continuous TSB flow. Recovery lag phase and gradients of a duplicate of each experiment were compared, assessing the influence of metabolic activity on desiccation responses.

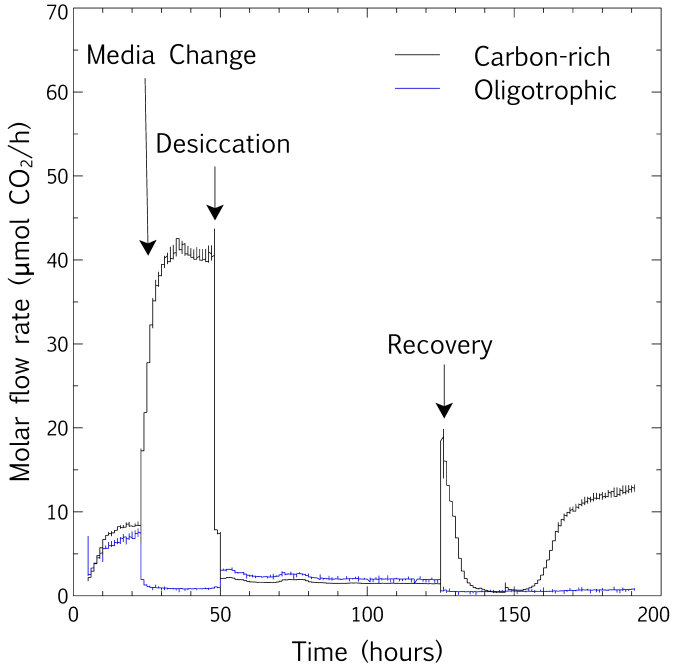

FIG 4.6 The effect of metabolic rate on the recovery of desiccated pure culture biofilms: testing the limits. Desiccation-sensitive *Pseudomonas aeruginosa* PAO1 biofilms were grown in duplicate on continuous TSB (0.3 g/L). At 1 day, one biofilm was switched to a continuous feed of tap water and the other to 3 g/L TSB for 24 hours, and both biofilms were run dry and desiccated for a further 3 days before re-starting continuous TSB flow. Recovery lag phase and gradients of a duplicate of each experiment were compared, assessing the influence of metabolic activity on desiccation responses. This experiment investigated greater metabolic extremes: higher carbon, shorter growth phase and longer desiccation phase.

4.5 Discussion

Microbial viability at surface-air interfaces is extended at low relative humidity and suppressed at high relative humidity, despite species variation (Turner and Salmonsen, 1973; Walters et al., 2005; Ronan et al., 2013). This biological principle of long-term survival at low RH is the scientific foundation of the dogma "the drier, the better", which finds extensive application in the storage of desiccated products, such as seeds or grains. However, a level of molecular rotational mobility in the cytoplasm improves desiccation resistance, and relative humidity below certain thresholds limits this mobility, suggesting that the relationship between dryness and longevity is not completely linear (Potts, 2001). On the higher end of the RH spectrum, this link between molecular mobility and water vapor has also been suggested as the central thermodynamic parameter that enables cellular aging at high RH (Walters et al., 2005), a proposal closely linked to the proposition of this work that persistent metabolism leads to a decrease in long-term community resilience.

Despite these ambiguities regarding the threshold details and molecular mechanisms of longevity, this work confirmed the bulk of literature, demonstrating that high (75%) RH inhibited the viability of both prokaryotes and eukaryotes (in communities and pure culture), as compared to low (30%) RH (Fig 3.4 and Fig 4.1). Ronan et al. (2013) used the large-droplet method to demonstrate that the survival of a desiccation-tolerant indoor air isolate, *Arthrobacter* sp., was significantly inhibited at high (75%) RH. This work aimed to extend that observation by exploring the interaction of surface hygroscopicity and water vapor, and their influence on

microbial longevity and metabolic persistence at surface-air interfaces. Due to its application as a buffer in nuclear fuel (Chapter 1-3), as well as the broader environmental occurrence of clays in soil and wetland environments, Wyoming MX-80 bentonite montmorillonite clay was chosen as the primary hygroscopic microbial substrate in this work. The viability of the natural eukaryotic and prokaryotic populations in as-received bentonite were inhibited by a year-long incubation at high (75%) RH, as compared to low (30%) RH (Chapter 3, Fig 3.4). In Fig. 4.1, the survival of desiccation-tolerant eukaryotes and prokaryotes was explored in pure culture, assessing the influence of relative humidity and surface hygroscopicity. The extended viability of *Cryptococcus* at both bentonite and glass surface-air interfaces, as compared to *Arthrobacter*, confirms several reports of increased desiccation-tolerance in eukaryotes (Fig 4.1; Brown, 1976). The extended survival of both species on bentonite, as opposed to glass, is likely due to the extra carbon (albeit limited), trace elements and buffering capacity of bentonite (Fig 4.1; Karnland et al., 2006). However, the trend of viability inhibition at high RH remained consistent throughout this study, despite the nature of the surface or the community or culture constituents.

Spore survival and viability is often explored in desiccated conditions, but even vegetative bacteria can survive for years, challenging our understanding of bacterial physiology and metabolism (Otter et al., 2015). On this note, many of the organisms explored in this dissertation are vegetative non-spore formers, including *Arthrobacter, Cryptococcus* and *Pseudomonas*, highlighting the emphasis on metabolic persistence in relation to long-term viability. In contrast to the suppression of long-term viability at high RH, microbial metabolism at bentonite-air interfaces was extended at high RH (Chapter 3, Fig 3.3). The hypothesis that the combination of hygroscopic surfaces and high RH extended microbial metabolism at surface-air interfaces was

supported, with significantly higher microbial CO_2 production at high RH on bentonite as compared to sand, and on PEG as compared to plastic surfaces (Fig 4.2). As mentioned in Chapter 3, the variation of microbial activity at high RH and hygroscopic interfaces is high, since some microcosms demonstrated high metabolism, whereas others showed no CO_2 production, without clearly observable causes for the variation. However, in both cases, only the combination of hygroscopic interfaces and high RH promoted microbial metabolism during desiccation and, despite the variation, the statistical differences between controls and inoculated samples were significant ($p<0.05$). The greater extension of metabolism at bentonite-air interfaces as compared to PEG-air interfaces is again likely due to the mineralogical properties of bentonite, providing the microbes low levels of carbon and trace elements (Fig 4.2; Karnland et al., 2006). In addition, the community comprises isolates of bentonite origin, likely more adapted to the bentonite than the PEG environment. The porosity and increased surface area of bentonite and PEG, as compared to sand and plastic, are intimately related to the hygroscopic capacities of these matrices. It has been emphasized that laboratory mineral dissolution rates are generally exaggerated, due to higher clay-surface reactive sights than natural clay deposits (Maher et al., 2006). Similarly, the activity of truly dry soil microbial populations is often difficult to extricate from the activity of microbial populations in occluded water within the soil (Stotzky and Pramer, 1972). A more fundamental link between hygroscopic surfaces, water vapor and microbial activity could be further pursued on flat surfaces coated with smooth chemical hygroscopic compounds, however these parameters of porosity and surface area are linked to hygroscopic surface-air interfaces in nature and are thus more relevant to this study. Although this study did address the challenge of measuring slower growth and metabolic rates at surface-air interfaces, as opposed to the better-studied rates in liquid culture, there are many elements that were not

representative of *in situ* scenarios. High cell concentrations was the primary unnatural parameter in most of the surface-air interface analyses, likely closest to the natural biofilms that may impact nosocomial, wastewater or food industries, rather than organisms that land on surfaces during air or vector dispersion.

ATP was assessed as a potential tool to corroborate the metabolic conclusions drawn from the CO_2 data. Hygiena swabs were selected as a tool for measuring ATP in microbial communities at surface-air interfaces. These swabs were designed as accessible, portable sanitation tests, based on the common measurement of photons generated by the luciferin-luciferase reaction. Controls demonstrated linear relationships around the cell concentrations assessed in this work based on linear regression models, in both liquid and desiccated systems (Appendix B). Although PEG interfered slightly with RLU measurements, as compared to microbial communities inoculated directly onto glass surfaces, linear associations and consistent trends were still evident within PEG samples. Making the intuitive association that more ATP/CFU is evidence of higher metabolic rates, the hypothesis suggested that if ATP is a viable tool to reflect CO_2 measurements, then microbial communities desiccated at hygroscopic surfaces and high RH will evidence higher ATP levels per viable cell in the initial phase of drying than microbial communities at glass-air interfaces at high RH, or at both PEG and glass interfaces at low RH.

The data showed an opposite trend to that expected, with almost immediate (within hours) inhibition of ATP/CFU at high RH, on both PEG and glass interfaces (Fig 4.3). A deeper exploration of literature does suggest that ATP pools are not necessarily directly coupled to respiration rates. ATP levels per cell in *Azotobacter* were shown to increase in the early log

phase, but reached a steady state that did not fluctuate despite 10-fold variations in respiration rates due to carbon influx manipulation. Anaerobic conditions significantly lowered this ATP steady state, however, demonstrating that the electron acceptor has a greater influence on ATP cell reservoirs than the electron donor (Knowles and Smith, 1970).

The uncoupling of ATP and energy flux rates has also been shown in C4 plants, where lower photosynthesis rates in the cold were shown to be independent of ATP levels, since ATP accumulated due to slower activity of the ATPase enzyme (Graham and Patterson, 1982). There is further evidence for the diverse factors that determine ATP coupling to energy fluxes in the microbial cell. For example, in *Zymomonas mobilis*, chloramphenicol led to an inhibition of protein synthesis, but not an inhibition of the monomers involved in the ATP-ADP cycle (Lazdunski and Belaich, 1972). Thus, chloramphenicol led to an increase in ATP pools, with an associated decrease in catabolic rates. In contrast, nitrogen is necessary for general catabolism as well as the monomers involved in ATP generation, and thus both catabolic rates *and* ATP pools decreased upon nitrogen starvation, again confirming that ATP pools are not necessarily directly coupled to respiration rates. These studies all suggest that ATP levels are not simple indicators of respiration rates, but are rather coupled to anabolic and catabolic fluxes and balances, influenced by many factors. Within a dry environment, the understanding of ATP levels will involve demonstrations of the distinct influence of water on catabolic and anabolic rates, and their consequent balance during desiccation. Likely, such balances are also species-specific, further complicating the use of this tool as a metabolic indicator. Interestingly, the consistent and dramatic inhibition of ATP at high RH (Fig 4.3) does suggest a complicating interpretive factor to consider in the widespread commercial use of this sanitation-monitoring system.

Since the conclusions of persistent metabolism at hygroscopic surfaces and high RH, based on CO_2 production, could not be corroborated with ATP data, further controls were designed to demonstrate that the gradients observed in the closed-loop CEMS were, in fact, due to microbial metabolism. In Fig 4.2, sterile controls did not indicate any CO_2 accumulation, suggesting that gradients were due to microbial activity. This was confirmed (FIG 4.4), as the addition of water to inoculated bentonite increased the CO_2 accumulation gradient, which was effectively zero after 7 days of desiccation (Fig 4.4A). A similar trend was evident in inoculated PEG samples (Fig 4.4B). The addition of sugar to an inoculated PEG sample produced an even more marked CO_2 accumulation gradient, whilst a sterile PEG control produced no CO_2 accumulation gradient (4.4C). Notably, when rewetting with water, the CO_2 generation lag phase was approximately twice as long in samples incubated for a week at 75% RH than samples incubated for a week at 30% RH, at both bentonite- and PEG-air interfaces. Similar *in situ* spikes in CO_2 production upon rewetting of dried agricultural and wild soils have been extensively documented, and the phenomenon has been coined the Birch Effect (Jarvis et al., 2007). The results from the present study suggest that the relative humidity at soil-air interfaces may influence the Birch Effect, due to the inhibition of microbial viability and community ATP levels at high RH (Fig 4.1-4.4).

Long-term microbial viability was inhibited in the same environment as short-term metabolic persistence (high RH, high hygroscopicity, Fig 3.4, 4.1 and 4.2), leading to the final hypothesis that persistent metabolism at surface-air interfaces would decrease the resilience of a microbial community. Previous studies of microbial populations in dust showed that lower temperature decreased the thermodynamic potential for high metabolic rates, thus lowering the aging of a population and extending survival rates (Lidwell and Lowbury, 1950). Similarly, studies concerning household mould suggest that high (80-90%) RH stimulates microbial metabolism in

house dust, as well as the growth of spore-bearing fungi, utilizing fatty acids and aldehydes in this nutrient-limited environment and producing methyl ketones and alcohols (Korpi et al., 1997). Also, relative humidity approaching saturation levels demonstrated some short-term increase in viable cells in dust microbial populations, prior to the typically reported long-term inhibition of viability at high RH (Lidwell and Lowbury, 1950). These authors proposed that the mechanism of inhibition at high RH was the concentrated salt ions dissolved at the hygroscopic interface. However, it is possible that metabolic persistence at high RH could mirror the negative thermodynamic influence of metabolic persistence at high temperatures on cell viability.

There is conflicting evidence regarding the influence of metabolic rates on desiccation tolerance. Some studies have shown that higher carbon fluxes lead to thicker biofilms, better suited to adaptation and stress responses (Condell et al., 2012). Others have rather emphasized adaptation due to stress exposure, claiming that the extensive morphological and physiological responses to desiccation are "not just indirect responses to stress, but rather responses of these cells to become more stress resistant" (de Goffau et al., 2009). Some of these morphological SOS responses include down-regulation of autolysin (leading to a lower growth rate) and the accompanying filamentation and decrease in cell separation, and increases in cell size, cell wall thickness and antibiotic resistance. At high RH more cell division is evidenced, supporting the proposal that persistent metabolic activity is linked to increased water availability and lower long-term viability.

Increased resistance to antibiotics within a biofilm, as opposed to within planktonic growth, has

been directly linked to slow growth (Otter et al., 2015). Within a biofilm, slow growth may be sustained by programmed cell death, predation or cannibalism. The concept of bacterial cell suicide was initially viewed with skepticism, since bacteria were considered single-cell organisms. However, increased evidence of programmed cell death within biofilms has strengthened the concept of biofilm as a "whole organism" (Bayles, 2014). This type of terminology has also been used within medicine, referring to the gut microbiome as an "organ" (Trinder et al., 2015). Thus, viewing a biofilm as a whole organism capable of metabolic pacing increases the legitimacy of the theory that cell suicide could contribute to survival at surface-air interfaces, and may be part of an adaptive mechanism of the slow nutrient cycling of vegetative bacterial species. Similarly, it was shown that predation influences metabolic regulation in biofilms, with ciliate predation of *Cryptococcus* biofilms preventing stagnation and stimulating persistent metabolism (Joubert et al., 2006). Thus, paced metabolism driven by the slow access to carbon from cell suicide or cell death could be a direct adaptive response linked to community desiccation resilience. Since this SOS response of programmed cell death might be directly linked to growth rate and viability (Bayles, 2014), an interesting future study would be to compare the rates of programmed cell death at high and low relative humidity. Bester et al. (2011) demonstrated that in a saturated system, planktonic cell output for proliferation only costs the biofilm 1.0±0.2% of the total carbon turnover. Within a liquid system, these cells are linked to biofilm spawning, however within a desiccated biofilm, reflecting a closed nutrient system, the same cell production could maintain a low level of persistent metabolism due to natural cell lysis, predation, cannibalism or cell suicide. The observation of Ronan et al. (2013), that cell viability during desiccation is greatly improved by the large droplet method as opposed to the spray method, supports this contention of nutrient cycling within a population. The deposition in

a larger volume of liquid, together with large numbers of other cells, may both provide important benefits over a small volume of liquid and fewer cells. Similarly, in the preliminary stages of this work, actively growing pure cultures were mixed, washed in tap water, added directly to the hygroscopic, oligotrophic substrate (bentonite or PEG), desiccated, and analyzed for CO_2 production (data not shown). There was no evidence of persistent metabolism at high RH and hygroscopic interfaces when the communities were not aged (grown into stationary phase, and subsequently washed and incubated with the oligotrophic, hygroscopic substrate for 3 days prior to inoculation and desiccation), suggesting the benefit of community adaptation to a substrate and the development of biofilm constituents like EPS.

An easily accessible and extensively studied macrobiological example of low resilience and adaptive strength as related to high carbon ingestion is the human obesity pandemic. Obesity is defined as an increased body weight of sufficient magnitude to produce adverse consequences (decrease fitness of the individual) and has been referred to as an "epidemic of energy storage" (Spiegelman and Flier, 2001). The term "storage" is critical, emphasizing that metabolic rates are not as critical as metabolic balances. The decreased fitness of the individual is caused directly by imbalances between the production and storage of energy. The measurement of CO_2 generated by a biofilm in a CEMS system reaches a steady state directly linked to the amount of carbon in the influent (Fig 4.5 and 4.6). This provides little information on the anabolic-catabolic balances within the system. Another study of population dynamics suggested the importance of carbon channeling in response to desiccation, with lower RH selecting for organisms capable of storing carbon as EPS, cell wall mucilage and phospholipids (Kakumanu et al., 2013). Carbon channeled to these adaptive shields is not involved in CO_2 or ATP generation by glycolysis and respiration.

A similar study suggested that carbon fluxes also had such predictable influences on community competition and population dynamics, suggesting that carbon channeling is a critical adaptive response linked to metabolism (Drenovsky et al., 2004). The channeling of carbon to EPS and mucilage at low RH (Kakumanu et al., 2013) is one of many intrinsic mechanistic factors that may influence, for instance, cell removal from substrates and thus the assessment of viable cell numbers in studies such as this (Fig 4.1 and 4.3). Similarly, factors such as biofilm thickness and community dynamics upon desiccation have not been addressed in this study. The distinction between immediate dormancy revival and cell growth upon rewetting can also not be elucidated using CO_2 metabolic profiles. However, the aim of the study was to attempt evaluation of the biofilm as a 'single' organism. The conclusions, although dependent on such detailed factors, are nevertheless relevant to whole-biofilm responses to desiccation. The obesity analogy is appropriate here, as it can be explored in terms of insulin responses, adipose tissue, hormonal imbalances, genetic predisposition and psychological elements. Also, as mentioned, the importance of carbon storage is crucial, and was not assessed within this study. However, despite the importance of each of these contributing factors, the ecological proposal of higher carbon input leading to lower resilience remains valid. Similarly, in this study, mechanisms like dormancy, growth rates, physiology and community dynamics are worthy of attention, but independent of these hypotheses and conclusions.

In order to explore the relation between metabolic slowness and biofilm adaptation, *Pseudomonas aeruginosa* was selected as a desiccation-sensitive candidate for the rewetting study, and *Arthrobacter* (Ronan et al., 2013) selected as a desiccation-tolerant candidate. The hypothesis evaluated the difference in desiccated biofilm recovery profiles for biofilms pre-exposed to oligotrophic conditions, as opposed to carbon-rich conditions. Oligotrophic

Pseudomonas biofilms desiccated for longer than 3 days in this study did not recover, whereas extreme carbon availability produced resilient biofilms (Fig 4.6). The parameters of desiccation resilience were the peak CO_2 production rate and steady state CO_2 production of continuous-flow re-saturated biofilms. Within oligotrophic conditions, *Pseudomonas* biofilms that had been starved showed no difference in both lag phase and increase in respiration rate to biofilms that had been metabolically active prior to desiccation (Fig 4.5A). In contrast, the desiccation-tolerant candidate, *Arthrobacter*'s, respiration profile supported the hypothesis. Oligotrophic biofilms demonstrated greater biofilm resilience (higher peak respiration rate and steady state during recovery) than carbon-rich biofilms. Interestingly, carbon-rich biofilms demonstrated low levels of persistent CO_2 generation during the desiccation period. This supports the hypothesis that higher metabolic rates may lead to lower survival. This interplay may be an adaptive mechanism in the desiccation-resistant species, and can be further investigated in other desiccation-sensitive and -resistant strains. As previously suggested, "the altered morphology and/or growth patterns of bacteria growing at low humidity might be more ecologically relevant than their textbook appearance at high humidity since their natural habitats are often dry" (Lidwell and Lowbury, 1950). Longer time periods of starvation may facilitate physiological adaptation due to metabolic pacing, and microscopy could narrow this window by direct observation of such morphological adaptation. A fascinating extension of the study would be to assess the response of desiccation-resistant species and mixed community biofilms to the same starvation and desiccation conditions, and compare whether carbon has the same positive influence on biofilm adaptation to desiccation in other well-adapted species. Potentially, in desiccation-tolerant species, metabolic pacing plays a role in community survival. In a study debunking the osmolyte accumulation hypothesis *in situ* in soils (Kakumanu et al., 2013), the adaptation response to desiccation was

more clearly linked to population diversity and dynamics than osmolyte accumulation or cell turnover, suggesting the importance of species studied. Furthermore, desiccation cycles and gradients (de Goffau et al., 2009) are more representative of natural cycles and could be incorporated into similar studies, since the impact of cycles such as the circadian rhythm on metabolism is extensive (Trinder et al., 2015; Kovac et al., 2009).

Thus, it was shown that high (75%) RH does inhibit long-term cell viability, in both prokaryotic and eukaryotic populations on neutral and hygroscopic surfaces. It was also shown that a combination of high RH and hygroscopic surfaces promotes short-term measurable respiration of microbial communities at surface-air interfaces. ATP was shown to be largely uncoupled with respiration rates at surface-air interfaces, but the addition of water and carbon to the desiccated communities confirmed the closed-loop CEMS gradient to be indicative of microbial metabolism. Finally, the notion that desiccation resilience may be improved by oligotrophy was only supported in a desiccation-tolerant *Arthrobacter* species, and not in a desiccation-sensitive *Pseudomonas* species. The interactive influence of relative humidity and surface properties on the metabolic persistence and long-term viability of microbial populations was thus explored. Both of these properties have application in natural biogeochemical cycles, nuclear waste management, and industrial settings, with increased viability promoting the potential of a community to influence its surroundings upon rewetting, and persistent, slow metabolism facilitating the potential for corrosion, dissolution, fermentation and the deposition of unwanted metabolites or biogeochemical cycling in natural environments during desiccation. An appreciation of the microbial ability to harness their matrix for access to water vapor, and the interaction of this metabolic persistence with long-term survival, is both applicable in the

modeling, monitoring or engineering of these industrial environments, and is an intriguing picture of the response of these versatile organisms to the vast challenges within which they so remarkably persist.

CHAPTER 5

Desiccation Microbiology: Context and Implications

5. Context and Implications

This study began as an investigation of microbial activity at bentonite-air interfaces, borne as part of a collaborative effort to understand microbial implications in near-field nuclear waste storage. Particularly when modeling over million-year timespans, the fundamental question regarding microbial implications in inhospitable environments is the tension between dormancy (survival) and persistent, low-level metabolism (activity) – a challenge to measure due to technological limits. From this nuclear waste application, the study grew into a more ecological and fundamental exploration of the interaction between microbial metabolism and survival at surface-air interfaces, and the influence of relative humidity and surface properties on these dynamics. As microbes are ubiquitous at surface-air interfaces, and rarely studied under desiccation, this investigation has both ecological, medical, industrial and engineering relevance outside the nuclear waste field. This chapter will firstly place the nuclear waste implications into context by describing the project within the collaborative framework commissioned by the NWMO. Subsequently, it will consider the implications of microbial metabolism under desiccation in broader industrial fields and microbial ecology. Finally, the inevitable questions that arose from these observations are proposed as areas of further investigation.

5.1 Nuclear Waste Management Organization: Collaborative Context

The foundational contribution of Stroes-Gascoyne to the field of nuclear waste microbiology in Canada has been repeatedly emphasized throughout this study. As an engineer at the AECL (Atomic Energy Canada, Ltd: a precursor crown organization to the NWMO), she identified the importance of microbes in the DGR as catalysts for some of the physical and chemical dynamics

within this harsh environment. The engineering flavor she brought to microbiological studies was practical, proposing a widely-referenced bentonite compaction density to limit microbial numbers in the DGR upon clay saturation. With the multiple barriers of corrosive-resistant copper, extensively-researched highly-compacted bentonite and well-selected geological sites (with low seismic activity and far from water sources), further biological research is pursued largely for legislative integrity, identifying areas of risk that may be less obvious, or less likely than the typical microbiological risk of sulphate reduction under saturated conditions.

This investigation was designed as part of an NWMO collaborative effort to explore any further microbiological questions in the DGR, and develop microbiological standard protocols, expertise and experience in preparation for *in situ* experiments when the first repositories are built in Canada. As indicated in Fig 5.1, the infamous molecular challenge was mandated to the research team under Josh Neufeld (Waterloo University). A deeper understanding of microbial population dynamics within the DGR would be facilitated by the extraction of DNA, RNA or metabolites from the complex clay matrix. However, as extensively discussed in Chapter 2, this has proven impossible thus far, with research turning to phospholipids fatty acids and culturing (Stroes-Gascoyne 2007; Mauclaire, 2007). The Neufeld group is exploring novel ideas for the removal of DNA from the matrix, a necessary tool in the repertoire of techniques for exploring DGR microbiology. Within this dissertation, an element of genomics was explored to contribute to this toolbox, assessing the potential influence of pH on the removal of cells and DNA from bentonite, based on the premise that there might be a link between the two remarkable characteristics of bentonite: the high pH (9-10) and the inaccessibility of genetic material. Although a decrease to neutral pH did not influence the removal of DNA from bentonite, the ionic strength of the

solution is driven by more than the pH (protons) and, thus, ion-exchange polymers or resins may be used to further expound this idea of using ion exchange to influence the binding (and release) of DNA and cells to the clay matrix in future studies.

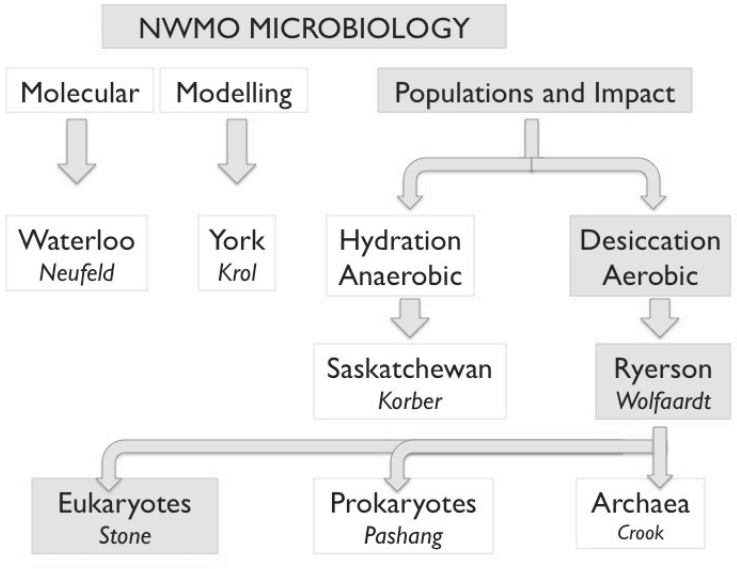

FIG 5.1 Microbiological studies in Canadian nuclear waste management: collaborations and mandates. Molecular tools are being developed by the Neufeld team (University of Waterloo) and all biological data is generated for corrosion models developed by the Krol team (York University, Toronto). The determination of culturable populations and microbial impact was mandated to two groups: Biological sulphur production under anaerobic, saturated, highly-compacted bentonite conditions is being explored by the Korber group (University of Saskatchewan) and interface microbiology is explored by the Wolfaardt group (Ryerson University, Toronto). Aerobic culturable populations in uncompacted bentonite were further divided within the Ryerson group, with a eukaryotic phylogenetic focus to this study (grey highlights). However, the DGR interface implications of metabolism and survival under desiccation were explored using both prokaryotes and eukaryotes in this study.

Although identification of microbial populations using both genomics and culturing techniques is useful, and previous studies have often focused on the numbers and species, the impacts of microbial populations are a crucial element of any microbiological study. A common microbiology mantra states that "everything is everywhere, and the environment selects", coined by Baas Becking and later termed the Baas-Becking hypothesis (O' Malley, 2007). Along with the idea of functional redundancy (Rousk et al., 2009), this suggests that within any niche, there are organisms capable of colonizing the energy and redox gradients. The integrity of the repository is thus dependent on (1) the suppression of microbial activity by the environment, (2) the potential for the dormant populations to become active if environmental limitations are lifted and (3) the potential for low-level persistent metabolism (not immediately apparent when monitoring with standard microbiological measurement techniques) to have implications over the timepans modeled for the DGR (100 000 -1 million years). Within this construct/notion, the tension between dormancy and survival again arises and underscores the importance of studying the impact of microbes: both typical microbial sulphide generation and the interaction of the broader bentonite microbiota with their environment and the sulphur reducers: across species, localizations and gradients of redox, oxygen and pH.

Corrosion models are being constructed for the NWMO by the York University research team under M. Krol, with data generated by physicists, chemists, geologists and microbiologists. Data for microbiological implications are being generated by the University of Saskatchewan (anaerobic, saturated, highly-compacted bentonite environments) and Ryerson University (desiccated, aerobic, interface bentonite environments). Within the context of this mandate, this dissertation focused on the eukaryotic phylogeny of aerobic bentonite, as prokaryotes and

archaea were assigned to two other academic studies. However, microbial interactions, impacts, survival and metabolism were explored in communities comprising both prokaryotes and eukaryotes isolated from bentonite. Within this deep geological context, the archaea and chemolithotrophs are particularly interesting, as their deep subsurface relevance has been extensively documented (Osburn, 2014), and further studies of the interactions between the various bentonite populations investigated under the NWMO mandate will add layers of understanding to microbial implications in the DGR.

Interfaces were identified as the primary area of potential microbial impact on the safe containment of used nuclear fuel, and assigned to the Ryerson group for further investigation (Stroes-Gascoyne et al., 2011A; Wolfaardt and Korber, 2012). The swelling pressure of highly compacted bentonite will only drop below the microbially-limiting threshold at these clay-air, clay-rock and rock-air interfaces during desiccation (Stroes-Gascoyne et al., 2010 and 2011A). Interfaces are also renowned for facilitating biological activity, since the harnessing of energy is driven by gradients: an inevitable consequence of the meeting of two environments at any interface. For instance, photosynthesis and most cellular chemical reactions are driven by the gradients at the intra-extracellular interface, defined by cell walls and membranes. Thus, this research demonstrated the influence of hygroscopic matrix interfaces on microbial access to water vapor during desiccation, and the potential consequence of persistent metabolism on bentonite properties. The interactions between (1) hygroscopicity and relative humidity, and (2) persistent metabolism and long-term survival were both demonstrated in this study. Tools were developed to assess microbial metabolism in this challenging matrix, and the dynamic interplay between relative humidity, hygroscopic matrices and microbial metabolism was expounded.

This study suggests that microbes could utilize a hygroscopic matrix to gain access to water vapor for persistent metabolism. It also suggests that persistent metabolism (although having potential impacts on bentonite properties) is associated with a decrease in long-term survival of bentonite populations. Thus, lower relative humidity would be associated with a higher dormant microbial population, potentially available for activity if any barrier is compromised. In contrast, if persistent microbial metabolism at high relative humidity influences the suppressive properties of bentonite in microenvironments, a cascade effect might occur. These results indicate that future *in situ* studies should consider microbial activity at bentonite-air interfaces, although such studies will likely demonstrate that the implications of metabolism during desiccation are slow enough to be negligible. In addition, the high natural salinity of Canadian groundwater (assuming any water leaks into the repository) was shown in this study to inhibit all saturated and desiccated microbial activity. Although the risk of bentonite weathering due to desiccated interface microbial activity is low, each level of risk in the multi-barrier system has to receive full attention for legislative and waste management integrity. The storage model of the NWMO includes a canister that is designed for the absolute minimum corrosion over 100 000 years, in terms of material (copper), thickness, and dynamics (bullet shape, sprayed on to eliminate welding weak points). Bentonite compaction should physically prevent the escape of radionuclides and malleability should protect the canisters from physical shock. Bentonite compaction and swelling should limit any microbial activity entirely, in the unlikely event of water availability. The placement of repositories away from underground water sources should prevent microbial access to water, other than water vapor. If water does enter the repository, the natural high salinity of Canadian groundwater will also limit microbial activity to halophiles, a much smaller pool for functional selection of microbial communities. Despite such an extensive

multi-barrier system, each level of the system is treated from the risk perspective as the only barrier, to ensure that each barrier is designed with urgency and the maximum safety possible.

5.2 Implications Outside of Nuclear Waste

Although this study was pursued with nuclear waste management as a primary focus, deep geological repositories are an example of a low-carbon, low-biomass environment. The primary conclusions of this work (microbial access to water vapor is facilitated by high relative humidity and hygroscopic matrices, and metabolic persistence may decrease desiccation tolerance) were explored as proof of principle at high cell numbers, since measuring metabolism under desiccated conditions is challenging. Thus, this study is even more relevant to niches conducive to higher cell numbers than such harsh environments as the deep subsurface. For instance, biofilms or microbial communities may grow prolifically and be exposed to desiccation (1) in pipes, (2) on rocks exposed to tides, (3) in dirty, moist built environments or (4) on food products. All of these biofilms or microbial communities could be exposed to desiccation, and could influence each environment in good or bad ways: from corrosion and degradation, to pathogen persistence or nutrient cycling and maintenance of species diversity in natural habitats. Thus the dynamic interplay between relative humidity and surface hygroscopicity, as well as the interplay between microbial metabolism and desiccation resilience, will influence microbiological implications in each of these environments.

5.3 Future research

This study can be extended within the nuclear waste context, as well as within the context of fundamental biology. Within the nuclear waste context, the obvious experimental system in continuation of this study would be *in situ* experiments in deep geological repositories. This work justifies the monitoring of bentonite-host rock interfaces. *In situ* studies may involve the long-term placement of highly compacted bentonite bricks in dry repositories, and removal of bentonite from (1) the interfaces and (2) the centre of the bricks for the assessment of the clay swell index and water retention capacity. In addition to these two parameters measured in this study, x-ray or electron diffraction could be utilized to monitor the molecular structure of the clay matrix, and compare degradation at the interfaces and the centre of the blocks. Variables to be evaluated in this experiment might include (1) relative humidity, (2) aerobic vs anaerobic interface activity or (3) localization and rates of bentonite weathering: investigating the potential of a cascade effect, if any bentonite microenvironments are compromised by aerobic surface microbial activity. Another interesting experiment would be to desiccate areas of sulphur-reducing activity in saturated bentonite, and monitor if relative humidity influences the production of sulphide, CO_2 or a change in bentonite properties in these more natural bentonite populations. In this dissertation, the impact of inoculated, aerobic bentonite microbiota was explored under desiccation, and the influence of relative humidity on this microbial activity investigated. This follow-up experiment might investigate the impact and influence of relative humidity on bentonite microbiota that are enriched *within* the bentonite by water saturation, rather than aerobic bentonite microbiota enriched under laboratory conditions and added to bentonite. Microbial communities that are stimulated in bentonite microcosms by the addition of water are presumably harnessing oxygen, pH and redox gradients and might have a greater

impact than the aerobic bentonite microbiota investigated in this study, if they can access water vapor during desiccation. Again, this would be an enriched study, which is unnatural in terms of cell numbers, but is necessary to predict whether microbes are persistently metabolizing at all below measurement detection limits, and whether this may have a long-term impact on bentonite properties, creating more conducive habitats for organisms of concern such as sulphate reducers.

In terms of fundamental research, a number of further experiments exploring the influence of relative humidity and surface hygroscopicity on microbial metabolism and survival at surface-air interfaces would be intriguing. For instance, the influence of coated surfaces on microbial metabolism, both hygroscopic and hydrophobic, and the interplay with relative humidity could be explored under pure culture conditions, to extricate the roles of surface hygroscopicity and physical surface structure on microbial access to water vapor. Furthermore, agar films would be another ideal environment in which to investigate surface-air biofilms, with the potential to utilize probes to monitor fine pH, redox and gas fluctuations during desiccation and exposure to varying relative humidity. The experiments demonstrating the potential influence of oligotrophy on desiccation resilience in *Arthrobacter*, but not *Pseudomonas*, could be further explored as a potential adaptive mechanism by repeating with other desiccation-resistant and desiccation-tolerant isolates, as well as mixed biofilm communities.

This study took on the challenge of exploring microbial activity during desiccation, as opposed to the more typical studies of desiccation survival. The ability of microbes to interact with surfaces to harness water vapor during desiccation was demonstrated, and potentially to harness

oligotrophy (the most ubiquitous natural condition facing microbes) for adaptation to desiccation. The interplay between community metabolic persistence and viability remains a fascinating ecological black box to be further unpacked.

APPENDIX A

To Chapter 3

APPENDIX A Eukaryotic bentonite isolates. The phylogenetic relationships between eukaryotic bentonite isolates (F1-F28 Consensus sequences, Y1&Y2 Consensus sequences) and closely-related species and type strains which were identified with a BLAST homology search and obtained from Genbank (accession numbers included). The dendrogram was generated with a Neighbor-Joining algorithm based on the Internal Transcribed Region of the rRNA gene cluster, with numbers on the nodes representing percentages from 1,000 bootstrap samples. *Melanogaster drosophila* was chosen as an outgroup. The strains used in this study are highlighted were deposited into Genbank (accession numbers included).

APPENDIX B

To Chapter 3

Consensus ITS Sequences for Phylogeny

F5

5’TGATGGTCTCGGCAGGCACCGGCCGGGCCTACAGAGCGGGTGACGAAGCCCCATA
CCCTCGAGGACCGGACGCGGTGCCGCCGCTGCCTTTCGGGCCCGTCCCGGGGGACG
AGGGCCCAACACACAAGCCGTGCTTGAGGGCAGCAATGACGCTCGGACAGGCATGC
CCCCCGGAATACCAGGGGGCGCAATGTGCGTTCAAAGACTCGATGATTCACTGAATT
CTGCAATTCACATTACGTATCGCATTTCGCTGCGTTCTTCATCGATGCCGGAACCAA
GAGATCCGTTGTTGAAAGTTTTAACGATTTAGCTTTTCGCTCAGACTGCAATCTTCAT
ACAGCGTTCACAGGTGTCTTCGGCGGGCGCGGACCCGGGGACGGAAGCCCCCCGGC
GGCCTGGCGGCGGGCCCGCCGAAGCAACAAGGTACGATAAACA 3’

F7

5’GTGTTTATCGTACCTTGTTGCTTCGGCGGGCCCGCCGCCAGGCCGCCGGGGGGCTT
CCGTCCCCGGGTCCGCGCCCGCCGAAGACACCTGTGAACGCTGTATGAAGATTGCA
GTCTGAGCGAAAAGCTAAATCGTTAAAACTTTCAACAACGGATCTCTTGGTTCCGGC
ATCGATGAAGAACGCAGCGAAATGCGATACGTAATGTGAATTGCAGAATTCAGTGA
ATCATCGAGTCTTTGAACGCACATTGCGCCCCCTGGTATTCCGGGGGGCATGCCTGT
CCGAGCGTCATTGCTGCCCTCAAGCACGGCTTGTGTGTTGGGCCCTCGTCCCCCGGG
ACGGGCCCGAAAGGCAGCGGCGGCACCGCGTCCGGTCCTCGAGCGTATGGGGCTTC
GTCACCCGCTCTGTAGGCCCGGCCGGTGCCTGCCGAGACCATCAATC 3’

F21

5’GGGTGTCGGCTGGCGCCGGCCGGGCCTACAGAGCGGGTGACAAAGCCCCATACGC
TCGAGGATCGGACGCGGTGCCGCCGCTGCCTTTCGGGCCCGTCCCCGGGGGAGGGG
ACGGGGCCCAACACACAAGCCGTGCTTGAGGGCAGCAATGACGCTCGGACAGGCAT
GCCCCCCGGAATACCAGGGGGCGCAATGTGCGTTCAAAGACTCGATGATTCACTGA
ATTCTGCAATTCACATTACTTATCGCATTTCGCTGCGTTCTTCATCGATGCCGGAACC
AAGAGATCCGTTGTTGAAAGTTTTAACTGATTATGATAATCAACTCAGACTGCATAC
TTTCAGAACAGCGTTCATGTTGGGGTCTTCGGCGGGCGCGGGCCCGGGGGCGCGAG
GCCTCCCCGGCGGCCGTCGAAACGGCGGGCCCGCCGAAGCAACAAGGTACGATAGA
CACGGGTGGGAGGTTGGACCCAGAGGGCCCTCACTCGGTAATGATCCTTCCGCAGG
TTCACC 3’

F8

5’TTTGGGTTGATCGGCAAGCGCCGGCCGGGCCTACAGAGCGGGTGACAAAGCCCCA
TACGCTCGAGGACCGGACGCGGTGCCGCCGCTGCCTTTCGGGCCCGTCCCCCGGGAT
CGGAGGACGGGGCCCAACACACAAGCCGGGCTTGAGGGCAGCAATGACGCTCGGA
CAGGCATGCCCCCCGGAATACCAGGGGGCGCAATGTGCGTTCAAAGACTCGATGAT
TCACTGAATTTGCAATTCACATTACGTATCGCATTTCGCTGCGTTCTTCATCGATGCC
GGAACCAAGAGATCCGTTGTTGAAAGTTTTAAATAATTTATATTTTCACTCAGACTT
CAATCTTCAGACAGAGTTCGAGGGTGTCTTCGGCGGGCGCGGGCCCGGGGGCGTGA
GCCCCCCGGCGGCCAGTAAAGGCGGGCCCGCCGAAGCAACAAGGTAAAATAAACA
CGGGTGGGAGGTTGGACCCAAAGGGCCCTCACTCGGTAATGATCCTTCCGCAGGT 3’

F19

5’TTGGGTTGATCGGCAAGCGCCGGCCGGGCCTACAGAGCGGGTGACAAAGCCCCAT
ACGCTCGAGGACCGGACGCGGTGCCGCCGCTGCCTTTCGGGCCCGTCCCCCGGAATC
GGAGGACGGGGCCCAACACACAAGCCGTGCTTGAGGGCAGCAATGACGCTCGGAC
AGGCATGCCCCCCCGGAATACCAGGGGGCGCAATGTGCGTTCAAAGACTCGATGATT
CACTGAATTTGCAATTCACATTACGTATCGCATTTCGCTGCGTTCTTCATCGATGCCG
GAACCAAGAGATCCGTTGTTGAAAGTTTTAAATAATTTATATTTTCACTCAGACTAC
AATCTTCAGACAGAGTTCGAGGGTGTCTTCGGCGGGCGCGGGCCCGGGGGCGTAAG
CCCCCCGGCGGCCAGTTAAGGCGGGCCCGCCGAAGCAACAAGGTAAATAAACACGG
GTGGGAGGTTGGACCCAGAGGGCCCTCACTCAGTAATGATCCTT 3’

F23

5’TTTGGGTTGATCGGCAAGCGCCGGCCGGGCCTACAGAGCGGGTGACAAAGCCCCA
TACGCTCGAGGACCGGACGCGGTGCCGCCGCTGCCTTTCGGGCCCGTCCCCCGGGAT
CGGAGGACGGGGCCCAACACACAAGCCGTGCTTGAGGGCAGCAATGACGCTCGGAC
AGGCATGCCCCCCCGGAATACCAGGGGGCGCAATGTGCGTTCAAAGACTCGATGATT
CACTGAATTTGCAATTCACATTACGTATCGCATTTCGCTGCGTTCTTCATCGATGCCG
GAACCAAGAGATCCGTTGTTGAAAGTTTTAAATAATTTATATTTTCACTCAGACTAC
AATCTTCAGACAGAGTTCGAGGGTGTCTTCGGCGGGCGCGGGCCCGGGGGCGTAAG
CCCCCCGGCGGCCAGTTAAGGCGGGCCCGCCGAAGCAACAAGGTAAATAAACACG
GGTGGGAGGTTGGACCCAGAGGGCCCTCACTCGGTAATGATCCTTCC 3’

F6

5’TGTTTGATGGGTGCGCGACGGGCGGGCCTACAGAGCGGGTGACAAAGCCCCATCC
CCTCGAGGACCAGACGCGGCGCCGCCGCTGCCTTTCGGGCCCGTCCCCCGGGGAGG
GGGACGAGACCCAACACACAAGCCGGGCTTGAGGGCAGCAATGACGCTCGGACAG
GCATGCCCCCCCGGAATACCAGGGGGCGCAATGTGCGTTCAAAGACTCGATGATTCA
CTGAATTCTGCAATTCACATTACGTATCGCATTTCGCTGCGTTCTTCATCGATGCCGG
AACCAAGAGATCCGTTGTTGAAAGTTTTAACTAATTTGTAATTCCACTCAGACTTCA
ATCTTCAGACAGAGTTCGAGATGTCTTCGGCGGGCGCGGGCGTAGGGGCAGGTGCC
CCCTAGCGGCCAGAATGGCGGGCCCGCCGAAGCAACAAGGTACAATAAACACGGGT
GGGAGGTTGGACCCAGAGGGCCCGTACTCGGCAATGATCCTTCCGCAGGTTCACCT
ACAGCGAAT 3’

F4

5’TGAATTGGTTGATCGGCAGGCGCCGGCCGGCCCTACAGAGCGGGTGACAAAGCCC
CATACGCTCGAGGACCAGACGCGGTGCCGCCGCTGCCTTTCGGGCCCGTCCCCCGGG
GAGGGGGACGAGACCCAACACACAAGCCGGGCTTGAGGGCAGCAATGACGCTCGG
ACAGGCATGCCCCCCGGAATACCAGGGGGCGCAATGTGCGTTCAAAGACTCGATGA
TTCACTGAATTCTGCAATTCACATTACGTATCGCATTTCGCTGCGTTCTTCATCGATG
CCGGAACCAAGAGATCCGTTGTTGAAAGTTTTAACTAATTTGTAATTCCACTCAGAC
TTCAATCTTCAGACAGAGTTCGAGATGTCTTCGGCGGGCGCGGGCGTAGGGGCAGG
TGCCCCCTAGCGGCCAGAATGGCGGGCCCGCCGAAGCAACAAGGTACAATAAACAC
GGGTGGGAGG 3’

F2

5’TTGGTTGATCGGCAGGCGCCGGCCGGGCCTACAGAGCGGGTGACAAAGCCCCATA
CGCTCGAGGACCAGACGCGGTGCCGCCGCTGCCTTTCGGGCCCGTCCCCGGGAGGG
GGGACGAGACCCAACACACAAGCCGGGCTTGAGGGCAGCAATGACGCTCGGACAG
GCATGCCCCCCCGGAATACCAGGGGGCGCAATGTGCGTTCAAAGACTCGATGATTCA
CTGAATTCTGCAATTCACATTACGTATCGCATTTCGCTGCGTTCTTCATCGATGCCGG
AACCAAGAGATCCGTTGTTGAAAGTTTTAACTAATTTGTATTTTCACTCAGACTTCAA
TCTTCAGACAGAGTTCGAGGTGTCTTCGGCGGGCGCGGGCGTAGGGGCAGGTGCCC
CTTAGCGGCCAGAATGGCGGGCCCGCCGAAGCAACAAGGTACAATAAACACGGGTG
GGAGGTTGGACCCAGAGGGCCCGCACTCGGTAATGATCCTTCCGC 3’

F15

5’TGGGGGTTGCTGGCAAGCACACGACCGGACCTCCAGAGCGAGAAGAATTACTACG
CTCGGAGCCGGACGGCACCGCCACTGACTTTAGGGCCCGCCGGGGCGGCGGGGCCC
AACACCAAGCTGAGCTTGAGGGTTGTAATGACGCTCGGACAGGCATGCCCCCCGGA
ATACCAGGGGGCGCAATGTGCGTTCAAAGATTCGATGATTCACTGAATTCTGCAATT
CACATTACTTATCGCATTTCGCTGCGTTCTTCATCGATGCCAGAACCAAGAGATCCG
TTGTTGAAAGTTTTAACTATTATATAGTACTCAGACATTATAGACAAACAGAGTTTA
GGTCCTCTGGCAGACGCTCGCCGGCCGGAGCCAGCAGCCCGAGGGCAGGCCTGCCA
AAGCAACAAAGTGTAATAAACAAAGGGTGGTAGGTTACCCGGGAGGCCTTGCGGCA
ACCCGGATGACTACTGTAAT 3’

F3

5’TGGGGTTGTTTTACGGCGTAGCCTCCCGAACACCCTTTAGCGAATAGTTTCCACAA
CGCTTAGGGGACAGAAGACCCAGCCGGACGATTTGAGGCACGCGGCGGACCGCGTT
GCCCAATACCAAGCGAGGCTTGAGTGGTGAAATGACGCTCGAACAGGCATGCCCCC
CGGAATACCAGGGGGCGCAATGTGCGTTCAAAGATTCGATGATTCACTGAATTCTGC
AATTCACATTACTTATCGCATTTCGCTGCGTTCTTCATCGATGCCAGAACCAAGAGA
TCCGTTGTTAAAAGTTTTAATTTATTAATTAAGTTTACTCAGACTGCAAAGTTACGCA
AGAGTTTGAAGTGTCCACCCGGAGCCCCCGCCCGAAGGCAGGGTCGCCCCGGAGGC
AACAGAGTCGGACAACAAAGGGTTATGAATAACCAGGCCGAAGCCCGGGCGTTCTT
GTAATGATCCCTCCGCAGGT 3’

F20

5’GTTGGGTGTTTTACGGCATGGCCGCGCCGCTCTCCAGTTGCGAGGTGTTAGCTACT
ACGCAATGGAAGCTGCGGCGGGACCGCCACTGTATTTGAGGGACGGCGTGTGCCCA
CAGGGGGCTTCCGCCGATCCCCAACGCCAGGCCCGGGGGCCTGAGGGTTGTAATGA
CGCTCGAACAGGCATGCCCGCCAGAATACTGGCGGGCGCAATGTGCGTTCAAAGAT
TCGATGATTCACTGAATTCTGCAATTCACATTACTTATCGCATTTCGCTGCGTTCTTC
ATCGATGCCAGAGCCAAGAGATCCGTTGTTGAAAGTTTTAATTTATTTGCTTGTTTAC
TCAGAAAAACATTATAAAAACAGAGTTAGGGGTCCTCTGGCGGGGGCGGCCCGTTG
TTACAGGGCCGTCTGTTCCCGCCGAAGCAACGTTTTAGGTATGTTCACAGGGTTGAT
GAGTTGTATAACTCGGTAATGATCCCTC 3’

F14

5’GTTGGGTGTTTAACGGCTGTGGACGCGCCGCGCTCCCGATGCGAGTGTGCAAACT
ACTGCGCAGGAGAGGCTGCGGCGAGACCGCCACTGTATTTCGGAGACGGCCACCCG
CTAAGGGAGGGCCGATCCCCAACGCCGACCCCCCGGAGGGGTTCGAGGGTTGAAAT
GACGCTCGGACAGGCATGCCCGCCAGAATACTGGCGGGCGCAATGTGCGTTCAAAG
ATTCGATGATTCACTGAATTCTGCAATTCACATTACTTATCGCATTTCGCTGCGTTCT
TCATCGATGCCAGAACCAAGAGATCCGTTGTTGAAAGTTTTGATTCATTTTCGAAAC
GCCTACGAGAGGCGCCGAGAAAGGCTCAGATTATAAAAAAACCCGCGAGGGGGTAT
ACAATAAGAGTTTTAGGTTGGTCCTCCG 3’

F25

5’GCCGGGCACTGCTTCACGGCGTGCGCGGCTGGGCCGGCCCTGCTGAATTATTCACC
CGTGTCTTTTGCGTACTTCTTGTTTCCTGGGTGGGCTCGCCCGCCATCAGGACCAACC
ACAAACCTTTTGCAATAGCAATCAGCGTCAGTAACAACGTAATTAATTACAACTTTC
AACAACGGATCTCTTGGTTCTGGCATCGATGAAGAACGCAGCGAAATGCGATACGT
AGTGTGAATTGCAGAATTCAGTGAATCATCGAATCTTTGAACGCACATTGCGCCCTT
TGGTATTCCAAAGGGCATGCCTGTTCGAGCGTCATTTGTACCCTCAAGCTTTGCTTGG
TGTTGGGCGTCTTTTGTCTCCAGTTCGCTGGAGACTCGCCTTAAAGTCATTGGCAGCC
GGCCTACTGGTTTCGGAGCGCAGCACAAGTCGCGCTCTTTGCCAGCCAAGGTCAGCG
TCCAGCAAGCCTTTTTTTTCAACCTTTGACCTCGGATCAGGTAGGGATACCCGCTGA
ACTTAAGCATATCA 3’

Y2

5’AGATGTCAAAGTTACACAATGAGTAACATCCAAAGATGCACTTAAAGTGATGGTT
TAGTTAGCAGACAGTAGTCTAGGTCCTGGCCATCCGAAGATGTCCTCAGCAAAATAC
TTATTATGCCAAGTCAAACCAGTCATATAGACAGATCCAAGCTAATACTTTTAAGAT
GAGTCGGTTCATCACCGGCAAACATCCAAATCCAAACTCAAGCATGGATCGAAATC
CAAAACTTGGGTTTGAGGGTTTCATGACACTCAAACAGGCATGCTCCTCGGAATACC
AAGGAGCGCAAGGTGCGTTCAAAGATTCGATGATTCACTGAATTCTGCAATTCACAT
TACTTATCGCATTTCGCTGCGTTCTTCATCGATGCGAGAGCCAAGAGATCCGTTGTTG
AAAGTTTTATTATGTTATAATAAGACTACATTTGTTACAATAATGTTTAGTTTAAAAG
TGGATGCAAGCATCCAACAGTGCACAGGTGTTATGGATATGAAAGAAGAACCACTG
GCTTTCGCCTATGGTTCAATCTAAATTCATTAATGATCCTTCCGCAGG 3’

Y1

5’GATGTCAAAGTTACACAATGAGTAACATCCAAAGATGCACTTAAAGTGATGGTTT
AGTTAGCAGACAGTAGTCTAGGTCCTGGCCATCCGAAGATGTCCTCAGCAAAATACT
TATTATGCCAAGTCAAACCAGTCATATAGACAGATCCAAGCTAATACTTTTAAGATG
AGTCGGTTCATCACCGGCAAACATCCAAATCCAAACTCAAGCATGGATCGAAATCC
AAAACTTGGGTTTGAGGGTTTCATGACACTCAAACAGGCATGCTCCTCGGAATACCA
AGGAGCGCAAGGTGCGTTCAAAGATTCGATGATTCACTGAATTCTGCAATTCACATT
ACTTATCGCATTTCGCTGCGTTCTTCATCGATGCGAGAGCCAAGAGATCCGTTGTTG
AAAGTTTTATTATGTTATAATAAGACTACATTTGTTACAATAATGTTTAGTTTAAAAG
TGGATGCAAGCATCCAACAGTGCACAGGTGTTATGGATATGAAAGAAGAACCACTG
GCTTTCGCCTATGGTTCAATCTAAATTCATTAATGATCCTTCCGCAGGTTA 3’

F1

5’ATCAAGTTGTTGAATGTTTTCTTTGGGAGGCCCCCAAGGCAATAATAAAGTTCTAG
TTCGCAAGAGCTTTCGCTTGAAATTAAGAAAAAGTTCAGGCGCAATCAAACTTTGGC
TTGCAGGCCTTTAGTCATTTAAAGCGTCTCCGGGCTAGAGATTTTACTTCTAAGCCA
GATACCCTCAATGTCCCCTTAAGAAAAAAATCTTAAGGGAAGAGTTGTTTCTGATAC
TGAAACAGGCGTACCTGCTGGAATACCAGCAGGTGCAAGATGCGTTCAAAGACTCG
ATGATTCACTGAATATGCAATTCACACTAGTTATCGCACTTTGCTACGTTCTTCATCG
ATGCGAGAACCAAGAGATCCGTTGTTAAAAGTTGTTTTATAGGCCACCTTTCAGCGA
GCCCATGTTACAATATTAATACTGAATTCATTTGGTAGAATAATTAATTTTTGGGGTA
CCAAGCTGAAAAAAAGTCGGCTTGACCATGGCTTCGATTAAAATCATCCTGTGCCGC
CTACCCCGTATGGCGGCTCAGGCATCTCTACTAGCGCCATGCTATAAGACAGTTCAC
GGTAAAAAATAAGAGAAAAACCAAGCCCGTAAGCCCAGTTTCCCCTCAAGTTTTATT
TAATGATCCTTCCGCA 3’

F11c

5’GTGGCTTCTGGACGCCGCCCTTGGTGGGAAGAGAGCGCGACTTGTGCTGCGTCCG
AAACCAGTAGGCCGGCTGCCAATGACTTTAAGGCGAGTCTCCCGCGAGCGGGAACA
ACAACGCCCAACACCAAGCAGAGTTGAGGGTACAAATGACGCTCGAACAGGCATGC
CCTTTGGATACCAAAGGGCGCATGTGCGTTCAAAGATTCGATGATTCACTGAATTCT
GCAATTCACACTACGTATCGCATTTCGCTGCGTTCTTCATCGATGC 3’

F10

5’TCAAGAGTGTAAAAATGTACTTTTGGACGTCGTCGTTATGAGTGCAAAGGCGAGA
TGTACTGCGCTCCGAAATCAATACGCCGGCTGCCAATTGTTTTAAGGCGAGTCTACA
CGCAGAGGCGAGACAAACACCCAACACCAAGCAGAGCTTGAAGGTACAAATGACG
CTCGAACAGGCATGCCCCATGGAATACCAAGGGGCGCAATGTGCGTTCAAAGATTC
GATGATTCACTGAATTCTGCAATTCACACTACTTATCGCATTTCGCTGCGTTCTTCAT
CGATGCCAGAACCAAGAGATCCGTTGTTGAAAGTTGTAACTATTATGTTTTTTCAGA
CGCTGATTGCAACTGC 3’

F12a

5’GCTGGACGCTGACCTTGGCTGGCAAAGAGCGCGACTTGTGCTGCGCTCCGAAACC
AGTAGGCCGGCTGCCAATGACTTTAAGGCGAGTCTCCAGCGAACTGGAGACAAAAG
ACGCCCAACACCAAGCAAAGCTTGAGGGTACAAATGACGCTCGAACAGGCATGCCC

TTTGGAATACCAAAGGGCGCAATGTGCGTTCAAAGATTCGATGATTCACTGAATTCT
GCAATTCACACTACGTATCGCATTTCGCTGCGTTCTTCATCGATGCCAGAACCAAGA
GATCCGTTGTTGAAAGTTGTAATTAATTACGTTGTTACTGACGCTGATTGCTATTGCA
AAAGGTTTGTGGTTGGTCCTGAGGGCGGGCGAGCCCACCCAGGAAACAAGAAGTAC
GCAAAAGACACGGGTGAATAATTCAGCAGGGCCGGCCCCGCCGCGCACGCCGTGAA
GCAGTGCCCAGCGGGGGGTGTCCAGCCCGCCTGGTTATTGTGTAATGATCCCTCCG
3’

F28

5’CACTGCTTCACGGCGTGCGCGGCTGGGCCGGCCCTGCTGAATTATTCACCCGTGTC
TTTTGCGTACTTCTTGTTTCCTGGGTGGGCTCGCCCGCCATCAGGACCAACCACAAA
CCTTTTGCAATAGCAATCAGCGTCAGTAACAACGTAATTAATTACAACTTTCAACAA
CGGATCTCTTGGTTCTGGCATCGATGAAGAACGCAGCGAAATGCGATACGTAGTGTG
AATTGCAGAATTCAGTGAATCATCGAATCTTTGAACGCACATTGCGCCCTTTGGTAT
TCCAAAGGGCATGCCTGTTCGAGCGTCATTTGTACCCTCAAGCTTTGCTTGGTGTTGG
GCGTCTTTTGTCTCCAGTTCGCTGGAGACTCGCCTTAAAGTCATTGGCAGCCGGCCT
ACTGGTTTCGGAGCGCAGCACAAGTCGCGCTCTTTGCCAGCCAAGGTCAGCGTCCAG
CAAGCCTTTTTTTTCAACCTTTGACCTCGGATCAGGTAGGGATACCCGCTGAACTTA
AGCATATCA 3’

F11e

5’GGCTTTGTGGATGCTGACCTTGGCTGGAAGAGAGCGCGACTTGTGCTGCGCTCCGA
AACCAGTAGGCCGGCTGCCAATAACTTTAAGGCGAGTCCCCAGCGAACTGGAGACA
AGACGCCCAACACCAAGCAAAGCTTGAGGGTACAAATGACGCTCGAACAGGCATGC
CCTTTGGAATACCAAAGGGCGCAATGTGCGTTCAAAGATTCGATGATTCACTGAATT
CTGCAATTCACACTACTTATCGCATTTCGCTGCGTTCTTCATCGATGCCAGAACCAAG
AGATCCGTTGTTGAAAGTTGTAATTATTATTATTGTTACTGACGCTGATTGCAATTAC
AAAAGGTTTATGGTTTGTCCTTGTGGTGGGCGAACCCACCAAGGAAACAAGAAGTA
CGCAAAAGACACGGGTGAATAATTCAGCAAGGCTGGCCCCAACAGCGCACGCCGCA
AAGCAACGCACTGCTGGGGGGAGTCCAGCCCGCTTTCATATTGTGTAATGATCCCTC
CG 3’

F9

5’GGCTTAATGGATGCTAGACCTTTGCTGATAGAGAGTGCGACTTGTGCTGCGCTCCG
AAACCAGTAGGCCGGCTGCCAATTACTTTAAGGCGAGTCTCCAGCAAAGCTAGAGA
CAAGACGCCCAACACCAAGCAAAGCTTGAGGGTACAAATGACGCTCGAACAGGCAT
GCCCTTTGGAATACCAAAGGGCGCAATGTGCGTTCAAAGATTCGATGATTCACTGAA
TTCTGCAATTCACACTACTTATCGCATTTCGCTGCGTTCTTCATCGATGCCAGAACCA
AGAGATCCGTTGTTGAAAGTTGTAATTATTAATTTGTTACTGACGCTGATTGCAATTA
CAAAAGGTTTATGTTTGTCCTAGTGGTGGGCGAACCCACCAAGGAAACAAGAAGTA
CGCAAAAGACAAGGGTGAATAATTCAGCAAGGCTGTAACCCCGAGAGGTTCCAGCC
CGCCTTCATATTTGTGTAATGATCCCTCCGCAGGTT 3’

F12b

5’TGGATGCTAGACCTTTGCTGATAGAGAGTGCGACTTGTGCTGCGCTCCGAAACCAG
TAGGCCGGCTGCCAATTACTTTAAGGCGAGTCTCCAGCAAAGCTAGAGACAAGACG
CCCAACACCAAGCAAAGCTTGAGGGTACAAATGACGCTCGAACAGGCATGCCCTTT
GGAATACCAAAGGGCGCAATGTGCGTTCAAAGATTCGATGATTCACTGAATTCTGCA
ATTCACACTACTTATCGCATTTCGCTGCGTTCTTCATCGATGCCAGAACCAAGAGAT
CCGTTGTTGAAAGTTGTAATTATTAATTTGTTACTGACGCTGATTGCAATTACAAAA
GGTTTATGTTTGTCCTAGTGGTGGGCGAACCCACCAAGGAAACAAGAAGTACGCAA
AAGACAAGGGTGAATAATTCAGCAAGGCTGTAACCCCGAGAGGTTCCAGCCCGCCT
TCATATTTGTGTAATGATCCCTCCGCA 3’

F12c

5’TGGATGCTAGACCTTTGCTGATAGAGAGTGCGACTTGTGCTGCGCTCCGAAACCAG
TAGGCCGGCTGCCAATTACTTTAAGGCGAGTCTCCAGCAAAGCTAGAGACAAGACG
CCCAACACCAAGCAAAGCTTGAGGGTACAAATGACGCTCGAACAGGCATGCCCTTT
GGAATACCAAAGGGCGCAATGTGCGTTCAAAGATTCGATGATTCACTGAATTCTGCA
ATTCACACTACTTATCGCATTTCGCTGCGTTCTTCATCGATGCCAGAACCAAGAGAT
CCGTTGTTGAAAGTTGTAATTATTAATTTGTTACTGACGCTGATTGCAATTACAAAA
GGTTTATGTTTGTCCTAGTGGTGGGCGAACCCACCAAGGAAACAAGAAGTACGCAA
AAGACAAGGGTGAATAATTCAGCAAGGCTGTAACCCCGAGAGGTTCCAGCCCGCCT
TCATATTTGTGTAATGATCCCT 3’

F26

5’TTGTGGACGCTACCTTTCAACGTTGCTTCGGCGGGCGGCCCGCTACCCTGGAAAGC
CCCTGTGGCCGCCCGGGGCTGCGAGCCCCCCGGCCCCCCTCGCGGGGGCGCCCGCC
GGAGGATACCCAACTCTTGATTATTTTAGGCCTCTCTGAGTCTTCTGTACTGAATAAG
TCAAAACTTTCAACAACGGATCTCTTGGTTCTGGCATCGATGAAGAACGCAGCGAAA
TGCGATAAGTAATGTGAATTGCAGAATTCAGTGAATCATCGAATCTTTGAACGCACA
TTGCGCCCGCCAGTATTCTGGCGGGCATGCCTGTTCGAGCGTCATTTCAACCATCAA
GCCCCAGGCTTGTGTTGGGGACCTGCGGCTGCCGCAGGCCCTGAAATCCAGTGGCG
GGTTCGCTGTCACCCC 3’

APPENDIX C

To Chapter 4

Microbial ATP, Age and Desiccation

1. Materials and Methods

1.1 Saturated microbial ATP measurements: Dilutions

Arthrobacter sp. was grown overnight in TSB (3 g/L, agitation, room temperature), washed 3 times and diluted to about 10^6 cells/mL in sterile tap water. A dilution series was set up, including 10, 25, 50 and 100 % (v/v) of this starting culture in sterile tap water. Of each dilution, 5 µL was added to a Hygenia commercial swab for ATP measurement in a luminometer. Each measurement was made in triplicate, and the mean ATP measurements (RLU/5 µL) were associated with the dilution, based on a linear regression model.

1.2 Saturated Microbial ATP measurements: Age

Arthrobacter sp. was grown for 7 days in TSB (3 g/L, agitation, room temperature). ATP levels and cell concentration were measured at 12 h, 24 h, 4 days and 7 days. ATP/mL, CFU/mL and

ATP/CFU were plotted against time, assessing the effect of culture age in the presence of rich media on ATP levels in a saturated culture.

1.3 Saturated Microbial ATP measurements: Age and Starvation

The ATP levels of the mixed bacterial inocula described in Chapter 4.3.2, incubated in tap water and PEG solution, respectively, were assessed at 2 days and 5 days. Again, the (ATP) RLU of 5 µL per swab was measured along with viable cell concentrations, in triplicate. ATP levels, CFU concentrations and ATP/CFU were compared at day 2 and day 5, assessing the effect of culture age under starvation on ATP levels in a saturated community.

1.4 Desiccated Microbial ATP Measurements: Dilutions

Arthrobacter sp. was grown overnight in TSB (3 g/L, agitation, room temperature), the undiluted culture was washed 3 times in sterile tap water and a dilution series set up in (A) tap water and (B) PEG (100 g/L tap water), including 1, 12.5, 25, 50 and 100% (v/v) bacterial culture.

Six glass coverslips per dilution were inoculated with the large droplet method described in Chapter 4.1 and desiccated for 3 hours. After desiccation, 3 coverslips per dilution were swabbed for ATP measurement, and 3 coverslips were vortexed (1 min) in 5 mL physiological saline solution (0.89% v/v NaCl) and dilutions were plated on TSB for viable cell concentrations. ATP, cell concentration and ATP/CFU are linearly associated with pre-desiccation dilutions, to assess the thresholds and integrity of this commercial and accessible photomultiplier upon desiccation.

2. Results

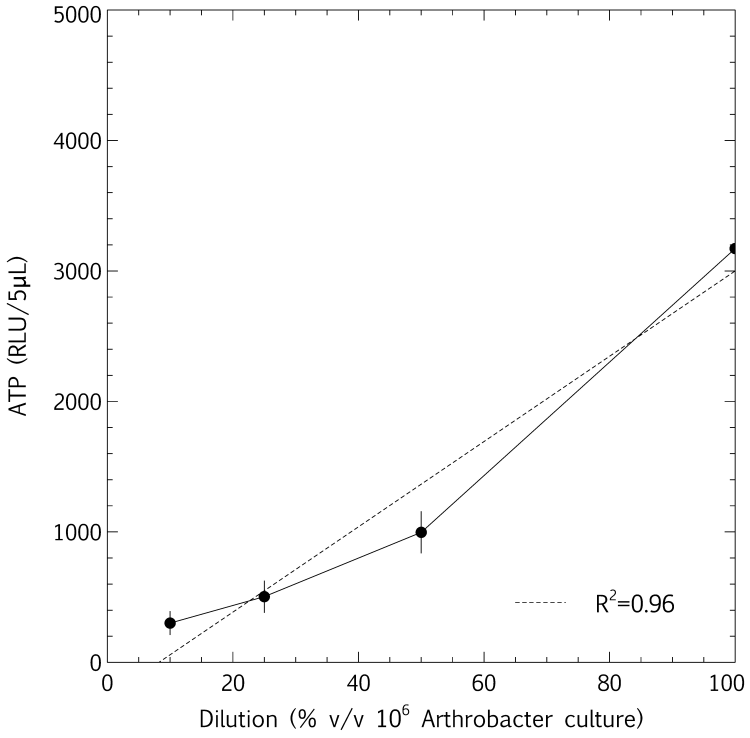

FIG 1 Saturated microbial ATP measurements: Dilutions. There was a strong association (R^2 = 0.96) between the dilution of a liquid *Arthrobacter* culture and the ATP levels measured (RLU per 5 µL of each dilution), based on a linear regression model. Thus, this commercial system designed to measure ATP at surface-air interfaces is adaptable to assess trends in liquid systems. Plots represent the means of triplicate samples and error bars the standard deviation.

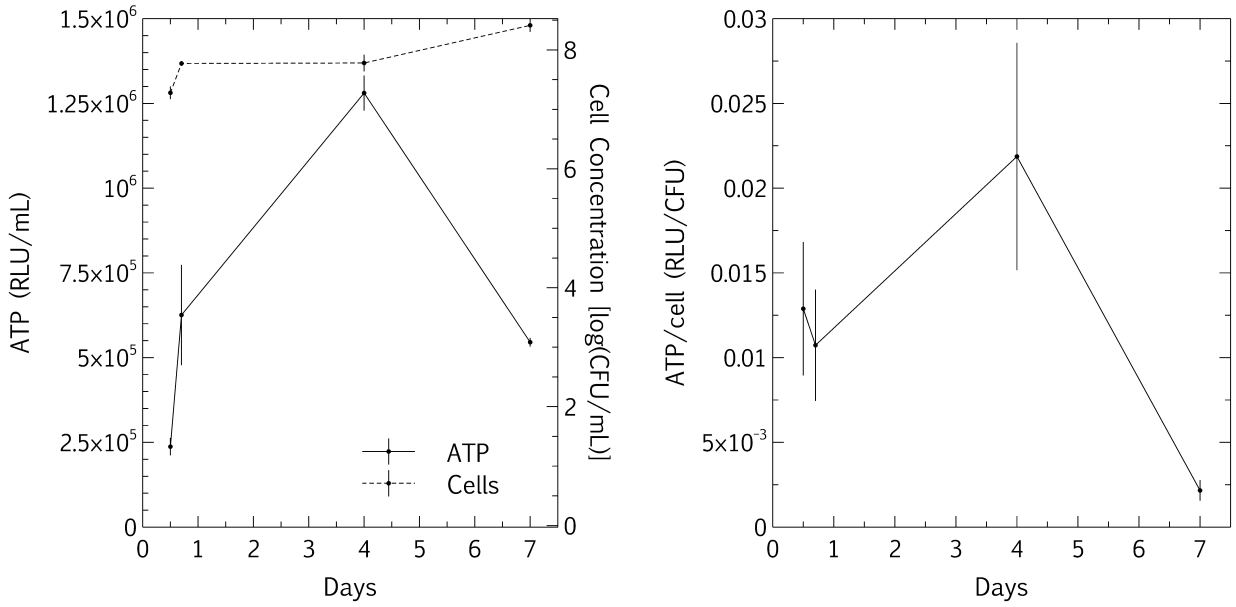

FIG 2 Saturated Microbial ATP measurements: Age. The ATP/viable cell levels in a liquid culture aged in rich carbon media remain relatively consistent at approximately 0.01-0.02 RLU/CFU over 4 days, but had dropped by a factor of ten by day 7. Over time, the aging of cells reflects a slow drop in ATP/viable levels in a nutrient-rich environment.

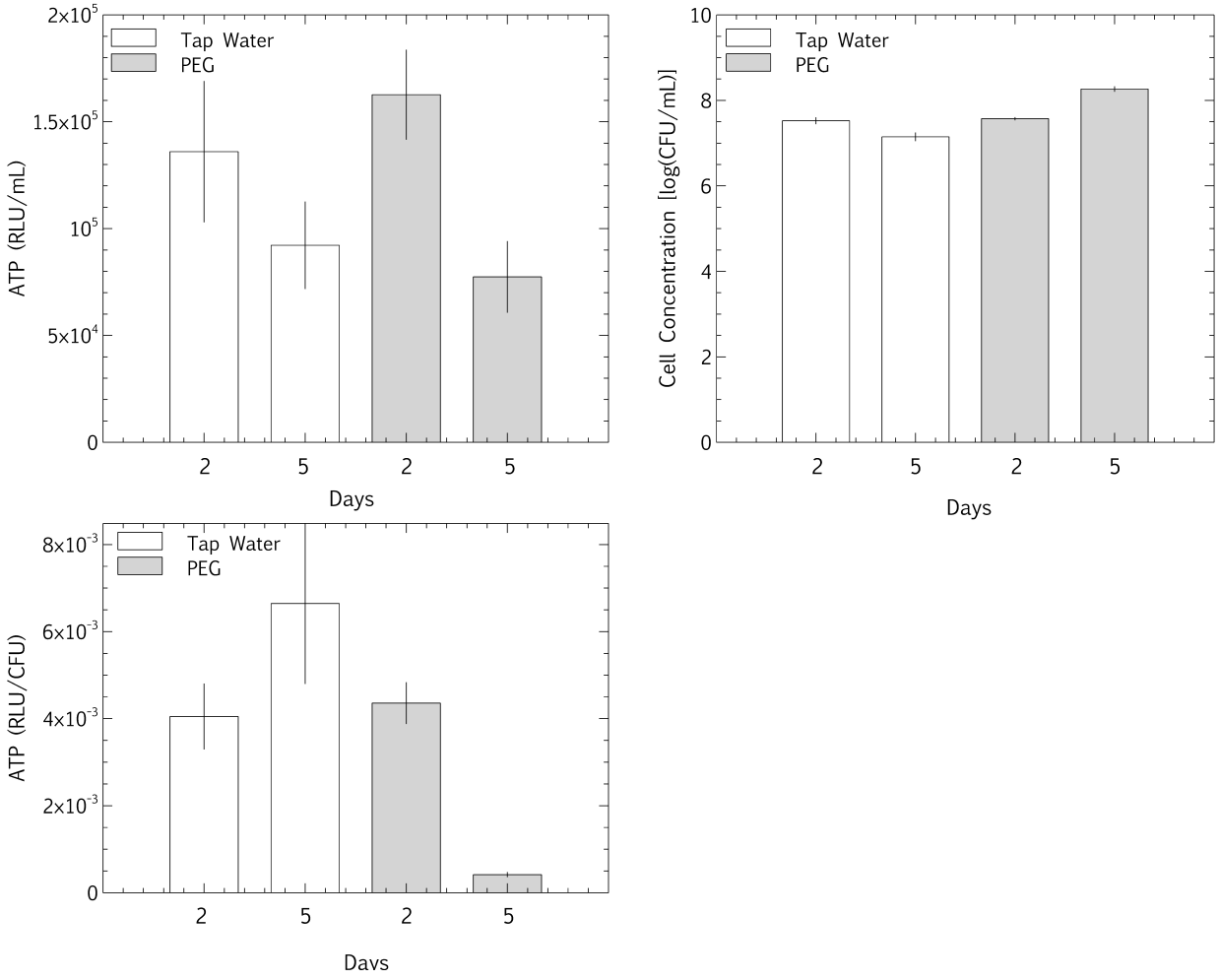

FIG 3 Saturated Microbial ATP measurements: Age and Starvation. Mixed microbial communities that were aged in sterile tap water showed an increase in ATP/viable cell over a period of 5 days, whereas PEG showed a decrease in ATP/cell over a period of 5 days, suggesting (in combination with Fig 2) that ATP reservoirs could potentially be depleted faster in the presence of a carbon source.

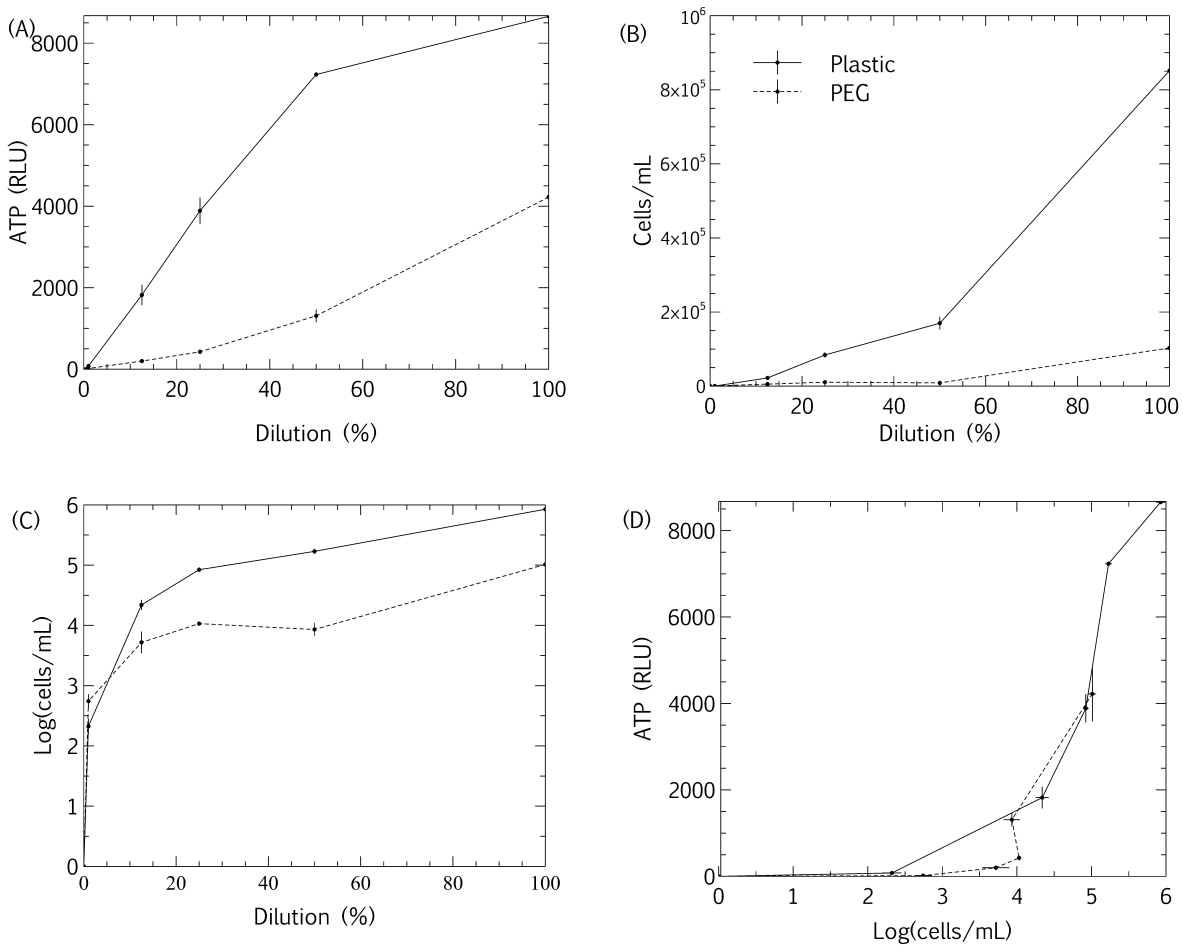

FIG 4 Desiccated Microbial ATP Measurements: Dilutions. A dilution series of an *Arthrobacter* sp. culture was inoculated onto coverslips with tap water and PEG and subsequently desiccated. Linear relationships were assessed between ATP levels, viable cell concentrations and dilutions, using linear regression. (A) ATP was linearly associated with pre-desiccation dilutions at glass-air interfaces ($R^2 = 0.895$) and PEG-air interfaces ($R^2 = 0.954$). (B) Similarly, post-desiccation cell numbers were linearly associated with the pre-desiccation dilutions at glass-air interfaces ($R^2 = 0.907$) and at PEG-air interfaces ($R^2 = 0.844$). After a log transformation of the CFU (C), the ATP/log[CFU] was shown to have a linear relationship higher than 2 log[CFU/mL], at both glass-air interfaces ($R^2 = 0.810$) and PEG-air interfaces (R^2

= 0.930). Notably, PEG consistently decreased post-desiccation ATP readings and cell concentrations at surface air interfaces.

Bibliography

1. Alakomi, H. L., Saarela, M., Gorbushina, A. A., Krumbeín, W. E., McCullagh, C., Robertson, P., & Rodenacker, K. (2006). Control of biofilm growth through photodynamic treatments combined with chemical inhibitors: In vitro evaluation methods. Proceedings of the International Conference on Heritage, Weathering and Conservation, HWC 2006 2, 713-717.
2. Alpert, P. (2005). The limits and frontiers of desiccation-tolerant life. *Integr Comp Biol,* 45(5), 685-695.
3. ASTM D5890-02. 2009. Standard test method for fluid loss of clay component of geosynthetic clay liners, ASTM International, West Conchohoken, PA. doi: 10.1520/D5891-02R09.
4. ASTM D5890-11. 2011. Standard test method for swell index of clay mineral component of geosynthetic clay liners, ASTM International, West Conchohoken, PA. doi: 10.1520/D5890-11.
5. Atlas, R. M. (2010). Handbook of microbiological media. CRC press, Florida.
6. Auerbach, I. D., Sorensen, C., Hansma, H. G., & Holden, P. A. (2000). Physical morphology and surface properties of unsaturated *Pseudomonas putida* biofilms. *J Bacteriol*, 182(13), 3809-3815.
7. Babauta, J. T., Nguyen, H. D., Harrington, T. D., Renslow, R., & Beyenal, H. (2012). pH, redox potential and local biofilm potential microenvironments within *Geobacter sulfurreducens* biofilms and their roles in electron transfer. *Biotechnol Bioeng*, 109(10), 2651-2662.

8. Barton, H. A., Taylor, N. M., Lubbers, B. R., & Pemberton, A. C. (2006). DNA extraction from low-biomass carbonate rock: an improved method with reduced contamination and the low-biomass contaminant database. *J Microbiol Meth*, 66(1), 21-31.
9. Bauermeister, A., Moeller, R., Reitz, G., Sommer, S., & Rettberg, P. (2011). Effect of relative humidity on *Deinococcus radiodurans*' resistance to prolonged desiccation, heat, ionizing, germicidal, and environmentally relevant UV radiation. *Microb Ecol,* 61(3), 715-722.
10. Bayles, K. W. (2014). Bacterial programmed cell death: making sense of a paradox. *Nat Rev Microbiol*, 12(1), 63-69.
11. Benoit, M. R., Conant, C. G., Ionescu-Zanetti, C., Schwartz, M., & Matin, A. (2010). New device for high-throughput viability screening of flow biofilms. *Appl Environ Microb*, 76(13), 4136-4142.
12. Berns, A. E., Philipp, H., Narres, H. D., Burauel, P., Vereecken, H., & Tappe, W. (2008). Effect of gamma-sterilization and autoclaving on soil organic matter structure as studied by solid state NMR, UV and fluorescence spectroscopy. *Eur J Soil Sci,* 59(3), 540-550.
13. Bester, E., Kroukamp, O., Hausner, M., Edwards, E. A., & Wolfaardt, G. M. (2011). Biofilm form and function: carbon availability affects biofilm architecture, metabolic activity and planktonic cell yield. *J Appl Microbiol*, 110(2), 387-398.
14. Bester, E., Kroukamp, O., Wolfaardt, G. M., Boonzaaier, L., & Liss, S. N. (2010). Metabolic differentiation in biofilms as indicated by carbon dioxide production rates. *Appl Environ Microb*, 76(4), 1189-1197.

15. Billi, D., Wright, D. J., Helm, R. F., Prickett, T., Potts, M., & Crowe, J. H. (2000). Engineering desiccation tolerance in *Escherichia coli*. *Appl Environ Microbiol,* 66(4), 1680-1684.

16. Billi, D. & Potts, M. (2002). Life and death of dried prokaryotes. *Res Microbiol,* 153(1), 7-12.

17. Binga, E. K., Lasken, R. S., & Neufeld, J. D. (2008). Something from (almost) nothing: the impact of multiple displacement amplification on microbial ecology. *ISME J*, 2(3), 233-241.

18. Bond, D. R., Holmes, D. E., Tender, L. M., & Lovley, D. R. (2002). Electrode-reducing microorganisms that harvest energy from marine sediments. *Science*, 295(5554), 483-485.

19. Borgesson, L. & Hernelind, J. (2014). Modelling of bentonite block compaction. Swedish Nuclear Fuel and Waste Management Report SKB P-14-10. Stockholm, Sweden.

20. Bos, R., H. C. van der Mei, & H. J. Busscher. (1999). Physico-chemistry of initial microbial adhesive interactions-its mechanisms and methods for study. *FEMS Microbiol Rev,* 23, 179-230.

21. Brown, A. D. (1976). Microbial water stress. *Bacteriol Rev*, 40(4), 803.

22. Butinar, L., Spencer-Martins, I., & Gunde-Cimerman, N. (2007). Yeasts in high Arctic glaciers: the discovery of a new habitat for eukaryotic microorganisms. *A Van Leeuw J,* 91(3), 277-289.

23. Chang, W. S., & Halverson, L. J. (2003). Reduced water availability influences the dynamics, development, and ultrastructural properties of *Pseudomonas putida* biofilms. *J Bacteriol*, 185(20), 6199-6204.

24. Chang, W. S., van de Mortel, M., Nielsen, L., de Guzman, G. N., Li, X., & Halverson, L. J. (2007). Alginate production by *Pseudomonas putida* creates a hydrated microenvironment and contributes to biofilm architecture and stress tolerance under water-limiting conditions. *J Bacteriol*, 189(22), 8290-8299.
25. Chen, J., Qin, Z., & Shoesmith, D. W. (2011). Long-term corrosion of copper in a dilute anaerobic sulfide solution. *Electrochim Acta*, 56(23), 7854-7861.
26. Cheng, L., House, M. W., Weiss, W. J., & Banks, M. K. (2015). Monitoring Sulfide-oxidizing Biofilm Activity on Cement Surfaces Using Non-Invasive Self-referencing Microsensors. *Water res,* 89, 321-329.
27. Chesterton, G. K. (1925). *The everlasting man*. Hendrickson Publishers.
28. Cline, J. D. (1969). Spectrophotometric determination of hydrogen sulphide in natural waters. *Limnol Oceanogr*, 14(3), 454-458.
29. Condell, O., Iversen, C., Cooney, S., Power, K. A., Walsh, C., Burgess, C., & Fanning, S. (2012). Efficacy of biocides used in the modern food industry to control Salmonella-links between biocide tolerance and resistance to clinically relevant antimicrobial compounds. *Appl Environ Microb*, AEM-07534
30. Corner, T. R. (1992). Ecology in a Jar. *TH YR SCH S*, 59(3), 32-36.
31. Dadachova, E., & Casadevall, A. (2011). Melanin and Resistance to Ionizing Radiation in Fungi. In *Extremophiles Handbook* (pp. 1147-1157). Springer Japan.
32. de Goffau, M. C. (2011). Microbial physiology in relation to the availability of water (Doctoral dissertation, University of Groningen).
33. de Goffau, M. C., van Dijl, J. M., & Harmsen, H. J. (2011). Microbial growth on the edge of desiccation. *Environ Microbiol*, *13*(8), 2328-2335.

34. de Goffau, M. C., Yang, X., Van Dijl, J. M., & Harmsen, H. J. (2009). Bacterial pleomorphism and competition in a relative humidity gradient. *Environ Microbiol*, *11*(4), 809-822.

35. Deng, X., Li, Z., & Zhang, W. (2012). Transcriptome sequencing of *Salmonella enterica* serovar *Enteritidis* under desiccation and starvation stress in peanut oil. *Food Microbiol*, 30(1), 311-315.

36. Dixon, D. A., Priyanto, D. G., Martino, J. B., De Combarieu, M., Johansson, R., Korkeakoski, P., & Villagran, J. (2014). Enhanced Sealing Project (ESP): evolution of a full-sized bentonite and concrete shaft seal. Geological Society, London, Special Publications, 400(1), 63-70. doi: 10.1144/SP400.33

37. Dontula, P., Macosko, C. W., & Scriven, L. E. (1998). Model elastic liquids with water-soluble polymers. *AIChE J*, 44(6), 1247.

38. Drenovsky, R. E., Vo, D., Graham, K. J., & Scow, K. M. (2004). Soil water content and organic carbon availability are major determinants of soil microbial community composition. *Microbial Ecol*, 48(3), 424-430.

39. Edgar, R. S., Green, E. W., Zhao, Y., van Ooijen, G., Olmedo, M., Qin, X., Xu, Y., Pan, M., Valekanja, U. K., Feeney, K. A., Maywood, E. S., Hastings, M. H., Baliga, N. S., Merrow, M., Millar, A. J., Johnson, C. H., Kyriacou, C. P., O' Neill, J. S. & Reddy, A. B. (2012). Peroxiredoxins are conserved markers of circadian rhythms. *Nature*, 485(7399), 459-464.

40. Ekendahl, S., O'Neill, A. H., Thomsson, E., & Pedersen, K. (2003). Characterisation of yeasts isolated from deep igneous rock aquifers of the Fennoscandian Shield. *Microbial Ecol*, 46(4), 416-428.

41. Feofilova, E. P., Ivashechkin, A. A., Alekhin, A. I., & Sergeeva, Y. E. (2012). Fungal spores: Dormancy, germination, chemical composition, and role in biotechnology (review). *Appl Biochem Micro+*, 48(1), 1-11.

42. Filip, Z. (1973). Clay minerals as a factor influencing the biochemical activity of soil microorganisms. *Folia Microbiol*, 18(1), 56-74.

43. Fisher, E. A. (1923). Some moisture relations of colloids. I. A comparative study of the rates of evaporation of water from wool, sand and clay. *Proc R Soc* A, 103(720), 139-161.

44. Fleige, S., & Pfaffl, M. W. (2006). RNA integrity and the effect on the real-time qRT-PCR performance. *Mol Aspects Med*, 27(2), 126-139.

45. Floryan, J. M., & Rasmussen, H. (1989). Numerical methods for viscous flows with moving boundaries. *Appl Mech Rev*, 42(12), 323-341.

46. Fredrickson, J. K., Zachara, J. M., Balkwill, D. L., Kennedy, D., Shu-mei, W. L., Kostandarithes, H. M., Daly, M. J., Romine, M. F., & Brockman, F. J. (2004). Geomicrobiology of high-level nuclear waste-contaminated vadose sediments at the Hanford Site, Washington State. *Appl Environ Microb*, 70(7), 4230-4241.

47. Fru, E. C., & Athar, R. (2008). In situ bacterial colonization of compacted bentonite under deep geological high-level radioactive waste repository conditions. *Appl Microbiol Biot*, 79(3), 499-510.

48. Garamszeghy, M. 2010. Nuclear Fuel Waste Projections in Canada–2010 Update. Nuclear Waste Management Organization Technical Report TR-2010-17. Toronto, Canada.

http://dgr.nwmo.ca/uploads_managed/MediaFiles/1678_nwmotr-2010-17_nuclearfuelwast.pdf

49. Garg, K. L., Jain, K. K., & Mishra, A. K. (1995). Role of fungi in the deterioration of wall paintings. *Sci Total Environ*, 167(1), 255-271.
50. Ghadakpour, M., Bester, E., Liss, S. N., Gardam, M., Droppo, I., Hota, S., & Wolfaardt, G. M. (2014). Integration and Proliferation of *Pseudomonas aeruginosa* PA01 in Multispecies Biofilms. *Microb Ecol*, 1-11.
51. Gómez-Suárez, C., H. J. Busscher, and H. C. van der Mei. 2001. Analysis of bacterial detachment from substrate surfaces by the passage of air-liquid interface. *Appl Environ Microb,* 67:2531-2537.
52. González-Pinzón, R., Haggerty, R., & Myrold, D. D. (2012). Measuring aerobic respiration in stream ecosystems using the resazurin-resorufin system. *J Geophys Res-Biogeo,* 117(G3).
53. Gorbushina, A. A. (2007). Life on the rocks. *Environ Microbiol, 9*(7), 1613-1631.
54. Gorbushina, A. A. & Broughton, W. J. (2009). Microbiology of the atmosphere-rock interface: How biological interactions and physical stresses modulate a sophisticated microbial ecosystem. *Annu Rev Microbiol,* 63, 431-450.
55. Gostinčar, C., Muggia, L., & Grube, M. (2012). Polyextremotolerant black fungi: oligotrophism, adaptive potential, and a link to lichen symbioses. *Front Microbiol, 390.*
56. Graham, D., & Patterson, B. D. (1982). Responses of plants to low, nonfreezing temperatures: proteins, metabolism, and acclimation. *Annu Rev Plant Physio*, 33(1), 347-372.

57. Greenspan, L. (1977). Humidity fixed points of binary saturated aqueous solutions. *J Res Nat Bur Stand*, 81(1), 89-96.

58. Grishkan, I. (2011). Ecological stress: Melanization as a response in fungi to radiation. In *Extremophiles Handbook* (pp. 1135-1145). Springer Japan.

59. Guglielminetti, M., Morghen, C. D. G., Radaelli, A., Bistoni, F., Carruba, G., Spera, G., & Caretta, G. (1994). Mycological and ultrastructural studies to evaluate biodeterioration of mural paintings. Detection of fungi and mites in frescos of the Monastery of St Damian in Assisi. *Int Biodeter Biodegr*, 33(3), 269-283.

60. Hallbeck, L., & Pedersen, K. (2012). Culture‐dependent comparison of microbial diversity in deep granitic groundwater from two sites considered for a Swedish final repository of spent nuclear fuel. *FEMS Microbiol Ecol*, 81(1), 66-77.

61. Harbers, G. M., Emoto, K., Greef, C., Metzger, S. W., Woodward, H. N., Mascali, J. J., Grainger, D. W. & Lochhead, M. J. (2007). Functionalized poly (ethylene glycol)-based bioassay surface chemistry that facilitates bio-immobilization and inhibits nonspecific protein, bacterial, and mammalian cell adhesion. *Chem Mat*, 19(18), 4405-4414.

62. Henderson, B. L., & Bui, E. N. (2002). An improved calibration curve between soil pH measured in waterand $CaCl_2$. *Soil Res*, 40(8), 1399-1405.

63. Hirsch, P., Eckhardt, F. E. W., & Palmer, R. J. (1995). Methods for the study of rock-inhabiting microorganisms—a mini review. *J Microbiol Meth*, 23(2), 143-167.

64. Hofstetter, T. B., Sosedova, Y., Gorski, C., Voegelin, A., & Sander, M. (2014). Redox properties of iron-bearing clays and MX-80 bentonite – Electrochemical and spectroscopic characterization. Nagra Technical Report 13-03. Zurich, Switzerland. https://www.researchgate.net/publication/275955029_Redox_properties_of_iron-

bearing_clays_and_MX-80_bentonite_-_Electrochemical_and_spectroscopic_characterization

65. Horneck, G., Stöffler, D., Ott, S., Hornemann, U., Cockell, C. S., Moeller, R., & Artemieva, N. A. (2008). Microbial rock inhabitants survive hypervelocity impacts on Mars-like host planets: first phase of lithopanspermia experimentally tested. *Astrobiol*, 8(1), 17-44.
66. Hunger, S., & Benning, L. G. (2007). Greigite: a true intermediate on the polysulfide pathway to pyrite. *Geochem Trans*, 8(1), 1.
67. IAEA (2013) Characterization of Swelling Clays as Components of the Engineered Barrier System for Geological Repositories Results of an IAEA Coordinated Research Project 2002–2007 IAEA-TECDOC-1718. http://www-pub.iaea.org/books/IAEABooks/8525/Characterization-of-Swelling-Clays-as-Components-of-the-Engineered-Barrier-System-for-Geological-Repositories
68. Jarvis, P., Rey, A., Petsikos, C., Wingate, L., Rayment, M., Pereira, J., Banza, J., David, J., Miglietta, F., Borghetti, M., Manca, G. & Valentini, R. (2007). Drying and wetting of Mediterranean soils stimulates decomposition and carbon dioxide emission: the "Birch effect". *Tree physiol,* 27(7), 929-940.
69. Jawad, A., Heritage, J., Snelling, A. M., Gascoyne-Binzi, D. M., & Hawkey, P. M. (1996). Influence of relative humidity and suspending menstrua on survival of Acinetobacter spp. on dry surfaces. *J Clin Microbiol*, 34(12), 2881-2887.
70. Jordan, R. N., Nichols, E. P., & Cunningham, A. B. (1999). The role of (bio) surfactant sorption in promoting the bioavailability of nutrients localized at the solid-water interface. *Water Sci Technol*, 39(7), 91-98.

71. Joubert, L. M., Wolfaardt, G. M., & Botha, A. (2006). Microbial exopolymers link predator and prey in a model yeast biofilm system. *Microb Ecol*, 52(2), 187-197.

72. Kakumanu, M. L., Cantrell, C. L., & Williams, M. A. (2013). Microbial community response to varying magnitudes of desiccation in soil: a test of the osmolyte accumulation hypothesis. *Soil Biol Biochem*, 57, 644-653.

73. Karnland, O., Olsson, S., & Nilsson, U. (2006). Mineralogy and sealing properties of various bentonites and smectite-rich clay materials. Stockholm: SKB. http://www.skb.se/publication/1419144/TR-06-30.pdf

74. Katra, I., Arotsker, L., Krasnov, H., Zaritsky, A., Kushmaro, A., & Ben-Dov, E. (2014). Richness and diversity in dust stormborne biomes at the southeast mediterranean. *Nature Sci Rep*, 4, 5265.

75. Kell, D. B., Kaprelyants, A. S., Weichart, D. H., Harwood, C. R., & Barer, M. R. (1998). Viability and activity in readily culturable bacteria: A review and discussion of the practical issues. *Anton Leeuw Int J G,* 73(2), 169-187.

76. Kempf, B., & Bremer, E. (1998). Uptake and synthesis of compatible solutes as microbial stress responses to high-osmolality environments. *Arch Microbiol*, 170(5):319-330.

77. Knowles, C. J., & Smith, L. (1970). Measurements of ATP levels of intact Azotobacter vinelandii under different conditions. *BBA-Bioenergetics*, 197(2), 152-160.

78. Kopf, S. H. (2015). From lakes to lungs: assessing microbial activity in diverse environments (Doctoral dissertation, California Institute of Technology).

79. Korpi, A., Pasanen, A. L., Pasanen, P., & Kalliokoski, P. (1997). Microbial growth and metabolism in house dust. *Int Biodeter Biodegr*, 40(1), 19-27.

80. Kotelnikova, S. (2002). Microbial production and oxidation of methane in deep subsurface. *Earth Sci Rev*, 58(3), 367-395.

81. Kovac, J., Husse, J., & Oster, H. (2009). A time to fast, a time to feast: the crosstalk between metabolism and the circadian clock. *Mol Cells*, 28(2), 75-80.

82. Kramer, A., Schwebke, I., & Kampf, G. (2006). How long do nosocomial pathogens persist on inanimate surfaces? A systematic review. *BMC Infect Dis,* 6(1), 130.

83. Kroukamp, O., & Wolfaardt, G. M. (2009). CO2 production as an indicator of biofilm metabolism. *Appl Environ Microb*, 75(13), 4391-4397.

84. Lazdunski, A., & Belaich, J. P. (1972). Uncoupling in bacterial growth: ATP pool variation in *Zymomonas mobilis* cells in relation to different uncoupling conditions of growth. *Microbiology+*, 70(2), 187-197.

85. Leenaars, A. F. M., & S. B. G. O'Brien. (1989). Particle removal from silicon substrates using surface tension forces. *Philips J Res*, 44, 183-209.

86. Li, X., Nielsen, L., Nolan, C., & Halverson, L. J. (2010). Transient alginate gene expression by *Pseudomonas putida* biofilm residents under water‐limiting conditions reflects adaptation to the local environment. *Environ Microbiol*, *12*(6), 1578-1590.

87. Lidwell, O. M., & Lowbury, E. J. (1950). The survival of bacteria in dust. II. The effect of atmospheric humidity on the survival of bacteria in dust. *J Hyg*, 48(01), 21-27.

88. Liu, D., Dong, H., Bishop, M. E., Zhang, J., Wang, H., Xie, S., & Eberl, D. D. (2012). Microbial reduction of structural iron in interstratified illite-smectite minerals by a sulfate-reducing bacterium. *Geobiol*, 10(2), 150-162.

89. Maher, K., Steefel, C. I., DePaolo, D. J., & Viani, B. E. (2006). The mineral dissolution rate conundrum: Insights from reactive transport modeling of U isotopes and pore fluid chemistry in marine sediments. *Geochim Cosmochim Ac* 70(2), 337-363.

90. Marshall, M. H., McKelvie, J. R., Simpson, A. J., & Simpson, M. J. (2015). Characterization of natural organic matter in bentonite clays for potential use in deep geological repositories for used nuclear fuel. *Appl Geochem,* 54, 43-53.

91. Masurat, P., Eriksson, S., & Pedersen, K. (2010) Microbial sulphide production in compacted Wyoming bentonite MX-80 under in situ conditions relevant to a repository for high-level radioactive waste. *Appl Clay Sci,* 47(1): 58-64.

92. Mathis, B. J., Marshall, C. W., Milliken, C. E., Makkar, R. S., Creager, S. E., & May, H. D. (2008). Electricity generation by thermophilic microorganisms from marine sediment. *Appl Microbiol Biotech*, 78(1), 147-155.

93. Mauclaire, L., McKenzie, J. A., Schwyn, B., & Bossart, P. (2007). Detection and cultivation of indigenous microorganisms in Mesozoic claystone core samples from the Opalinus Clay Formation (Mont Terri Rock Laboratory). *Phys Chem Earth, PT A/B/C*, 32(1), 232-240.

94. Meola, M., Lazzaro, A., & Zeyer, J. (2015). Bacterial composition and survival on Sahara dust particles transported to the European Alps. *Front Microbiol*, 6.

95. Mermillod-Blondin, F., Fauvet, G., Chalamet, A., & Creuzé des Châtelliers, M. (2001). A comparison of two ultrasonic methods for detaching biofilms from natural substrata. *Int Rev Hydrobiol*, 86(3), 349-360.

96. Meysman, F. J., & Middelburg, J. J. (2005). Acid-volatile sulfide (AVS)—A comment. *Mar Chem*, 97(3), 206-212.

97. Mottershead, D., Gorbushina, A., Lucas, G., & Wright, J. (2003). The influence of marine salts, aspect and microbes in the weathering of sandstone in two historic structures. *Build Environ*, 38(9), 1193-1204.

98. Mulder, M. (1996). Basic principles of membrane technology. Springer Science & Business Media.

99. Mulligan, C. N., Yong, R. N., & Fukue, M. (2009). Some effects of microbial activity on the evolution of clay-based buffer properties in underground repositories. *Appl Clay Sci*, 42(3), 331-335.

100. Murray, A. E., & Fritsen, C. H. (2007). Microbiota within the perennial ice cover of Lake Vida, Antarctica. *FEMS Microbiol Ecol*, 59(2), 274-288.

Muurinen, A. (2009). Studies on the chemical conditions and microstructure in the reference bentonites of alternative buffer materials project (ABM) in Äspö. Posiva Oy Working Report 2009-42. Eurajoki, Finland.

http://www.posiva.fi/files/989/WR_2009-42_web.pdf

101. Nakano, M., & Kawamura, K. (2010). Estimating the corrosion of compacted bentonite by a conceptual model based on microbial growth dynamics. *Appl Clay Sci,* 47(1), 43-50.

102. Nielsen, L., Li, X., & Halverson, L. J. (2011). Cell–cell and cell–surface interactions mediated by cellulose and a novel exopolysaccharide contribute to *Pseudomonas putida* biofilm formation and fitness under water‐limiting conditions. *Environ Microbiol*, *13*(5), 1342-1356.

103. North, N. N., Dollhopf, S. L., Petrie, L., Istok, J. D., Balkwill, D. L., & Kostka, J. E. (2004). Change in bacterial community structure during *in situ* biostimulation of

subsurface sediment cocontaminated with uranium and nitrate. *Appl Environ Microb*, 70(8), 4911-4920.

104. *Nuclear Fuel Waste Act*, S. C. 2002, c. 23.
105. Nuclear Waste Management Organization of Canada. (2005). Final Study: Choosing a Way Forward. The Future Management of Canada's Used Nuclear Fuel. http://www.nwmo.ca/uploads_managed/MediaFiles/2680_nwmo_final_study_nov_2005.pdf
106. Nuclear Waste Management Organization of Canada. (2010). Moving Forward Together: Process for selecting a site for Canada's deep geological repository for used nuclear fuel; Nuclear Waste Management Organization, May 2010. http://www.nwmo.ca/uploads_managed/MediaFiles/1545_processforselectingasiteforcan.pdf
107. Oliver, J. D. (2005). The viable but nonculturable state in bacteria. J Microbiol, 43, 93-100.
108. Oliver, J. D. (2010). Recent findings on the viable but nonculturable state in pathogenic bacteria. *FEMS Microbiol Rev,* 34(4), 415-425.
109. O'Malley, Maureen A. (2007) The nineteenth century roots of 'everything is everywhere'. *Nature Rev Microbiol* 5(8) 647-651.
110. Organization for Economic Co-operation and Development: Nuclear Energy Agency. (2012). Radioactive Waste Management Programs in OECD-NEA Member Countries: Canada (2012) National Nuclear Context. http://www.oecd-nea.org/rwm/profiles/Canada_profile_web.pdf

111. Osburn, M. R., LaRowe, D. E., Momper, L. M., & Amend, J. P. (2014). Chemolithotrophy in the continental deep subsurface: Sanford Underground Research Facility (SURF), USA. *Front. Microbiol*, 5, 610.

Otter, J. A., Vickery, K., Walker, J. D., deLancey Pulcini, E., Stoodley, P., Goldenberg, S. D., Salkald, J. A. G., Chewins, J., Yezli, S., & Edgeworth, J. D. (2015). Surface-attached cells, biofilms and biocide susceptibility: implications for hospital cleaning and disinfection. *J Hosp Infect*, 89(1), 16-27.

112. Paget, E., Monrozier, L. J., & Simonet, P. (1992). Adsorption of DNA on clay minerals: protection against DNaseI and influence on gene transfer. *FEMS Microbiol Lett*, 97(1-2), 31-39.

113. Pedersen, K. (1997). Microbial life in deep granitic rock. *FEMS Microbiology Reviews*, *20*(3-4), 399-414.

114. Pedersen, K. (2010) Analysis of copper corrosion in compacted bentonite clay as a function of clay density and growth conditions for sulfate‐reducing bacteria. *J Appl Microbiol,* 108(3): 1094-1104.

115. Pedersen, K., Motamedi, M., Karnland, O., & Sandén, T. (2000). Cultivability of microorganisms introduced into a compacted bentonite clay buffer under high-level radioactive waste repository conditions. *Eng Geol* 58(2):149-161.

116. Pfeffer, C., Larsen, S., Song, J., Dong, M., Besenbacher, F., Meyer, R. L., Kjeldsen, K. U., Schreiber, L, Gorby, Y. A., El-Nagger, M. Y., Leung, K. M., Schramm, A., Risgaard-Petersen, N., & Nielsen, L. P. (2012). Filamentous bacteria transport electrons over centimetre distances. *Nature*, 491(7423), 218-221.

117. Post, J. C., Ehrlich, G. D., & Costerton, J. W. (2013). Biofilm remediation of metal containing wastewater. *U.S. Patent No. 8,425,776*. Washington, DC: U.S. Patent and Trademark Office.

118. Potts, M. (1994). Desiccation tolerance of prokaryotes. *Microbiol Rev,* 58(4), 755-805.

119. Potts, M. (2001). Desiccation tolerance: a simple process? *Trends Microbiol*, 9(11), 553-559.

120. Ramirez, M. L., Chulze, S. N., & Magan, N. (2004). Impact of osmotic and matric water stress on germination, growth, mycelial water potentials and endogenous accumulation of sugars and sugar alcohols in *Fusarium graminearum*. *Mycologia*, 96(3), 470-478.

121. Rawlings, D. E. (2002). Heavy metal mining using microbes. *Ann Rev Microbiol*, 56(1), 65-91.

122. Reese, B. K., Finneran, D. W., Mills, H. J., Zhu, M. X., & Morse, J. W. (2011). Examination and refinement of the determination of aqueous hydrogen sulfide by the methylene blue method. *Aq Geochem,* 17(4-5), 567-582.

123. Rickard, D., & Morse, J. W. (2005). Acid volatile sulfide (AVS). *Mar Chem*, 97(3), 141-197.

124. Ritchie, F., McQuilken, M. P., & Bain, R. A. (2006). Effects of water potential on mycelial growth, sclerotial production, and germination of *Rhizoctonia solani* from potato. *Mycol Res*, 110(6), 725-733.

125. Ronan, E., Yeung, C. W., Hausner, M., & Wolfaardt, G. M. (2013). Interspecies interaction extends bacterial survival at solid–air interfaces. *Biofouling*, 29(9), 1087-1096.

126. Rousk, J., Brookes, P. C., & Bååth, E. (2009). Contrasting soil pH effects on fungal and bacterial growth suggest functional redundancy in carbon mineralization. *Appl Env Microbiol*, 75(6), 1589-1596.

127. Rutter, P. R., & Vincent, B. (1988). Attachment mechanisms in the surface growth of microorganisms, p. 87-107 *In* M. J. Bazin and J. I. Prosser (ed.) Physiological models in microbiology, vol. II. CRC Press, Boca Raton, Fla.

128. Safonov, A. V., Ershov, B. G., & Gorbunova, O. A. (2012). Control of microbiological processes during long-term storage of radwastes. *Atom Energy+*, 112(4), 255-260.

129. Samarian, D. S., Jakubovics, N. S., Luo, T. L., & Rickard, A. H. (2014). Use of a High-throughput In Vitro Microfluidic System to Develop Oral Multi-species Biofilms. *JoVE,* (94), e52467-e52467.

130. Schmitt, D. M., O'Dee, D. M., Cowan, B. N., Birch, J. W. M., Mazzella, L. K., Nau, G. J., & Horzempa, J. (2013). The use of resazurin as a novel antimicrobial agent against Francisella tularensis. *Front Cell Infect Microbiol*, 3, 93.

131. Schofield, R. K., & Taylor, A. W. (1955). The measurement of soil pH. *Soil Sci America J*, 19(2), 164-167.

132. Sherwood Lollar, B. (2011) Far-field Microbiology Considerations Relevant to a Deep Geological.Repository: State of Science Review. Nuclear Waste Management Organization Technical Report TR-2011-09. Toronto, Canada. http://www.nwmo.ca/uploads_managed/MediaFiles/1902_nwmotr-2011-09_far-fieldmicrobiologyconsiderationsrelevanttoadeepgeologicalrepository-state-of-scien.pdf

133. Sikorski, J., & Nevo, E. (2007). Patterns of thermal adaptation of Bacillus simplex to the microclimatically contrasting slopes of 'Evolution Canyons' I and II, Israel. *Environ Microbiol*, 9(3), 716-726.

134. Skjerdal, O. T., Lorentzen, G., Tryland, I., & Berg, J. D. (2004). New method for rapid and sensitive quantification of sulphide-producing bacteria in fish from arctic and temperate waters. *Int J Food Microbiol*, 93(3), 325-333.

135. Snowdon, J. A., & Cliver, D. O. (1996). Microorganisms in honey. *Int J Food Microbiol*, 31(1), 1-26.

136. Spiegelman, B. M., & Flier, J. S. (2001). Obesity and the regulation of energy balance. *Cell*, 104(4), 531-543.

137. Sterflinger, K., Tesei, D., & Zakharova, K. (2012). Fungi in hot and cold deserts with particular reference to microcolonial fungi. *Fungal Ecol*, 5(4), 453-462.

138. Stone, W., Kroukamp, O., Moes, A., McKelvie, J., Korber, D. R., & Wolfaardt, G. M. 2016. Measuring microbial metabolism in atypical environments: Bentonite in used nuclear fuel storage. *J Microbiol Meth*, 120, 79-90.

139. Stotzky, G., & Pramer, D. (1972). Activity, ecology, and population dynamics of microorganisms in soil. *CRC CR Rev Microbiol*, 2(1), 59-137.

140. Stroes‐Gascoyne, S., & West, J. M. (1997). Microbial studies in the Canadian nuclear fuel waste management program. *FEMS Microbiol Rev*, 20(3‐4), 573-590.

141. Stroes-Gascoyne, S., Lucht, L. M., Oscarson, D. W., Dixon, D. A., Hume, H. B., & Miller, S. H. (1997). Migration of bacteria in compacted clay-based material. Atomic Energy of Canada Limited, Pinawa, Manitoba (Canada). http://www.iaea.org/inis/collection/NCLCollectionStore/_Public/31/010/31010425.pdf

142. Stroes-Gascoyne, S., Schippers, A., Schwyn, B., Poulain, S., Sergeant, C., Simonoff, M., & Matray, J. M. (2007A). Microbial community analysis of Opalinus clay drill core samples from the Mont Terri underground research laboratory, Switzerland. *Geomicrobiol J*, 24(1), 1-17.

143. Stroes-Gascoyne, S., Hamon, C. J., Dixon, D. A., & Martino, J. B. (2007B). Microbial analysis of samples from the tunnel sealing experiment at AECL's Underground Research Laboratory. *Phys Chem Earth*, 32(1):219-231.

144. Stroes-Gascoyne, S., Hamon, C. J., Maak, P., & Russell, S. (2010). The effects of the physical properties of highly compacted smectitic clay (bentonite) on the culturability of indigenous microorganisms. *Appl Clay Sci*, 47(1), 155-162.

145. Stroes-Gascoyne, S., Hamon, C. J., & Maak, P. (2011A). Limits to the use of highly compacted bentonite as a deterrent for microbiologically influenced corrosion in a nuclear fuel waste repository. *Phys Chem Earth, PT A/B/C*, 36(17), 1630-1638.

146. Stroes-Gascoyne, S., Sergeant, C., Schippers, A., Hamon, C. J., Nèble, S., Vesvres, M. H. & Le Marrec, C. (2011B). Biogeochemical processes in a clay formation *in situ* experiment: Part D–Microbial analyses–Synthesis of results. *Appl Geochem*, *26*(6), 980-989.

147. Stroes-Gascoyne, S. and Hamon, C. J. (2014). Microbial Analysis of Highly Compacted Bentonite Samples from Two Large *In Situ* Tests at the Äspö Hard Rock Laboratory, Sweden. Nuclear Waste Management Organization Report NWMO TR-2014-15. Toronto, Canada. http://dgr.nwmo.ca/uploads_managed/MediaFiles/2473_nwmo_tr-2014-15_microbial_analysis_of_highly_compa.pdf

148. Takada-Hoshino, Y., & Matsumoto, N. (2004). An improved DNA extraction method using skim milk from soils that strongly adsorb DNA. *Microbes Environ*, 19(1).

149. Tavares, F. W., Bratko, D., Blanch, H. W., & Prausnitz, J. M. (2004). Ion-specific effects in the colloid-colloid or protein-protein potential of mean force: role of salt-macroion van der Waals interactions. *J Phys Chem B,* 108(26), 9228-9235.

150. Trinder, M., Bisanz, J. E., Burton, J. P., & Reid, G. (2015). Bacteria Need "Sleep" Too?: Microbiome Circadian Rhythmicity, Metabolic Disease, and Beyond. *U Toronto Med J*, 92(3).

151. Trüper, H. G., & Schlegel, H. G. (1964). Sulphur metabolism in Thiorhodaceae I. Quantitative measurements on growing cells of *Chromatium okenii*. *Anton Van Leeuw*, 30(1), 225-238.

152. Turner, A. G. & Salmonsen, P. A. (1973). The effect of relative humidity on the survival of three serotypes of *Klebsiella*. *J Appl Bacteriol,* 36(3), 497-499.

153. Van Houdt, R., & Michiels, C. W. (2010). Biofilm formation and the food industry, a focus on the bacterial outer surface. *J Appl Microbiol*, 109(4), 1117-1131.

154. Varin, T., Lovejoy, C., Jungblut, A. D., Vincent, W. F., & Corbeil, J. (2010). Metagenomic profiling of Arctic microbial mat communities as nutrient scavenging and recycling systems. *Limnol Oceanogr*, 55(5), 1901-1911.

155. Vilks, P. (2009). Sorption in highly saline solutions–State of the science review. Nuclear Waste Management Organization Report NWMO TR-2009-18. Toronto, Canada. https://www.researchgate.net/publication/267854920_Sorption_in_Highly_Saline_Solutions_-_State_of_the_Science_Review

156. Vishniac, H. S., & Onofri, S. (2003). *Cryptococcus antarcticus* var. *circumpolaris* var. nov., a basidiomycetous yeast from Antarctica. *Anton Van Leeuw*, 83(3), 231-233.

157. Vreulink, J. M., Stone, W., & Botha, A. (2010). Effects of small increases in copper levels on culturable basidiomycetous yeasts in low-nutrient soils. *J Appl Microbiol*, 109(4), 1411-1421. doi:10.1111/j.1365-2672.2010.04770.x

158. Walker, S. G., Flemming, C. A., Ferris, F. G., Beveridge, T. J., & Bailey, G. W. (1989). Physicochemical interaction of *Escherichia coli* cell envelopes and *Bacillus subtilis* cell walls with two clays and ability of the composite to immobilize heavy metals from solution. *Appl Environ Microb*, 55(11), 2976-2984.

159. Walters, C., Hill, L. M., & Wheeler, L. J. (2005). Dying while dry: Kinetics and mechanisms of deterioration in desiccated organisms. *Integr Comp Biol*, 45(5), 751-758.

160. Weimerskirch, H., Martin, J., Clerquin, Y., Alexandre, P., & Jiraskova, S. (2001). Energy saving in flight formation. *Nature*, 413(6857), 697-698.

161. White, T. J., Bruns, T., Lee, S. J. W. T., & Taylor, J. W. (1990). Amplification and direct sequencing of fungal ribosomal RNA genes for phylogenetics, p. 315-322. *In* PCR protocols: a guide to methods and applications. Innis, M.A., D.H. Gelfand, J.J. Sninsky, and T.J. White (eds.). Academic Press, Inc., New York.

162. Wolfaardt, G. M., & Korber, D. R. (2012). Near-field microbiological considerations relevant to a deep geological repository for used nuclear fuel - State of science review. Nuclear Waste Management Organization Report NWMO TR-2012-02. Toronto, Canada.

http://www.nwmo.ca/uploads_managed/MediaFiles/2067_nwmo-tr-2012-02_near-field-microbiological-conside.pdf

163. Wolfaardt, G. M., Lawrence, J. R., & Korber, D. R. (1999). Function of EPS, p. 171-200. *In* Microbial extracellular polymeric substances. Wingender, J., Neu, T. R., and Flemming (eds.). H. C. Springer, Berlin Heidelberg.

164. Xu, K. D., Stewart, P. S., Xia, F., Huang, C. T., & McFeters, G. A. (1998). Spatial physiological heterogeneity inPseudomonas aeruginosa biofilm is determined by oxygen availability. *Appl Environ Microb*, 64(10), 4035-4039.

165. Zavarzin, G. A. (2006). Winogradsky and modern microbiology. *Microbiol,* 75(5), 501-511.

166. Zhdanova, N. N., Zakharchenko, V. A., Vember, V. V., & Nakonechnaya, L. T. (2000). Fungi from Chernobyl: mycobiota of the inner regions of the containment structures of the damaged nuclear reactor. *Mycol Res*, 104(12), 1421-1426.

167. Zolensky, M. E. (2005). Extraterrestrial water. *Elements,* 1(1), 39-43. 20.